AD-A173 747 COMBUSTION PERFORMANCE OF CONTAMINATED MARINE DIESEL FUELS IN A T63 GAS T (U) SOUTHWEST RESEARCH INST SAN ANTONIO TX BELVOIR FUELS AND LUBR D W NAEGELI ET AL 1/2

UNCLASSIFIED DEC 85 BFLRF-208 DAAK70-85-C-0007 F/G 21/4 NL

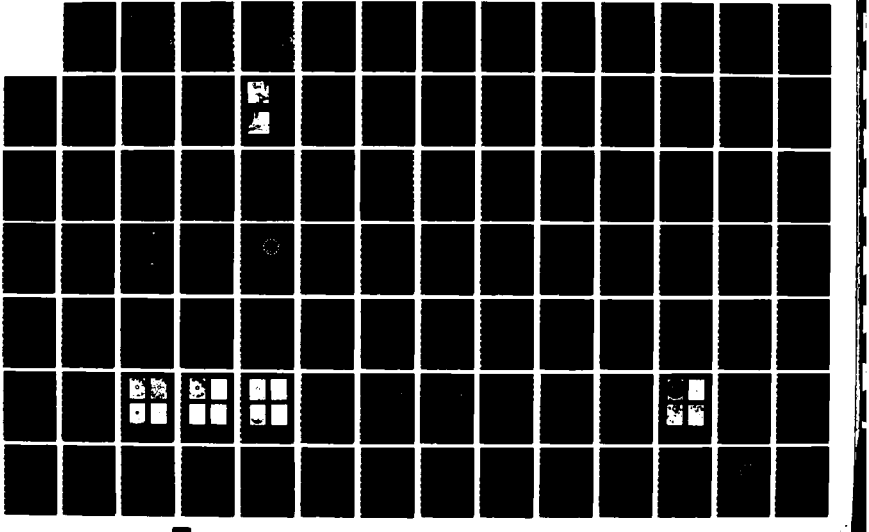

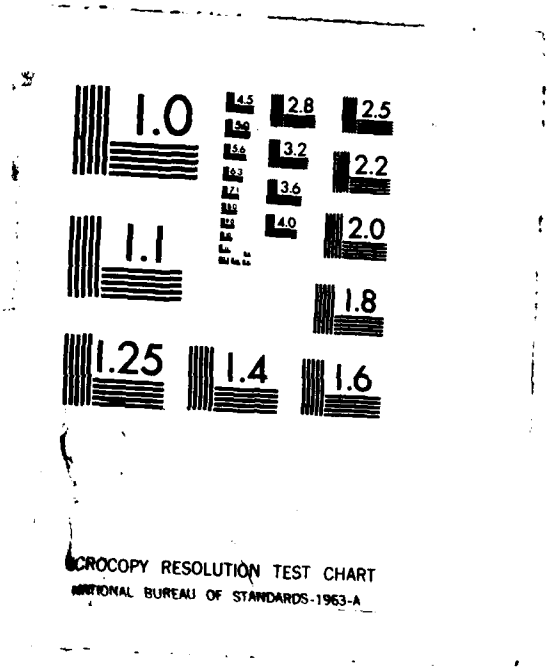
1.0
1.1
1.25
1.4
1.6
1.8
2.0
2.2
2.5
2.8
3.2
3.6
4.0
4.5
5.0
5.6
6.3
7.1
8.0
9.0
CROCOPY RESOLUTION TEST CHART
NATIONAL BUREAU OF STANDARDS-1963-A

(12)

COMBUSTION PERFORMANCE OF CONTAMINATED MARINE DIESEL FUELS IN A T63 GAS TURBINE COMBUSTOR

INTERIM REPORT
BFLRF No. 208

By

D.W. Naegeli
L.G. Dodge
Belvoir Fuels and Lubricants Research Facility (SwRI)
Southwest Research Institute
San Antonio, Texas

Prepared for

David Taylor Naval Ship R&D Center
Annapolis, MD

Under Contract to

U.S. Army Belvoir Research, Development and Engineering Center
Materials, Fuels and Lubricants Laboratory
Fort Belvoir, Virginia

Contract No. DAAK70-85-C-0007

December 1985

Disclaimers

The findings in this report are not to be construed as an official Department of the Army position unless so designated by other authorized documents.

Trade names cited in this report do not constitute an official endorsement or approval of the use of such commercial hardware or software.

DTIC Availability Notice

Qualified requestors may obtain copies of this report from the Defense Technical Information Center, Cameron Station, Alexandria, Virginia 22314.

Disposition Instructions

Destroy this report when no longer needed. *Do not return it to the* originator.

Unclassified
SECURITY CLASSIFICATION OF THIS PAGE

AD-A173947

REPORT DOCUMENTATION PAGE

1a. REPORT SECURITY CLASSIFICATION Unclassified	1b. RESTRICTIVE MARKINGS None
2a. SECURITY CLASSIFICATION AUTHORITY N/A	3. DISTRIBUTION/AVAILABILITY OF REPORT Approved for public release; distribution unlimited
2b. DECLASSIFICATION/DOWNGRADING SCHEDULE	
4. PERFORMING ORGANIZATION REPORT NUMBER(S) Interim Report BFLRF No. 208	5. MONITORING ORGANIZATION REPORT NUMBER(S)
6a. NAME OF PERFORMING ORGANIZATION Belvoir Fuels and Lubricants Research Facility (SwRI) 6b. OFFICE SYMBOL (If applicable)	7a. NAME OF MONITORING ORGANIZATION U.S. Army Belvoir Research, Development and Engineering Center
6c. ADDRESS (City, State, and ZIP Code) Southwest Research Institute 6220 Culebra Road San Antonio, TX 78284	7b. ADDRESS (City, State, and ZIP Code) Attn: STRBE-VF Fort Belvoir, VA 22060-5606
8a. NAME OF FUNDING/SPONSORING ORGANIZATION David Taylor Naval Ship R&D Center 8b. OFFICE SYMBOL (If applicable) MFG, Code 2759	9. PROCUREMENT INSTRUMENT IDENTIFICATION NUMBER DAAK70-85-C-0007; WD 18 & 19
8c. ADDRESS (City, State, and ZIP Code) Annapolis Laboratory Annapolis, MD 21402	10. SOURCE OF FUNDING NUMBERS PROGRAM ELEMENT NO. / PROJECT NO. / TASK NO. / WORK UNIT ACCESSION NO.

11. TITLE (Include Security Classification)

Combustion Performance of Contaminated Marine Diesel Fuels in a T63 Gas Turbine Combustor

12. PERSONAL AUTHOR(S)
Naegeli, D.W.; Dodge, L.G.

13a. TYPE OF REPORT	13b. TIME COVERED	14. DATE OF REPORT (Year, Month, Day)	15. PAGE COUNT
Interim	FROM Nov 83 TO Sept 85	1985 December	121

16. SUPPLEMENTARY NOTATION

17. COSATI CODES			18. SUBJECT TERMS (Continue on reverse if necessary and identify by block number)
FIELD	GROUP	SUB-GROUP	Navy Fuel Distillate Contaminated Fuel Combustor

OCT 29 1986
D
S E

19. ABSTRACT (Continue on reverse if necessary and identify by block number)

The combustions performance of 26 fuel blends of Navy distillate fuel (NDF), heavy marine gas oil (HMGO), and a Jet A reference fuel contaminated with residuals containing various concentrations of asphaltenes, resins, and ash was measured in a T63 gas turbine combustor rig. The combustion performance measurements included cold start ignition, combustion efficiency, gaseous exhaust emissions, flame radiation, exhaust smoke, liner temperature, and combustor can deposit formation. Except for ignition, these measurements were made at four operating conditions, 10 percent of full power (idle), 55, 75, and 100 percent of full power. Cold-start ignition measurements were made on nine of the test fuels at burner inlet air temperatures ranging from 238K to 300K and fuel temperatures ranging from 263K to 300K.

Droplet size measurements were made of fuel sprays from the T63, LM2500, DDA 501-K17, and the TF40B atomizers using a Malvern light scattering apparatus. These measurements were made on

20. DISTRIBUTION/AVAILABILITY OF ABSTRACT	21. ABSTRACT SECURITY CLASSIFICATION	
☒ UNCLASSIFIED/UNLIMITED ☐ SAME AS RPT. ☐ DTIC USERS	Unclassified	
22a. NAME OF RESPONSIBLE INDIVIDUAL F.W. Schaekel	22b. TELEPHONE (Include Area Code) (703) 664-3576	22c. OFFICE SYMBOL STRBE-VF

DD FORM 1473, 84 MAR — 83 APR edition may be used until exhausted. All other editions are obsolete.

SECURITY CLASSIFICATION OF THIS PAGE
Unclassified

19. ABSTRACT (Cont'd)

~~seven~~ fuels over a range of low fuel flow rates comparable with those used for the ignition conditions of the respective engines. Correlation equations were developed relating Sauter mean droplet diameter to fuel properties and flow conditions. The correlation equation developed for the T63 atomizer was used in a charcteristic time model calculation of the cold start ignition data.

Flame radiation and exhaust smoke ~~were found to~~ correlated with hydrogen-carbon ratio. Fuels contaminated with residuals did not deviate significantly from the H/C ratio correlation.

When neat NDF and HMGO were contaminated with residuals there appeared to be a slight decrease in combustion efficiency and increase in total hydrocarbon and CO emissions. The NO_x emissions were essentially independent of fuel quality.

Deposit formation in the dome and primary zone sidewall of the combustor can was found to be a major problem with contaminated fuels. Significant deposits formed in less than one hour of operation. Subsequent operation with neat NDF and JP5 burned off as much as 65 percent of the deposit in five hours of operation.

FOREWORD

This work was prepared at the Belvoir Fuels and Lubricants Research Facility (SwRI) under DOD Contract Nos. DAAK70-82-C-0001 and DAAK70-85-C-0007. The project was administered by the Fuels and Lubricants Division, U.S. Army Belvoir Research, Development, and Engineering Center, Ft. Belvoir, VA 22060, with Mr. F.W. Schaekel, STRBE-VF, serving as Contracting Officer's Representative. This was funded by the U.S. Navy with Mr. R. Strucko, Department of the Navy, serving as Technical Monitor. This report covers the period of performance from November 1983 through September 1985.

ACKNOWLEDGEMENTS

The authors wish to thank Messrs. R.C. Haufler and F.H. Lessing of Southwest Research Institute for their excellent work in conducting the combustor experiments. Special thanks is awarded to R.C. Haufler for his efforts in photographing the combustor desposits formed from contaminated fuels and for carrying out droplet size measurements on fuel atomizers.

We wish to thank Messrs. Stephen Rutter, Sidney Watkins, and George Opdyke, Jr. of Avco Lycoming Division for information about the TF40B and parts necessary for this test. Similarly, Bruce Sanneman of General Electric provided information about the LM2500. John McGroarty of Naval Ship Systems Engineering Station provided help and consultation as well as parts for the DDA 501-K17 atomizer tests.

TABLE OF CONTENTS

LIST OF ILLUSTRATIONS

LIST OF ILLUSTRATIONS (CONT'D)

LIST OF TABLES

I. INTRODUCTION

With the successful introduction of the General Electric Co. (GE) LM2500 gas turbine engine as the main propulsion system for the DD963 Destroyer Class in 1975, gas turbines have become the preferred main propulsion powerplants for the modern fossil-fueled cruisers, destroyers, frigates, and large hydrofoil ships. The move to gas turbine propulsion is a result of more sophisticated ship design, emphasizing weight, compactness, and efficiency. In essence, gas turbines have a higher power output-to-weight ratio and volume ratio than diesels and boilers. However, there is a problem; fuels commonly used in marine diesels and boilers may not be entirely compatible with the needs of gas turbine engines.

The performance impacts on gas turbine engines using nonspecification fuels are manifested in many different areas: efficiency, reliability, fuel heating requirements, power output, exhaust temperatures, and smoke. The most important of these are efficiency and reliability, which depend substantially on the combustion performance of the fuel in the gas turbine combustor. Combustion performance includes cold start ignition, combustion efficiency, flame radiation, smoke, and deposit formation.

The fuel properties that effect cold start ignition and combustion efficiency are viscosity, surface tension, and the boiling point distribution.(1,2)* The size of droplets formed in fuel sprays depends on the fuel viscosity and surface tension. The rate of droplet evaporation is primarily dependent on droplet size, but the boiling point distribution is also important. These properties have a significant effect on the ignitability of the fuel and the completeness of combustion. They also affect deposit formation on combustor surfaces, but while the ignition process is thought to depend mainly on the viscosity and the volatility of low boiling components, the formation of deposits depends on the high boiling components or end point. When fuel droplets evaporate incompletely during combustion, the highest boiling components can stick to combustor surfaces and pyrolyze, forming deposits. If the fuel also contains contaminants such as metals and dirt, these materials will concentrate in the fuel as the droplets evaporate. The effects of metal contaminants are not well known, but it is fairly certain that they will accumulate in deposits and may have some effect on the deposit formation.

* Underscored numbers in parentheses refer to the list of references at the end of this report.

Flame radiation and exhaust smoke are both related to the tendency of the fuel to form solid carbon or soot in the combustion process. While smoke is not a particularly troublesome aspect of gas turbine combustion onboard ships, the flame radiation within the combustion chamber, caused by incandescent soot particles, can pose a significant threat to engine reliability. The increased radiant heat transfer to the combustor liner causes increased liner temperatures, which can lead to increased cycle fatigue. This fatigue may result in premature engine overhaul. It is well documented that soot formation in gas turbine combustors is, for the most part, dependent on the hydrogen content of the fuel.(1-5) There is little evidence that the final boiling point has any effect on soot formation. However, the sooting tendencies of heavy fuels, such as heavy marine gas oil (HMGO) and diesel fuel marine contaminated with asphaltenes, and resins have not been thoroughly investigated.

Based on the current understanding of the effects of fuel properties on combustion performance, it seems reasonably certain that the fuel property specifications for gas turbines used in marine vessels could be broadened substantially compared to the aviation fuel specifications. Fuel availability data indicate that broadening the surface fleet fuel specification to include a wider range of commercially available marine middle distillates would greatly increase the amount of fuel that the Navy could use both for continuous and emergency operations. This move to broadening the fuel specifications for gas turbines used in marine applications is still somewhat uncertain and requires some engine testing to determine the effects of off-specification fuels on combustion performance.

In the present study, the effects of marine fuel properties on combustion performance are examined in a T63 gas turbine combustor. The test fuels examined in this program consist of neat marine diesel fuels (Navy fuel distillate, NDF, and heavy marine gas oil, HMGO) and blends containing high boiling contaminants, asphaltenes, resins, catfine bottoms, and dirt. Jet A was used as a reference fuel.

II. APPROACH: Experimental Facilities And Methods

A. General Description

Combustion performance measurements on several fuel blends based on Navy Distillate Fuel, NDF, and Heavy Marine Gas Oil, HMGO, containing different levels of contami-

nants were made in a T63 gas turbine combustor rig. The areas investigated for fuel sensitivity were:

- Ignition
- Flame Radiation
- Liner Temperature
- Exhaust Smoke
- Gaseous Emissions
- Combustion Efficiency
- Deposits

This work was performed in the combustor facility of the Belvoir Fuels and Lubricants Research Facility (BFLRF) at Southwest Research Institute. This combustor facility was specially designed to study fuel-related problems in the operation of turbine engines. The air supply system provides a clean, smooth flow of air to the combustion test cell with mass flow rates up to 1.1 kg/s, pressure to 1620 kPa (16 atm), and temperatures to 1086K (1500°F) (unvitiated). Turbine flowmeters and strain-gage pressure transducers are used to measure flow properties of the air and fuel. Thermocouples are referenced to a 338.5K (150.0°F) oven. Data reduction is performed on-line with test summaries available immediately; these summaries provide average flow data as well as standard deviations (typically less than 1 percent of average value), exhaust temperature, profiles, emissions data, and combustion efficiencies.

B. T63 Combustor Rig

The combustor used in this study was fabricated from T63 engine hardware. This combustor has been used in previous programs to study the fuel effects on ignition, combustion stability, combustion efficiency, exhaust pattern factor, radiation, and smoke. Table 1 presents the operating conditions which represent the air flow conditions in the actual engine for the four different power points used for these tests (idle to full power). Figure 1 is a schematic of the combustor can showing also the location of the radiation sensor and liner thermocouples.

TABLE 1. T-63 COMBUSTOR RIG OPERATING CONDITIONS

Mode	% Power	BIP kpa(psia)	BIT K(°F)	W_a, kg/s(lb/s)	W_f, kg/m(lb/m)	F/A	FF	BOT, K(°F)
Ground Idle	10	230(33.4)	422(300)	0.64(1.40)	0.42(0.92)	0.0109	1.158	833(1040)
Cruise	55	369(53.6)	494(430)	0.93(2.06)	0.93(2.06)	0.0145	1.141	1033(1400)
Climb/Hover	75	418(60.7)	518(472)	1.02(2.24)	1.01(2.23)	0.0166	1.123	1122(1560)
Takeoff	100	477(69.2)	547(524)	1.10(2.42)	1.30(2.87)	0.0198	1.094	1244(1780)

BIP: Burner inlet air pressure
BIT: Burner inlet air temperature
W_a: Air flow rate
W_f: Fuel flow rate
F/A: Fuel/air ratio
FF: $W_a\sqrt{BIT/BIP}$
BOT: Typical burner outlet temperature

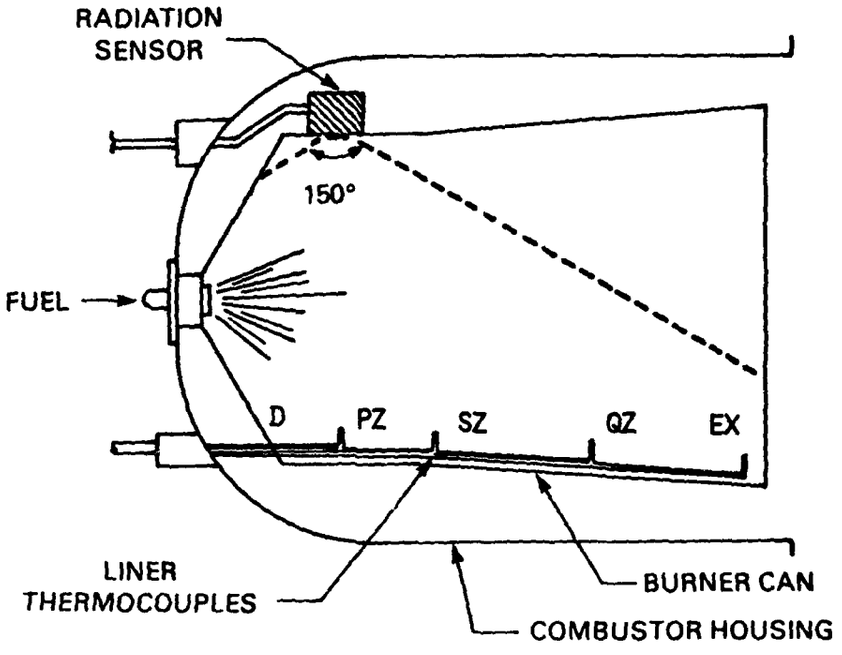

FIGURE 1. T63 COMBUSTOR LINER AND HOUSING
(Liner Thermocouples Were Placed on the Dome, D; Primary Zone, PZ; Secondary Zone, SZ; Quench Zone, QZ; and Exhaust, EX)

C. Combustor Facility

A detailed layout of the BFLRF combustor laboratory is shown in Figure 2. The facility consists of a variable pressure-temperature air supply, a control room for operating the air flow system, the fuel flow system, the combustor and its exhaust system; also, there are components for the data acquisition system (see Figures 3 and 4 for views of the control panel).

1. Air Flow System

A flow diagram of the "air factory" is shown in Figure 5. The compressed air for the lab is generated in two stages: two Ingersoll Rand "Pack-Air" rotary-screw compressors are connected in parallel, each delivering 0.573 m^3/sec (1000 SCFM) at 700 kPa (100 psig). This air goes through an inter-cooler and then to a single-cylinder reciprocating compressor where it is compressed to 1.75 mPa (250 psia). From there, the air passes through an aftercooler, a receiver, and an oil filter before going to the flow controls.

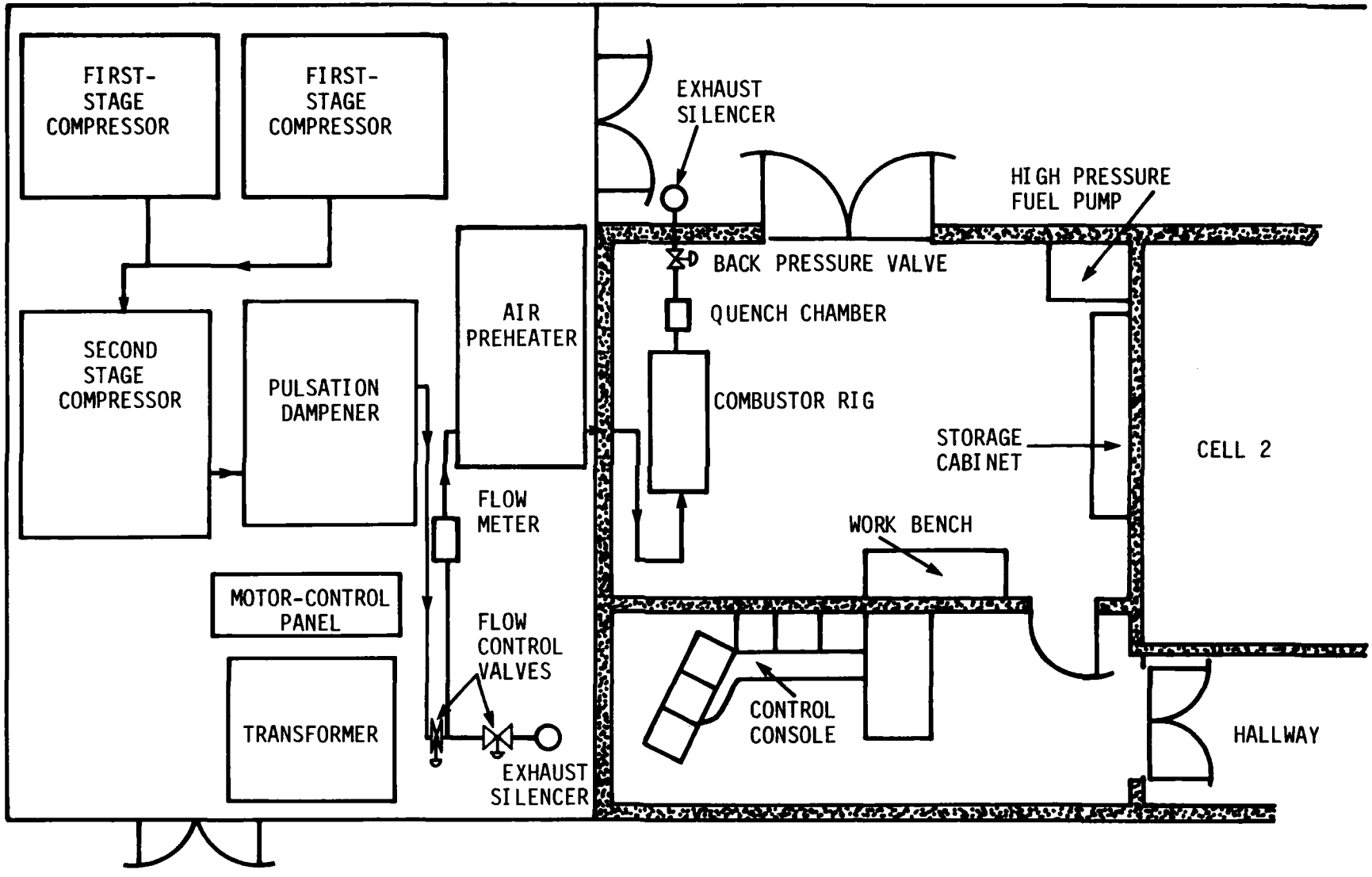

FIGURE 2. LAYOUT OF TURBINE FUEL RESEARCH COMBUSTOR LABORATORY

a. Air Heater Control System
b. Compressor Motor Controls
c. Pressure Transducer Reference System
d. Thermocouple Reference Oven
e. Moisture Readout
f. Quench Water Control
g. Air Flow Control
h. Ignition and Fuel Flow Control
i. Window Looks Into Combustion Room

FIGURE 3. VIEW OF CONTROL CONSOLE

a. Programmable Calculator
b. Printer
c. X-Y Plotter
d. Scanner and Digital Voltmeter
e. Magnetic Tape Cassette

FIGURE 4. VIEW OF CONTROL CONSOLE SHOWING DATA ACQUISITION SYSTEM

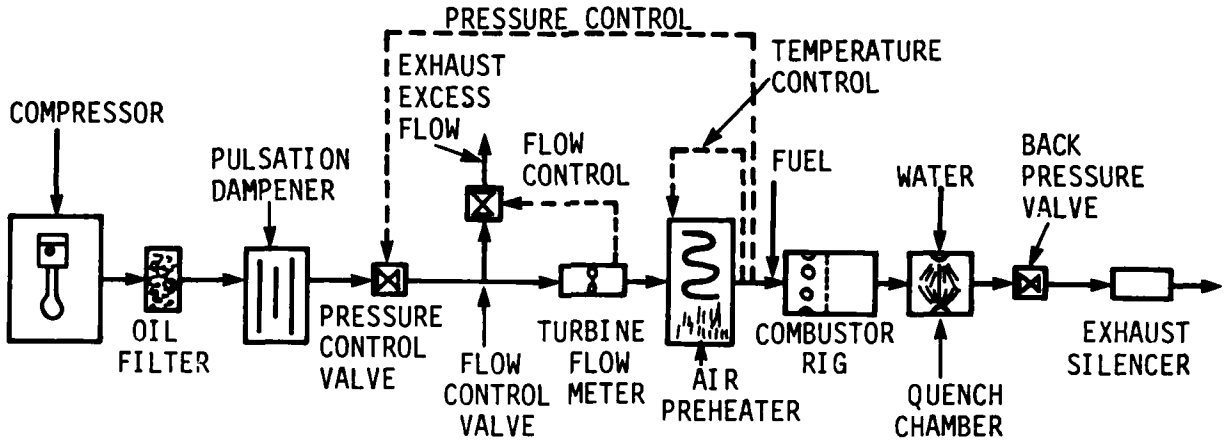

FIGURE 5. FLOW DIAGRAM OF TURBINE COMBUSTOR SYSTEM

The oil carryover is less than 5 ppm. Suction and discharge bottles are on the booster compressor which, in conjunction with the receiver, were designed on an analog computer by Ingersoll Rand to eliminate pulsations from the air flow. At the downstream side of the receiver, the pressure fluctuation (a frequency of about 45 Hz) was less than 700 Pa (0.1 psi) when the actual pressure was 1.6 mPa (235 psia).

The flow control system operates in two parts: one valve is used to provide a pressure drop to the system, while a second valve bypasses any excess air flow through an exhaust silencer. The compressors are always operating at full capacity--a method which uses more total energy but eliminates any surging caused by the compressors uncycling.

A 3-inch (7.62-cm) turbine flowmeter is used to measure the air flow rates. Because a turbine meter measures volumetric flow, the pressure and temperature are also sensed at the meter so the flow measurement can be converted to mass flow rate. The air flow then enters a preheater which is able to heat the flow from roughly 310K (100°F) to 1116K (1550°F). This heater is an indirect, gas-fired system with a counterflow heat exchanger; the air remains unvitiated. The combustion control system was designed in accordance with federal safety standards. The preheater will shut down automatically in event of a malfunction in the fuel supply or when temperatures exceed established limits. The final air temperature is automatically controlled by a Honeywell recorder-

controller system which regulates the air/fuel ratio in the combustion chamber and dilutes the hot exhaust gases going to the tube bundle.

The air flow is piped into the test cell and, for all practical purposes, is the same as the air from any turbine engine compressor. It is essentially pulsation and oil free, and its moisture content is controlled. The air flow rate, pressure, and temperature are independently adjustable to any value within the operating envelope.

2. The Fuel Supply System

The fuel supply system is capable of pumping fluids ranging in properties from gasoline to No. 5 diesel at flow rates of over 0.063 lb/sec (1 gal./min) and pressures up to 7 MPa (1000 psi). For this program, the fuel was forced from drums to the fuel selection manifold system (see Figure 6) with pressurized inert gas. The manifold employs 12 solenoid valves (for 12 fuels). After the manifold, a high-pressure pump delivers fuel to the combustor. The plumbing from the pump to the combustor is stainless steel to facilitate cleaning when special fuels or fuel additives are used. A turbine flowmeter measures the flow rate of the fuel. On starting, a system of valves and bypasses is used to increase the flow rate to the desired level before introducing it to the combustion chamber. On shutdown, the lines can be drained and purged with an inert gas.

3. Exhaust System

A pneumatically-controlled valve is located downstream of the quench section to maintain the pressure in the combustor system. A silencer is used to attenuate the exhaust noise.

D. Data Acquisition System

The data acquisition system used a Hewlett-Packard 9820 programmable calculator with associated hardware. Figure 7 shows a flowchart of the system. A digital voltmeter is coupled to a 50-channel scanner which samples the voltage outputs from the various sensor systems and then feeds the corresponding digital values to the calculator. The calculator handles all of the data reduction and any necessary calculations, e.g., combustion efficiency, flow factor, and exhaust emissions coefficients. The resulting data are then processed in one of three ways:

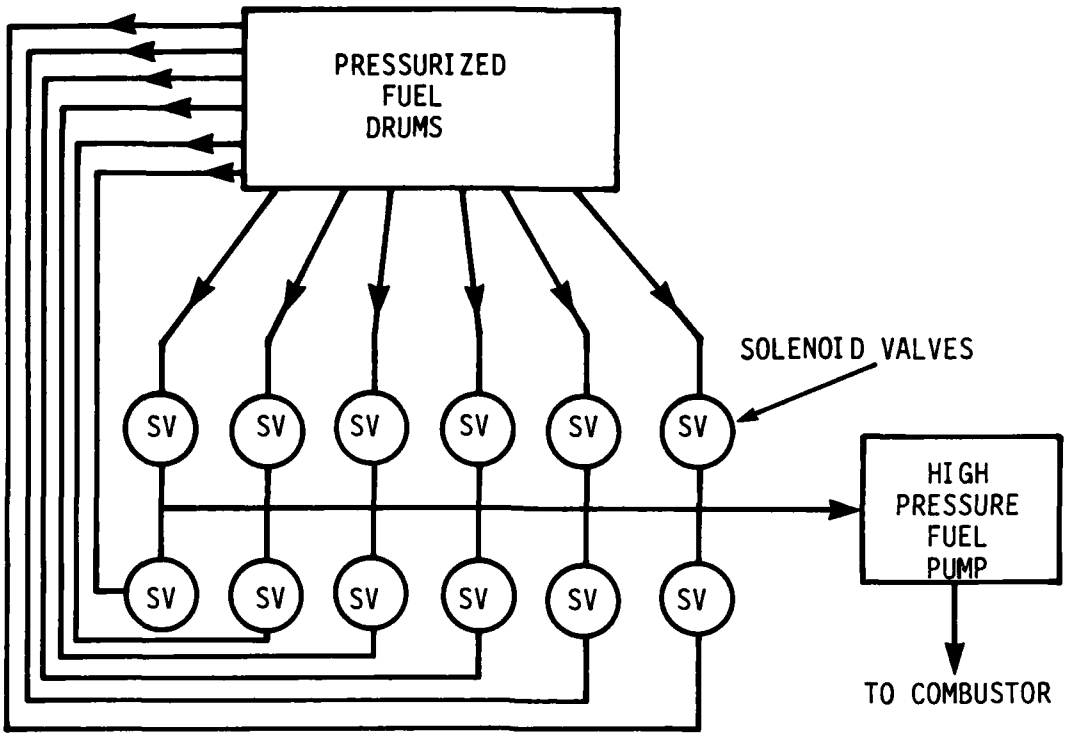

FIGURE 6. FUEL SELECTION MANIFOLDING SYSTEM

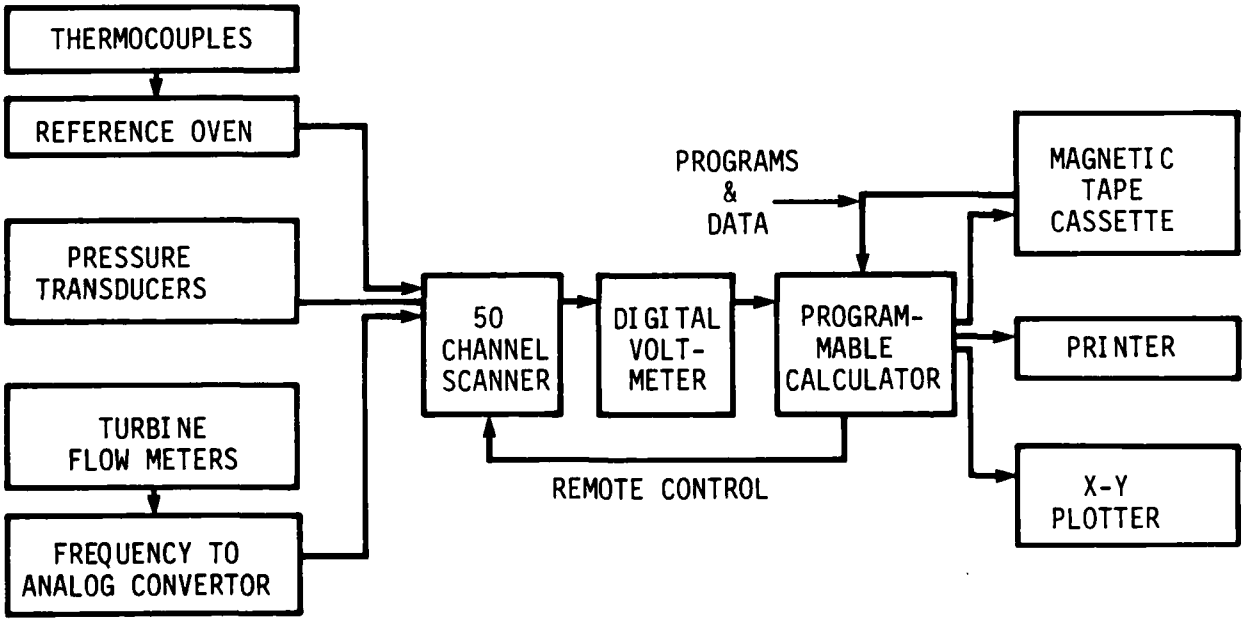

FIGURE 7. DATA ACQUISITION SYSTEM

1. The data can be stored on magnetic tape for further reduction at a later time;

2. The data can be output graphically on an X-Y plotter, or

3. The data can be output on a printer along with any appropriate alphanumeric titles or column headings.

Figure 8 shows an example of graphical output. Table 2 illustrates the use of the printer for the continuous monitoring of several channels of data, while Figure 9 is an example of a complete test report available immediately after the data were taken. The 50 channels can be scanned, the data reduced, and a report such as Figure 9 printed out in less than 2 minutes.

The sensing systems consist of strain-gauge pressure transducers, thermocouples, and turbine flowmeters. Regulator power supplies are used with the pressure transducers. A vacuum/pressure reference system is used to calibrate the transducers against a Wallace and Tiernan gauge; use of three-way valves allow this to be done during a test without disconnecting the transducers. The thermocouples are referenced to a 338.5K (150.0°F) oven; the unit will handle up to 50 thermocouples of any kind, including platinum.

E. Exhaust Analysis Instrumentation

Exhaust emissions are measured on-line using the following instruments in accordance with SAE-ARP 1256 with the exception of the NO/NO_x measurements. These measurements are performed by chemiluminescence.

Sample	Instrument	Sensitivity
Carbon Monoxide	Beckman Model 315B NDIR	50 ppm to 16%
Carbon Monoxide	Beckman Model 315B NDIR	330 ppm to 16%
Unburned Hydrocarbons	Beckman Model 402 FID Hydrocarbon Analyzer	0.5 ppm to 10%
Nitric Oxide	Thermo-Electron 10A Chemiluminescence Analyzer	3 ppm to 10,000 units
Total Oxides of Nitrogen	Thermal-Electron 10A Chemiluminescence Analyzer *with NO_x Converter*	3 ppm to 10,000 units
Oxygen	Beckman Fieldlab Oxygen Analyzer	0.1 ppm to 100%

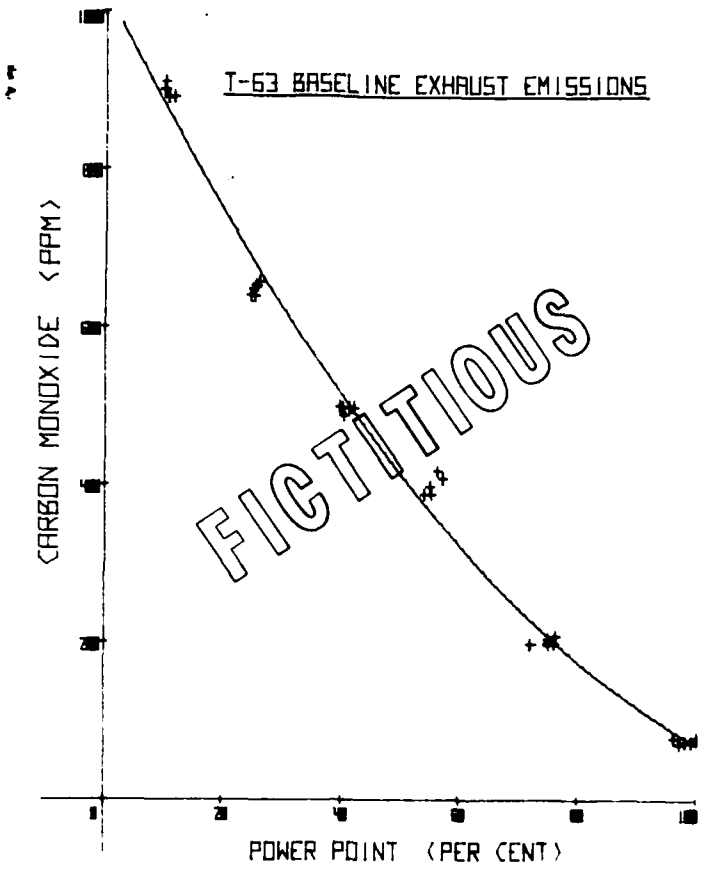

FIGURE 8. EXAMPLE OF GRAPHIC OUTPUT

TABLE 2. FUEL TEMPERATURE REQUIREMENTS TO REDUCE FUEL VISCOSITY TO THAT OF NDF AT 26.7°C (299.9K OR 80.0°F), OR 3.65 CST

	°C	°K	°F
Blend No. 1	38	311	100
Blend No. 2	50	323	122
HMGO	62	335	144
NDF + 5% Asphaltenes	32	305	89
NDF + 10% Asphaltenes	37	310	98

U. S. ARMY FUELS & LUBRICANTS RESEARCH LABORATORY
TURBINE COMBUSTOR FACILITY

***** EFFECTS OF HIGH AVAILABILITY FUELS ON COMBUSTION PERFORMANCE *****
U.S. NAVY AIR ENGINE CENTER

DATE: 10/ 3/84 TIME: 9: 0
COMBUSTOR SYSTEM: T-63 POWER POINT: 100%
FUEL NO. 10
FLAME RADIATION 14.66BTU/SQFT 166.5KW/SQM

***** EXPERIMENTAL TEST CONDITIONS *****

	AVERAGE	STD.DEV.	DESIRED	LAST SCAN
INLET AIR PRESSURE, PSIA	68.25	.17	53.60	68.10
INLET AIR TEMPERATURE, DEG F	526.02	2.54	430.00	522.82
AIR FLOW RATE, LBS/SEC	2.448	.013	2.060	2.455
FUEL FLOW RATE, LBS/MIN	2.872	.009	1.790	2.866
FUEL/AIR RATIO	.01956	.00012	.01450	.01945
AIR FLOW LOADING FACTOR	1.1263	.0061	1.1470	1.1302

FUEL PRESSURE= 285
FUEL TEMPERATURE= 77.1 DEG F

* BURNER OUTLET TEMPERATURE SURVEY *

BOT AVG=1361.2 DEG F
BOT HOT SPOT: TC# 2 = 1644 DEG F
BOT PATTERN FACTOR = .3382

	TC#	AVERAGE	STD DEV
OUTER ANNULUS	1	488	31
	4	1519	16
	7	853	61
	10	1299	50
	13	743	44
CENTER ANNULUS	2	1644	31
	5	451	62
	8	1090	20
	11	737	50
	14	1513	12
INNER ANNULUS	3	516	15
	6	1088	7
	9	1337	122
	12	741	39
	15	1399	10

* EXHAUST CHEMISTRY *

CO.. .049 % CO2..5.69 % O2..13.8 % UBH.. 96.6 PPM <CARBON>
NO.. 96.0 PPM NOX.. 99.0 PPM NO2.. 3.0 PPM <NOX-NO>
CO.EI. 23.9G/KG UBH.EI. 7.4G/KGF NOX.EI. 7.6G/KGF
SMOKE NUMBER.

COMBUSTION EFFICIENCY, CALCULATED FROM EXHAUST CHEMISTRY. 99.4023 %
FUEL/AIR RATIO, CALCULATED FROM EXHAUST CHEMISTRY. .026075
REMARKS.

FIGURE 9. EXAMPLE OF A TEST REPORT

The exhaust sample is routed to the instruments through a 177°C (350°F) heated Teflon® line and then appropriately distributed.

F. Smoke Analysis System

The system used for measuring exhaust smoke level is in accordance with the requirements of SAE-ARP 1179. Basically, a sample of the exhaust is passed through a strip of filter paper. Particulates from the exhaust are trapped on the surface, leaving a spot ranging in "grayness" from white to black, depending on the sample size and particulate content of the exhaust. The "grayness" of the spot is evaluated with a reflectometer. The smoke number, SN, of each spot is then calculated by:

$$SN = 100\ (1 - R_S/R_W)$$

where R_S and R_W are the diffuse reflectance of the sample spot and the clean filter paper. Exhaust samples are taken over a range of sample sizes around W/A = 0.023 pound of sample per square inch of filter area. Note, W is the weight of the soot sample in pounds, and A is the area of the filter paper in square inches. The resulting smoke numbers are plotted against log (W/A). These are least-squares fitted with a straight line; the interpolated value of SN at W/A = 0.023 is the reported smoke number for the engine operation condition.

Champagne (6) gives a complete description of the procedure and relates the results to particulate concentration and exhaust plume visibility. Troth, et al., (7) provide a numerical relationship for that correlation:

$$d_S = a_1 \exp(a_2\ SN)(1-\exp(-a_3\ SN)) + a_4 \exp(-a_5\ (SN-a_6)$$

where:
- d_S = true smoke density, mg/m^3
- SN = EPA Smoke Number
- a_1 = 0.8
- a_2 = 0.057565
- a_3 = 0.1335
- a_4 = 0.0942
- a_5 = 0.005
- a_6 = 27.5

G. Flame Radiation Measurement

Flame radiation measurements in the T63 combustor are made with a sensor fabricated by Hy-Cal Engineering. The measurements are broad-band, extending out to 6.5 microns in the infrared. As shown in Figure 1, the sensor is mounted on the combustor wall and has a 150° viewing angle; it is, therefore, insensitive to changes in flame structure.

H. Liner Temperature

Seven thermocouples were attached to the outside surface of the combustor can to measure the liner temperature. In reference to Figure 1, the thermocouples were placed, one on the dome (D), two on the primary zone (PZ), two on the secondary zone (SZ), one on the quench zone (QZ), and one on the exhaust side (ES).

I. Droplet Size Measurement

Ignition tests with the T63 combustor have highlighted the critical importance of atomization characteristics on the ignition process. Degraded atomization caused by increased fuel viscosity due to more viscous fuels or lower fuel temperatures leads to higher fuel/air ratio requirements for ignition, and finally at viscosities in excess of 10 cSt combined with low air temperatures, a failure to ignite at any fuel/air ratio. These ignition problems occur with degraded atomization because of the decreased fuel surface area available for evaporation and the increased spark energy required for droplet evaporation.

In order to better understand the T63 ignition tests, atomization quality, as measured by drop-size distribution and cone angle, were measured for seven different fuels including Navy Distillate Fuel (NDF) specification MIL-F-16884H, five distillate fuels too viscous or contaminated to meet the NDF specification, and Jet A (very similar to JP-5) as a reference to aircraft-type fuels. These fuels are described in detail in Table 4 (in the "Test Fuels" section) as Fuel Nos. 1, 2, 3, 4, 5, 8, and 9, and the viscosity characteristics are shown in Figure 10. (Figure 10 uses viscosity scales, i.e., log-log viscosity versus log temperature, to linearize the relationship.) Detailed atomization tests were also performed for fuel nozzles from three types of gas turbines in the Navy fleet -DDA 501-K17, GE LM2500, and AVCO TF40B - as discussed in Appendix A. These three atomizers

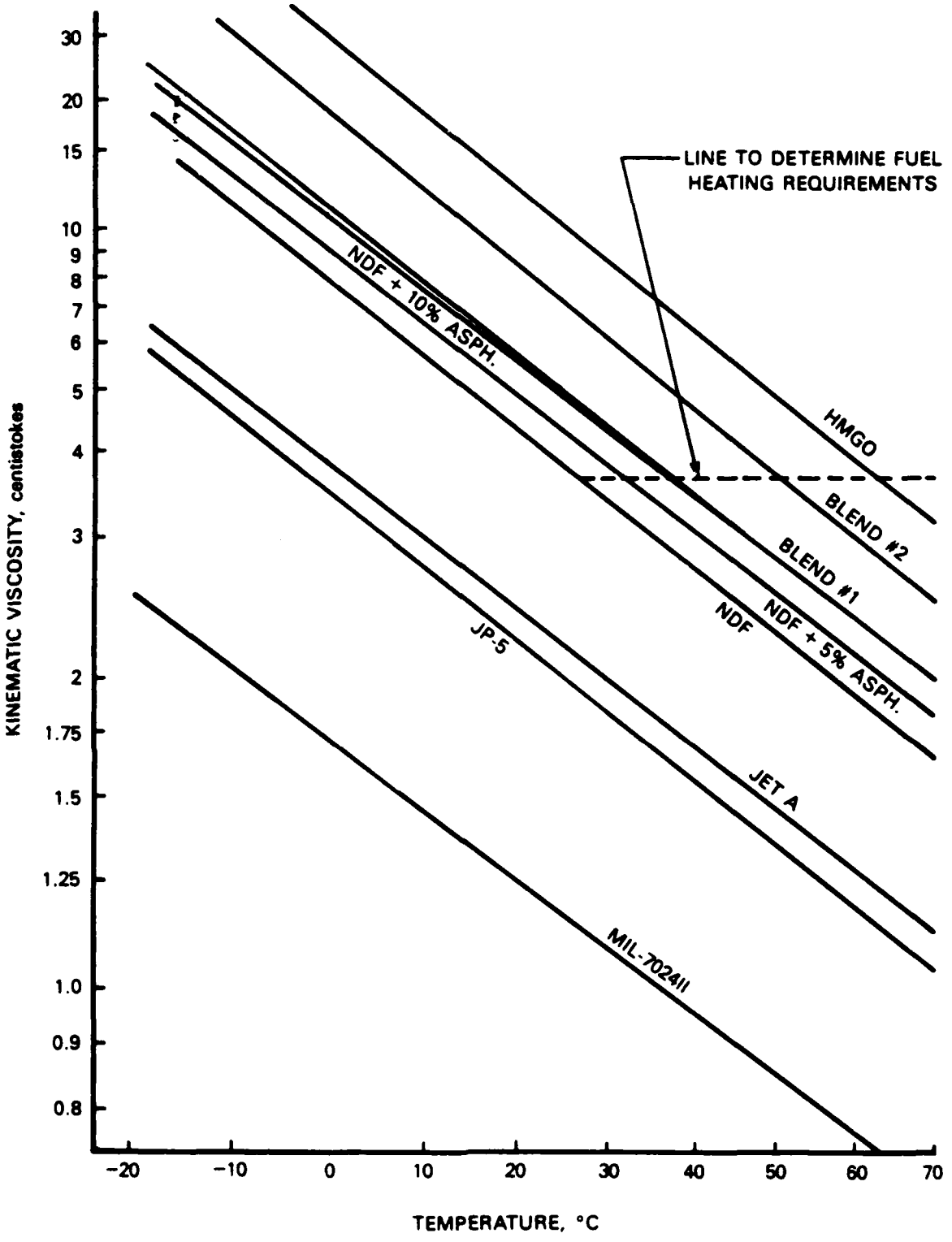

FIGURE 10. EFFECT OF FUEL TEMPERATURE ON KINEMATIC VISCOSITY

and the T63 were tested at fuel flow rates for ignition, idle, and an intermediate power condition. The T63 atomization tests were performed at atmospheric conditions with the fuel at 296K ± 1K (73°F ± 1°F) except for the NDF which was at 291K (65°F). In support of low-temperature ignition tests, T63 atomization tests at ignition conditions were also performed with the fuels cooled to 271K ± 1K (28°F ± 2°F). For the three atomizers other than the T63, atomization tests were performed with all fuels at 300K (80°F), and then limited tests were performed with all fuels more viscous than NDF heated to a temperature sufficient to reduce their viscosity to that of NDF at 300K (80°F). The purpose of heating the fuels was to determine if the atomization quality of NDF could be achieved by heating the fuels. The fuel temperatures required are shown in Table 2 and Figure 10.

As discussed in the Results and Discussion section, the T63 atomization tests resulted in a good overall evaluation of the effect of fuel property variations on spray formation. They also indicated that the fuel effects varied markedly, depending upon the flow rate through the nozzle and whether the majority of the flow was through the primary nozzle, used for ignition, or the secondary, used at higher power conditions. Even limiting the analysis to the primary nozzle used for the ignition studies, the fuel effects (principally viscosity) were found to be very significant at low fuel flow rates and less significant at higher fuel flow rates. This variation is ignored in published correlations used to predict minimum ignition energies. The atomization data obtained for this program were limited to two different flow rates for ignition and were insufficient by themselves to predict atomization performance over the range of flow rates used in ignition tests at SwRI. However, based on the flow rate sensitivity observed in this program, more extensive measurements over a range of flowrates spanning the ignition condition were performed on the same T63 atomizer using some of the same fuels for a contract for the Naval Air Propulsion Center (NAPC) (Contract No. N00140-80-C-2269). These results were used to correlate the ignition studies for this program. The liquids used for the NAPC study were JP-4, JP-5, NDF, HMGO, HMGO cooled to 274K (1°F), and water. The NDF and HMGO are the same fuels as used in this program and reported in Table 4. Water was used to examine the effects of surface tension, independent of viscosity. The test fluids, test temperature and viscosity, surface tension, and density at the test temperature are given in Table 3.

TABLE 3. TEST FLUIDS USED IN T63 ATOMIZATION STUDY TO GENERATE THE CORRELATION FOR SAUTER MEAN DIAMETER (SMD) FOR IGNITION STUDIES

Fluid	Test Temperature, K	Kinematic Viscosity at Test Temp, cSt	Surface Tension at Test Temp, dynes/cm	Density of Test Temp, g/mL
JP-4	298.8	0.85	23.89	0.7458
JP-5	298.8	1.16	26.62	0.8012
NDF	299.4	3.77	28.39	0.8410
HMGO	298.8	9.80	31.14	0.8683
HMGO (Gold)	273.8	28.0	33.45	0.8869
Water	301.0	0.84	71.58	0.9966

Drop-size data were obtained with a Malvern Model 2200 Particle Sizer based on the diffraction angle produced by drops when illuminated by a beam of monochromatic, coherent, collimated light from a HeNe laser. A 300-mm focal length f/7.3 lens was used to collect the scattered light. The laser beam diameter was 9 mm with a Gaussian intensity distribution truncated at the edge by the 9-mm aperture. Data were recorded at an axial distance of 38.1 mm (1.5 in.) downstream of the nozzle tip, through various chords in 5 or 10 mm radial steps from the top to the bottom edge of the spray. The effective cone angle at the measurement location was also determined by measuring the attenuation of the laser beam, indicative of the concentration of drops in the beam.

Two procedures were necessary to ensure the proper calibration of the particle sizing instrument. The drop size distribution is computed from the relative scattered light intensity measured at different scattering angles by a set of 30 annular ring photodiodes. For an ideal optical and electronic system and uniform responsivity between photodiodes, the signal intensity may be used to compute the drop-size distribution without resorting to external calibration standards. Tests at this laboratory have shown that the nonidealities of the system are negligible except for the detector responsivities which must be determined for each instrument in order to get accurate results. The calibration procedure is described by Dodge.(8) This was the first procedure performed to assure proper calibration of the system.

The second procedure was necessary to correct for the very dense (optically) fuel sprays obtained at the higher fuel flow rates. In the standard configuration, the instrument monitors the unscattered laser beam intensity with a photodiode mounted on the centerline of the optical system. The instrument instruction manual indicates that if the scattered light intensity exceeds the unscattered light intensity, there are a significant number of photons being scattered by more than one drop. Since the theory relating scattered light intensity to drop-size assumes diffraction by a single drop, these multiply-scattered photons will result in errors in the computed size distribution. In order to evaluate the problem and develop correction procedures, experiments have been conducted at this laboratory (9) and others (10). This second procedure (10) was used to correct the data recorded in dense sprays for this program.

All tests were performed at atmospheric conditions in a test chamber of square cross-section 30 cm on a side and 76 cm long, with air pulled through the chamber at a velocity of about 2.1 m/s by an explosion-proof exhaust fan. A set of twisted metal screens in the exhaust duct removed the fuel mist from the air before exhausting to the atmosphere.

Fuel pressures were measured with a Wallace and Tiernan Penwalt Model 61B-1A-0150, 150 psia pressure gauge and a Helicord Model 2290-0, 500 psig gauge. Flow rates were measured volumetrically using a graduated cylinder. Because the T63 atomizer uses a flow divider valve internal to the nozzle body which determines the fuel flow split between the primary and secondary spray nozzles, the individual flow rates to each nozzle are not easily measurable. For that reason, and the fact that the flow divider valve responds to pressure rather than mass or volume flow rate, these tests for the T63 atomizer were performed at constant differential pressure drop (psid) for a given condition and the flow rates were then measured for each fuel.

The matrix of test conditions used for the T63 atomizer was as follows:

	Ignition (low flow)	Ignition (high flow)	Idle	Intermediate Power
ΔP, kPa	296.0	827.0	1310.0	1862.0
psid	43.0	120.0	190.0	270.0
Nominal Fuel Flow, NDF				
mL/min	187.0	360.0	657.0	1280.0
lbm/hr	21.0	40.4	73.7	143.6

All spray data were reduced assuming a Rosin-Rammler drop-size distribution, which is specified by two parameters X and N, defined by,

$$R = \exp(-((D/X)^N))$$

where R is the cumulative volume (or mass) fraction of the spray contained in drops whose diameters are larger than D. Thus X is a size parameter, in micrometers, and N indicates the width of the distribution. Large values of N imply narrow distributions and vice versa. Fuel sprays are usually characterized by an "average" size based on the volume-area mean diameter (D_{32}), more commonly called the Sauter Mean Diameter (SMD), defined by,(11)

$$SMD = D_{32} \quad \frac{\Sigma_i D_i^3 N_i}{\Sigma_i D_i^2 N_i}$$

where D_i is the drop diameter and N_i is the population of drops in the size class D_i. The SMD is a mean diameter which represents a fictitious uniform spray composed of drops of uniform size having the same total drop surface and volume as the actual spray. The SMD is computed from the Rosin-Rammler parameters by,(11)

$$SMD = X/\Gamma(1-1/N)$$

where Γ is the gamma function.

J. Combustion Efficiency

Combustion efficiencies (ϵ) were calculated from the exhaust gas analysis according to the relationship developed by Hardin.(12)

$$\epsilon = 1 - \left[\frac{A\ f(UBH) - 121{,}745\ f(CO) - 38{,}880\ f(NO) - 14{,}654\ f(NO_2)}{A\ f(CO_2) + f(CO) + f(UBH)}\right] 100\%$$

where f(i) is the concentration of "i" in the exhaust, A is a constant based on the heat of combustion and hydrogen/carbon ratio of the fuel, and UBH is unburned hydrocarbons.

K. Cold Start Ignition

In order to perform cold start ignition tests in the T63 combustor rig, a capability to cool the burner inlet air supply had to be incorporated into the air supply system. Combustor inlet air is cooled by injecting liquid nitrogen and oxygen gas through a manifold placed upstream of the combustor. A rotometer is used to measure the oxygen flow rate, and the oxygen concentration is measured at the combustor exhaust by a Beckman Fieldlab oxygen analyzer. Note that fuel is not injected during this measurement. To set a particular flow condition, the oxygen flow is increased until the oxygen concentration is the same as that of air (approximately 21 percent). The net mass flow rate of combustor inlet air is then determined by adding the compressor air flow, measured by the turbine flow meter, the oxygen flow, measured by the rotometer, and the liquid nitrogen flow, calculated in terms of the oxygen flow.

The liquid nitrogen cooling system is capable of lowering the burner inlet air supply to -30°F (-34°C) for the mass flow rates (0.2 to 0.6 lb/min) used in the ignition tests.

Ignition tests are carried out by first establishing the desired air flow conditions of temperature, pressure, and mass flow rate. Then the spark ignitor is activated, producing sparks at the rate of 8 per second, with energies of approximately 0.8 joules. Fuel flow is then initiated and gradually increased until ignition occurs. At the point of ignition, the fuel and air flow conditions are noted and the fuel is turned off to extinguish the fire.

L. Deposit Formation

In this program, deposit formation in the T63 combustor was given special emphasis because of the nature of the fuel contamination. The heavy components, asphalts, and slurry oil with catalytic fines, which were blended with Jet A, NDF, and HMGO were

very high boiling materials known to form high carbon residues in ASTM Test D 524. In fact, one of the main objectives in planning the combustion performance test procedure was to evaluate the fuels for deposit-forming tendencies. Normally, the combustion performance measurements can be made in less than 15 minutes at each operating condition. To evaluate deposits, the test duration was extended to 30 minutes at each operating condition. The full power condition was tested first; this was followed by the 75 percent, 10 percent, and 55 percent of the full power condition in that order. After this test sequence was completed for a fuel, the combustor was disassembled and examined for deposit formation. Photographs of the dome and primary zone sidewall of the combustor were taken as a record of deposit. The combustor can was weighed before and after each test to determine the amount of deposit formed by a test fuel over a known period of time. Samples of the deposits were retained for analysis of their chemical composition.

M. Test Fuels

There were two basic objectives in choosing the test fuels. The first objective was to compare the combustion performance of U.S. Navy type DFM fuels with typical gas turbine aviation fuels such as Jet A and JP-5. Two base fuels, Navy distillate (NDF) and heavy marine gas oil (HMGO), were used to prepare the test fuel blends. The second objective was to determine the possible degradation in combustion performance that might arise from DFM contamination by high boiling asphaltic materials such as No. 6 fuel oil. Sometimes fuel tanks contain significant quantities of No. 6 fuel oil and the like prior to being filled with DFM. This form of contamination can amount to the presence of as much as 10 percent of a high boiling asphalt type material.

According to Marcusson (13), the components of asphalt are the asphaltic acids and their anhydrides, oily constituents, resins, and asphaltenes. The components of main concern are the polar materials, resins, and asphaltenes; they are believed to be most deleterious to combustion performance because of their greater tendency to form deposits in fuel systems and combustion chamber surfaces. Asphaltenes precipitate when a large excess of petroleum ether or pentane is added to the asphalt. Asphaltenes are thus regarded as pentane insolubles. When asphaltenes are subjected to a relatively polar solvent such as toluene, a good share of the material dissolves. The fraction that does not dissolve is known as a resin. This variety of resin is known as a toluene insoluble.

Not all resins are insoluble; asphalts also contain a class of lower molecular weight resins that are less polar than asphaltenes and appear to be less deleterious to gas turbine combustion performance. These resins are found in the oily constituent after the asphaltenes have been precipitated with pentane. The oily constituents and resins are separated by absorption on fuller's earth. The oily constituents are extracted from the fuller's earth with petroleum naphtha, and the resins are then removed by extraction with toluene. These less polar resins from herein will be defined as toluene-soluble resin.

The test fuel matrix defined in Table 4 consists of 26 fuel blends based on Jet A, Navy distillate (NDF) and heavy marine gas oil (HMGO), which contain different levels of contaminants, R_1, R_2, R_3, and R_4. The Jet A is a low aromatic kerosene, which is used mainly as a reference fuel in this work. NDF is a diesel fuel marine type middle distillate supplied by the Navy. HMGO is a heavier diesel fuel marine consisting of 50 percent NDF and 50 percent telura oil. The essential physical and chemical properties of these base fuel stocks and contaminants are given in Table 5.

R is an asphalt material that is relatively rich in asphaltenes (pentane insolubles) and low in toluene insolubles. It was derived from an extraction process at Kerr McGee Refinery, Wyunewood, OK. According to Streiter's (13) method of asphalt analysis, R_1 contains 7.75 percent asphaltenes, 78.10 percent oily constituents, 14.15 percent toluene soluble resins, and a negligible concentration of toluene-insoluble resins (see Table 5).

R_2 was blended by adding a toluene-insoluble coke-like material to R_1. This material was a delayed petroleum coke that was insoluble in fuel. The material had to be ground to a find powder with a particle size of less than 1 micron. A mixture of R_1 containing 2-percent delayed coke was ground in a ball mill attriter. During the course of the grinding process, the particle size distribution of the coke was measured by a HIAC/ROYCO Model Pc-320 particle size analyzer. The grinding was complete when the average particle size was less than 1 micron. Particle settling rates were measured by allowing the R_2 blend to stand in a graduated cylinder. After standing, samples were pipetted out from different depths in the cylinder. The samples were analyzed for toluene insolubles. A significant gradiant in the concentration of toluene insolubles was apparent after a few hours of standing. It was clear from these measurements that the R_2 blend had to be stirred prior to and during a combustor test.

TABLE 4. BLENDING FRACTIONS AND PHYSICAL AND CHEMICAL PROPERTIES OF TEST FUELS

Fuel No.	Fuel Type	Distillate (Percent)			Residual Blends (Percent)				Hydrogen, Percent	H/C Atom Ratio	Properties Net Heat of Combustion, Btu/lb	Specific Gravity	Kinematic Viscosity @ 40°C, cSt	Kinematic Viscosity @ 20°C, cSt	Kinematic Viscosity @ 0°C, cSt	Surface Tension @ 23°C, dynes/cm	T 10% off Temp, °C D 2887 Method	Pentane Insolubles, wt%	Toluene Insolubles, wt%	Ash, wt%
		Jet A	NDF	HMGO	R1	R2	R3	R4												
	Distillates																			
1	Jet A	100							14.2	1.964	18,753	0.8049	1.71	2.46	3.83	25.2	202			0.0
2	NDF		100						12.89	1.763	18,349	0.8484	2.75	4.32	7.90	28.67	208			0.0
3	Blend 1		70	30					12.85	1.757	18,327	0.8565	3.42	5.69	11.00	29.15	213			0.0
4	Blend 2		30	70					12.80	1.749	18,298	0.8670	4.76	8.42	18.50	29.52	221			0.0
5	HMGO			100					12.77	1.744	18,226	0.8756	6.25	12.03	28.52	31.40				0.0
	Residual Blends																			
6		98			2				13.92	1.913	18,745	0.8069								
7	High Asphaltenes		98		2				12.88	1.762	18,342	0.8496								
8	Low resins		95		5				12.86	1.758	18,331	0.8513	3.09	4.82	9.01	28.67	206	0.32	0.01	
9			90		10				12.83	1.754	18,314	0.8543	3.46		10.53	28.41	206	0.68	0.02	0.001
10				98	2				12.76	1.743	18,271	0.8719								
11				95	5				12.75	1.741	18,263	0.8724						0.29	0.01	
12				90	10				12.72	1.737	18,249	0.8748						0.63	0.02	0.001
13			98			2			12.87	1.760	18,342	0.8496						0.12	0.01	
14	High Asphaltenes		95			5			12.85	1.757	18,331	0.8519	3.08	5.57	9.04	28.36	206	0.31	0.03	
15	High Resins		90			10			12.81	1.751	18,314	0.8544	3.50		10.47	28.49	206	0.66	0.04	0.001
16				98		2			12.76	1.743	18,271	0.8719						0.16	0.07	
17				95		5			12.74	1.740	18,263	0.8730						0.46	0.17	
18				90		10			12.71	1.735	18,249	0.8749						0.97	0.38	0.001
19			98				2		12.87	1.760	18,341	0.8496								0.01
20	High Asphaltenes		95				5		12.86	1.758	18,331	0.8513						0.35	0.03	0.025
21	High Ash		90				10		12.83	1.754	18,313	0.8546						0.73	0.04	0.051
22				98			2		12.76	1.743	18,270	0.8720								0.01
23				95			5		12.74	1.740	18,261	0.8732						0.31	0.03	0.025
24				90			10		12.72	1.736	18,248	0.8751						0.67	0.06	0.051
25	Cat. Cracked		90					10	12.69	1.732	18,237	0.8623						0.16	0.01	
26	with fines			90				10	12.45	1.694	18,097	0.8967						0.22	0.02	

TABLE 5. PROPERTIES OF BASE FUELS AND BLENDING STOCKS

	Fuel Type							
	Jet A	NDF	Telura Oil	HMGO	R_1	R_2	R_3	R_4
Heat of Combustion Net (J/g)	43,575	42,680	42,345	42,389	41,908	41,697	41,842	40,559
Carbon, wt%	85.78	86.12	86.47	86.31	86.28	86.50	86.20	86.30
Hydrogen, wt%	14.20	12.89	12.67	12.77	12.33	12.18	12.26	11.20
Sulfur, wt%	—	0.20	—	—	0.76	0.75	0.75	1.96
Aromatics by UV, wt%								
Single Ring	4.60	5.80	6.82	6.32	5.93	5.82	5.92	—
Double Ring	1.30	7.17	4.24	5.67	4.43	4.34	4.44	—
Triple Ring	0.02	1.56	1.43	1.49	3.10	2.98	3.20	—
Total	5.92	14.53	12.49	13.48	13.46	13.14	13.58	—
Aromatics by FIA, vol%								
Aromatics	7.94	26.3	—	—	—	—	—	—
Olefins	1.44	1.80	—	—	—	—	—	—
Saturates	90.61	71.90	—	—	—	—	—	—
Viscosity at 313K, cSt	1.68	2.75	13.17	6.25	75.36	—	—	49
Specific Gravity	0.801	0.8484	0.8939	0.8756	0.9071	0.9092	0.9103	1.060
Ash, wt%	*0.00*	*0.00*	*0.00*	*0.01*	*0.06*	*0.06*	*0.57*	*0.03*
Carbon Residue, wt%	0.00	0.16	0.31	0.09	9.22	—	—	—
Pour Point, °C	—	-30	-21	-30	-26	-26	-26	-13
Distillation by D 2887, °C								
IBP	182	94	159	118	—	—	—	—
10%	202	208	285	232	—	—	—	—
50%	221	273	374	334	—	—	—	—
90%	243	346	453	428	—	—	—	—
FBP	299	440	561	521	—	—	—	—
Metals, ppm								
Vanadium	—	1	5	3	98	98	98	5
Sodium	—	1	1	1	43	43	43	1
Nickel	—	1	1	1	46	46	46	3
Silicon	—	5	10	7	50	50	1200	23
Aluminum	—	1	5	2	10	10	450	46
Iron	—	1	1	1	15	15	1150	6
Pentane Insolubles, wt%	—	0.01	0.01	0.01	7.93	—	—	1.3
Toluene Insolubles, wt%	—	0.001	0.01	0.01	0.12	—	—	0.1

R_3 was blended to emphasize fuels with high ash content and possible contamination with dirt. It was prepared by adding 1.65 grams of ferric oxide (Fe_2O_3), 2.5 grams of silicon dioxide (SiO_2), and 0.85 grams of aluminum oxide (Al_2O_3) per kilogram of R_1. These metal oxides were in the form of fine powders of approximately 1 micron particle size. Because of particle settling, R_3 was also well stirred prior to blending with NDF and HMGO. Also, when the NDF/R_3 and HMGO/R_3 blends were tested in the combustor, they were thoroughly mixed before the test and continuously stirred during the test.

R_4 is a low viscosity No. 6 oil contaminated with catalyst fines. It is the "Bottoms" from a catalytic cracker fractionator.

III. RESULTS AND DISCUSSION

A. Cold Start Ignition

Sea-level cold-start ignition measurements were made at several operating conditions in a T63 combustor rig. As shown in Table 6, the ignition measurements were carried out at essentially atmospheric pressure whereas the burnler inlet temperature was varied from ambient down to about -34°C. The mass flow rate of air was varied to change the reference velocity in the combustor.

Table 6. Operating Conditions for Ignition

Pressure, kPa:	103 to 124
Burnler Inlet Temperature, °C:	25, 10, 0, -24, -34
Fuel Temperature, °C:	0 to 30
Mass Flow Rate, Kg/sec:	0.09, 0.18, 0.27
Reference Velocity, m/sec:	5, 10, 15

Fuel temperature was varied in order to examine the effect of fuel viscosity on ignition. About 30 percent of the ignition tests, however, were performed at fuel temperatures of approximately 80°F (27°C). This is the temperature to which the fuels used in Navy ships are heated prior to being admitted to the engine.

Ignition tests were performed on Fuel Nos. 1 through 5, 8, 9, 14, and 15 described in Table 4. Fuel No. 1 (Jet A) was used as a reference fuel and for adjusting combustor conditions. Combining the nine test fuels with the conditions given in Table 5 gave a total of 135 run conditions examined. Each run condition was carried out in triplicate, giving a total of 405 data points.

The ignitability of the test fuels was measured in terms of the fuel/air ratio required to achieve ignition at a given set of operating conditions, i.e., fuel temperature (T_f) burner inlet temperature (BIT) and reference velocity (Vref). Figures 11 and 12 show the effect of the burner inlet temperature on the fuel/air ratio required to ignite the test fuels. Note that these experiments were done at constant fuel temperature and that test Fuel Nos. 14 and 15 are not displayed because their ignition properties were essentially the same as test fuel Nos. 8 and 9, respectively. Figures 11 and 12 show that the fuel/air ratio for ignition is very weakly dependent on the burner inlet temperture. It is apparent that ignition is much more dependent on the fuel properties than the burner inlet temperature. Comparing Figures 11 and 12 shows that increasing the reference velocity in the combustor reduces the fuel/air ratio required for ignition. The reference velocities in Figures 11 and 12 are 5 and 10 m/sec, respectively. When the reference velocity is increased, the mass flow rates of fuel and air are increased. As the mass flow rate of fuel passing through the atomizer is increased, the fuel atomization is substantially improved, and ignition occurs with greater ease at a lower fuel/air ratio. Atomization is also significantly improved when the viscosity of the fuel is decreased. The ignitability of the test fuels appears to follow this trend. Figure 13 shows that the fuel/air ratio for ignition correlates strongly with the fuel viscosity. Figure 14 shows the results of ignition test on Fuel Nos. 1 through 5; the fuels were all tested at approximately the same fuel temperature (275K) and reference velocity. However, in one case the burner inlet temperature was 262K and in the other it was 251K. The results reaffirm that fuel viscosity plays a much more important role in ignition than burner inlet temperature.

It can be concluded that heavier fuels such as HMGO have ignition characteristics similar to aviation fuels. Similar to middle distillates such as JP-5, the ignitability of heavier distillates depends on their viscosity. Even the blending of asphalts with NDF had nothing more than a viscosity effect on the ignition.

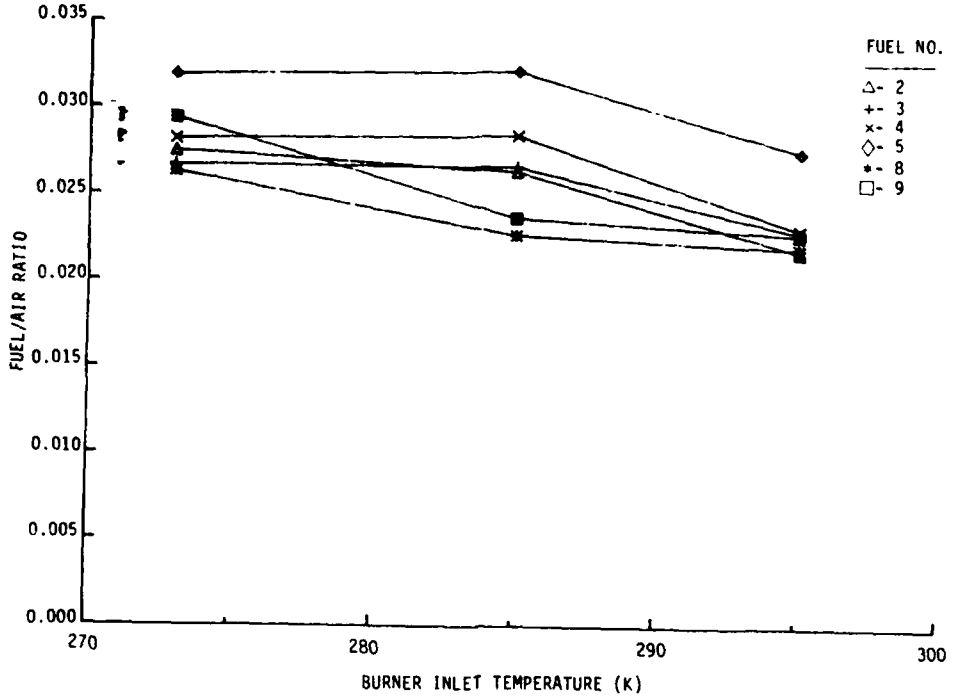

FIGURE 11. EFFECT OF BURNER INLET TEMPERATURE ON THE FUEL/AIR RATIO REQUIRED FOR IGNITION
(T_f = 300K, BIP = 113 kPa, Vref = 5.0 m/sec)

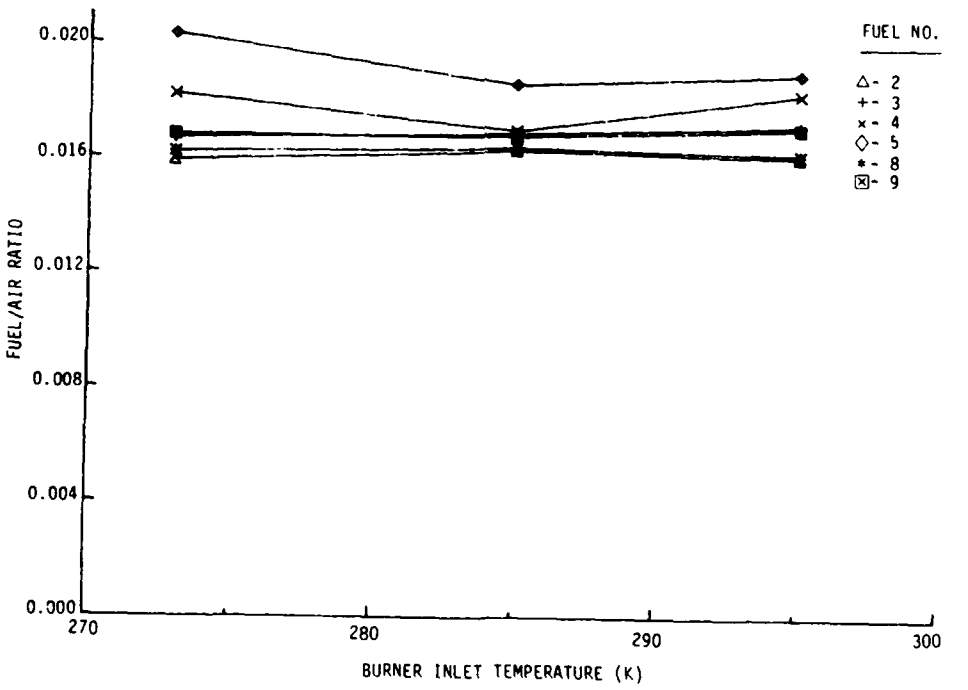

FIGURE 12. EFFECT OF BURNER INLET TEMPERATURE ON THE FUEL/AIR RATIO REQUIRED FOR IGNITION
(T_f = 300K, BIP = 118 kPa, Vref = 10.4 m/sec)

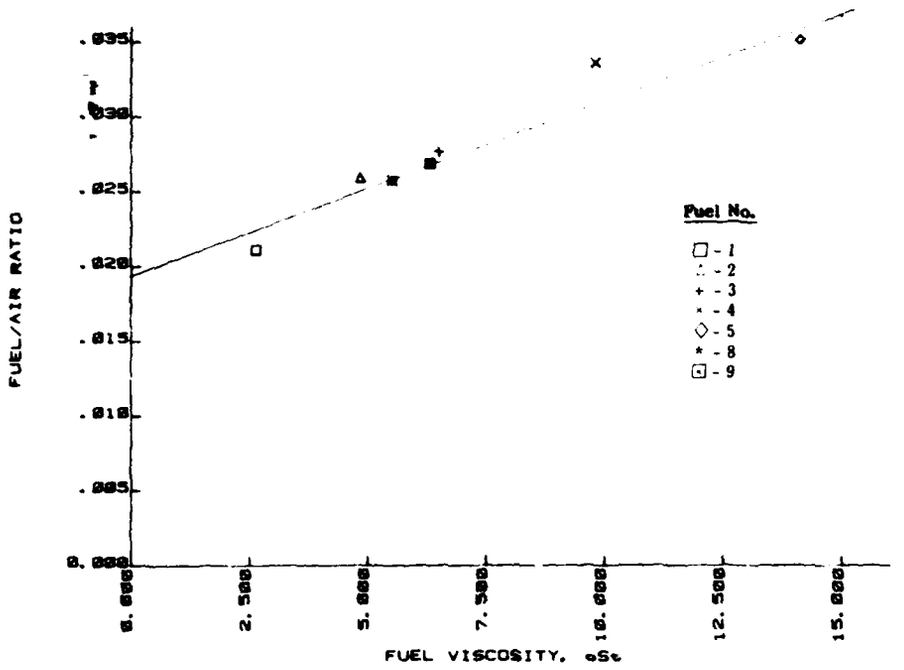

FIGURE 13. EFFECT OF FUEL VISCOSITY ON THE FUEL/AIR RATIO REQUIRED FOR IGNITION
(Ignitions were made at BIT = 284K, T_f = 288K, and Vref = 5 m/sec)

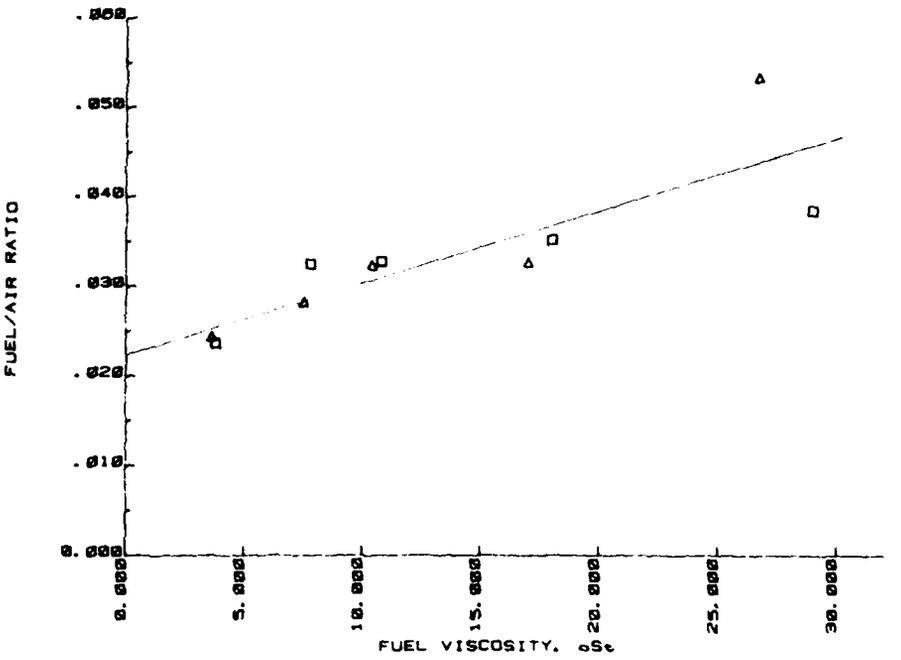

FIGURE 14. EFFECT OF FUEL VISCOSITY ON THE FUEL/AIR RATIO REQUIRED FOR IGNITION AT DIFFERENT BURNER INLET TEMPERATURES
(Fuel Nos. 1-5 Plotted at: □-BIT = 262K, T_f = 274K; Δ-BIT = 251K, T_f = 276K; Vref = 5 m/sec)

When fuel temperatures are greater than 300K (80°F), the viscosity of the heaviest fuel, HMGO does not exceed 10 cSt. Because of the relatively small effect of burner inlet temperature on ignition, the test fuels are expected to ignite without fail at BITs down to 239K (approximately -30°F) if the fuel temperature is in the range of 80° to 90°F which is used onboard ship. In actual tests with the T63 combustor, ignition was achieved with Fuel Nos. 1 and 2 at a BIT of 238K (-31°F) and a fuel temperature of 267K (22°F); the viscosity of Fuel No. 2, NDF, at this temperature is 10 cSt. Fuel Nos. 3, 4, and 5 with viscosities of 14, 25, and 41 cSt at 267K would not ignite. Therefore, a viscosity of 10 cSt seems to be an acceptable limit for ignition at a BIT of 238K.

Characteristic Time Model--The ignition data were analyzed using the characteristic time model for ignition developed by Peters and Mellor.(14,15) The criteria for ignition in the model is that the energy of the spark must heat an initial volume such that the heat release rate within the volume is greater than the loss rate. The method of analyzing the ignition event is to express the heat generation and loss rates in terms of times which are characteristic of the controlling processes.(16,17) Since fuel must evaporate to burn, heat generation is limited first by droplet vaporization and then the chemical reaction rate; the heat loss in a gas turbine spark gap environment is controlled by turbulent mixing as opposed to conduction or radiation. It follows that an ignition limit is reached when τ_{sl}, turbulent mixing time (heat loss), equals the sum of τ_{hc}, the chemical time, and τ_{eb}, the droplet evaporation time (heat generation). The basic equation defining the ignition limit becomes

$$\tau_{sl} \sim \tau_{hc} + a\, \tau_{eb} \tag{1}$$

where the proportionality $\sim$ and the constant weighting factor a are required because the characteristic times are not absolute and can only be calculated as relative values.

A detailed analysis of each time in Equation 1 is available (18); a brief description is given here.

$$\tau_{eb} = d^2_o/\beta\phi \tag{2}$$

where d_o is the Sauter mean diameter of the spray, β is the droplet evaporation coefficient and ϕ is the equivalence ratio in the primary zone of the combustor.

ϕ appears in Equation 2 because τ_{eb} is defined as the mass of fuel to be evaporated divided by the evaporation rate.(17,18)

The mixing time is defined as:

$$\tau_{sl} = d_q/V \tag{3}$$

where V is the flow velocity at the spark gap and d_q is the spark kernel diameter, or the diameter of the sphere that could be heated to the stoichiometric flame temperature by the minimum ignition energy. In gas turbine applications, the reference velocity is substituted for the spark gap velocity because the former is readily available and it is assumed that they are proportional. The minimum ignition energy is defined as the rated energy of the spark plug.

The chemical time is derived for the ignition of fuel lean mixtures typical of gas turbine ignition conditions. It is expressed in terms of the rate of gas phase hydrocarbon oxidation

$$\tau_{hc} = \frac{A \exp(E/RT_{\phi = 1})}{\rho_g} \tag{4}$$

where A is the pre-exponential factor (10^{-5}); E is the activation energy (26,100 cal/mole); R is the universal gas constant; $T_{\phi=1}$ is the stoichiometric adiabatic flame temperature; and ρ_g is the gas density. The constants A and E were determined by Plee and Mellor (19) using Fenn's (20) work on the ignition of propane and pentane. Because they depend on molecular cross sections and bond energies, jet fuels would tend to have slightly lower values of A and E. Thus, the chemical time for ignition of jet fuels may be slightly lower than those for propane and pentane. However, in the overall model, the droplet evaporation time dominates the heat generation side of the equation so any small differences in the chemical time are of little significance.

Calculations of the characteristic times for ignition were carried out on an HP Model 1000 computer with a code supplied by Professor A. Mellor, Drexel University. The code was used to calculate the characteristic times and perform a statistical correlation of the τ_{sl} with (τ_{hc} + a τ_{eb}). The proportionality constant, a, was assumed to be 0.021. This value was found to give the most favorable correlation in previous applications of

the model. In the present work it was found that the correlation coefficient, R, was insensitive to changes of ± 2a.

Two factors were varied in order to achieve the best correlation of the data. First, it was assumed that in-situ drop-size measurements of the T63 atomizer sprays were not available. The Sauter mean diameters of droplets in sprays from the T63 atomizer were calculated with an empirical equation experimentally derived for pressure swirl atomizers by Jasuja.(21) Later, droplet size measurements of sprays from the T63 atomizer were determined in-house by a light scattering technique. In addition to droplet size measurements of the T63 atomizer, the light scattering method was also used to measure droplet size distributions in the sprays from atomizers of the LM2500, TF40B, and DDA 501-K17 engines. A discussion of droplet size measurements may be found in the next subsection of this report. The second parameter of importance in the model was the equivalence ratio near the spark gap. It was first assumed that it could be approximated as the equivalence ratio in the primary zone of the combustor. The equivalence ratio in the primary zone was estimated from the overall equivalence ratio and the relative air flow split in the combustor. However, this approach was tried and failed to work. Instead, as found in earlier work (22), the best correlations were obtained when the equivalence ratio in the spark gap was held constant. Since it is assumed in the model that the spark energy heats the gas kernel to the stoichiometric flame temperature, the correlations were developed with an equivalence ratio of unity.

The results of the characteristic time model calculations are shown in Figures 15 and 16. These plots of τ_{sl} versus $(\tau_{hc} + 0.021\ \tau_{eb})$ define the limiting curve for the ignition process in the T63 combustor. The limiting curve for ignition can be used to predict if a given operating condition, burner inlet temperature, fuel temperature and mass flow rate, etc., will give rise to ignition. If the characteristic time coordinates lie below and to the right of the limiting curve, ignition is not possible; ignition can occur if the coordinates lie to the left and above the line.

Basically, the limiting curve relates the gas velocity at the spark gap to the Sauter mean diameter (SMD) of the spray. Note that the time τ_{eb} for droplet vaporization is most strongly dependent on SMD, d_o. Other parameters such as burner inlet temperature which affect the fuel droplet evaporation constant, β, have a relatively small effect on the characteristic times. The fuel properties that affect the SMD are viscosity and

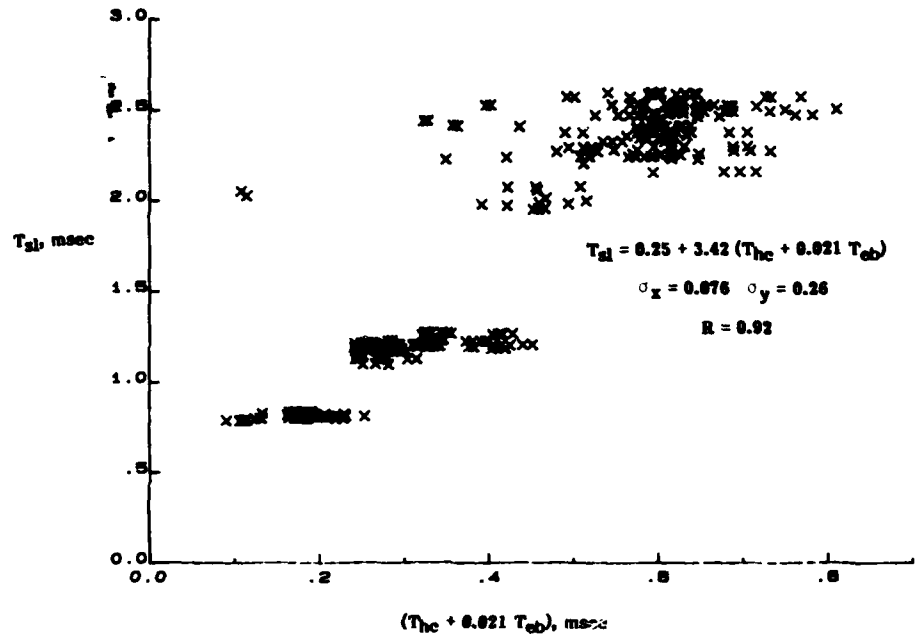

FIGURE 15. CHARACTERISTIC TIME CORRELATION FOR IGNITION IN THE T63 COMBUSTOR USING JASUJA'S EQUATION FOR PRESSURE SWIRL ATOMIZERS TO CALCULATE SMD

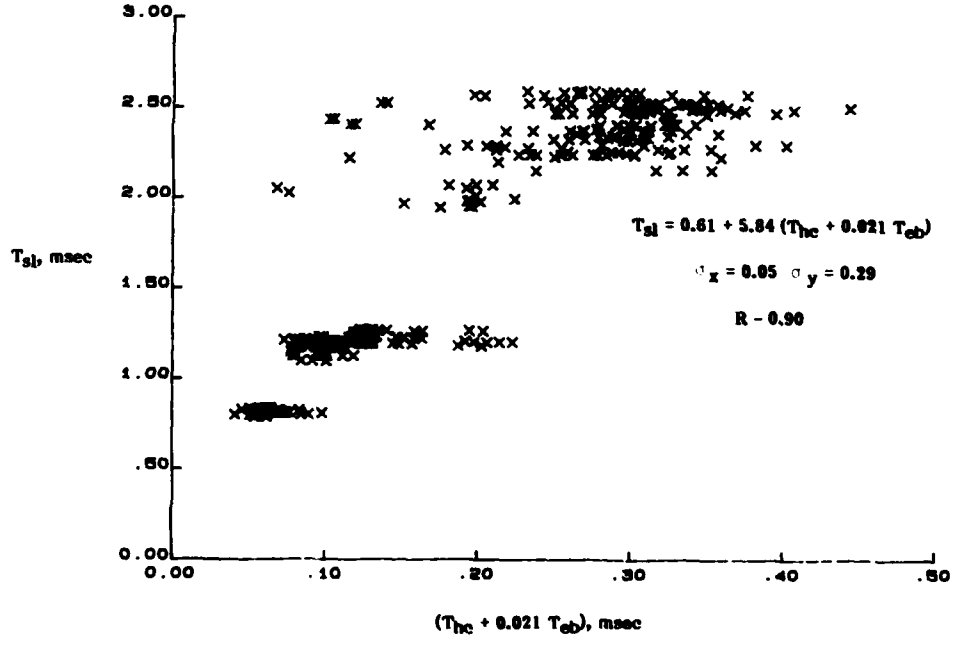

FIGURE 16. CHARACTERISTIC TIME CORRELATION FOR IGNITION IN THE T63 COMBUSTOR USING EXPERIMENTAL MEASURED SMDs

surface tension. Viscosity is the most important property because it changes most dramatically with fuel temperature. As fuel viscosity and surface tension increase, the SMD of the spray increases and τ_{eb} increases, thus reducing the probability of ignition. The effects of fuel viscosity and surface tension, and the fuel flow rate through the atomizer on the SMD of the spray are discussed in in the next subsection of this report.

Figure 15 shows the correlation (A) of characteristic times obtained using Jasuja's (21) equation to predict the Sauter mean diameter of droplets in the T63 atomizer spray. Figure 16 shows a similar correlation (B) obtained using measured Sauter mean diameters of droplets in the T63 atomizer spray. Both correlations represent reasonably good fits to the data, with correlation coefficients of 0.92 and 0.90 for correlations (A) and (B), respectively. The intercept of (A) is closer to zero than that of (B). In theory, the intercept should be zero. It is evident from the difference in slopes of the correlations that the measured SMDs are significantly smaller than those calculated from Jasuja's expression. The marked differences between the calculated and measured SMDs are discussed in the next subsection of this report.

Because correlation (B) is based on actual measured SMDs as opposed to predicted SMDs, it is considered to be the more appropriate form.

B. Droplet Size Measurements

Overall Spray Structure—The performance of gas turbine combustors depends strongly on the average fuel drop size produced by the atomizer, particularly in the areas of ignition, combustion efficiency, soot formation, and gaseous emissions. Changes in fuel properties led to significant changes in combustor performance, and some of these combustor performance effects were directly attributable to atomization performance. In order to interpret these fuel effects on atomization, it is necessary to examine the overall spray structure.

The structure of the T63 fuel spray is typical of most pressure swirl atomizer sprays in that the average drop size varies considerably as a function of the radial distance from the centerline of the spray. This is shown schematically in Figure 17, which represents an end-on view of a cross-section of the spray. These sprays are (approximately) axially symmetric with larger drops towards the outer part of the spray cone and smaller drops

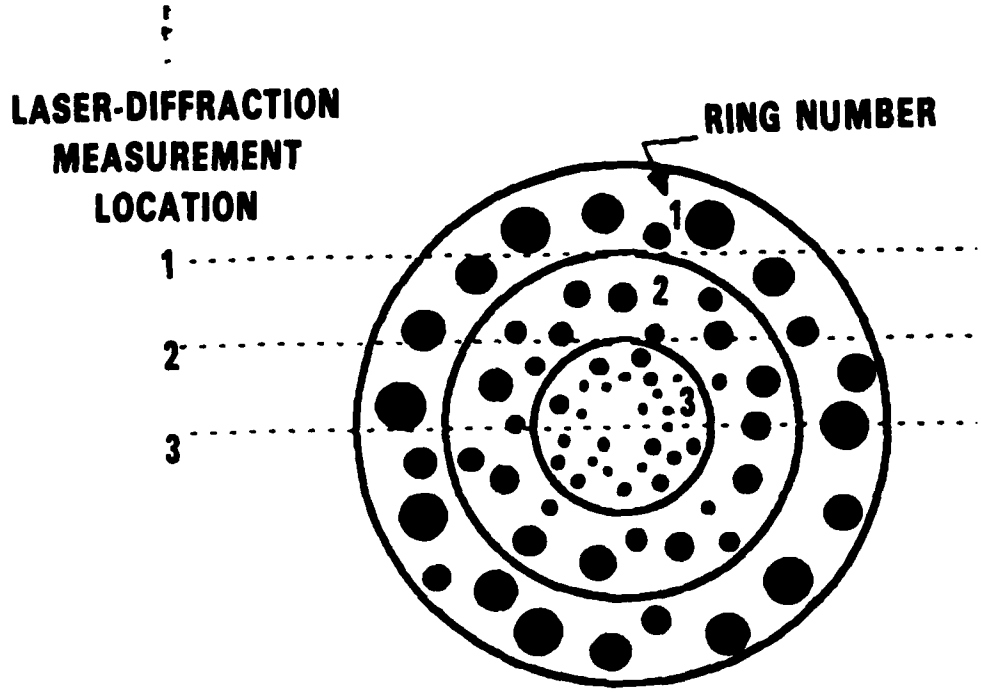

LINE-OF-SIGHT MEASURED VALUES

MEAS. LOCATION		INCREASING MEAS. AVG. SIZE	INCREASING MEAS. WIDTH OF DIST.
1	$SIZE_{AVG.} = SIZE_1$	↑	↓
2	$SIZE_{AVG.} = (CONC_1)(L_{21})(SIZE_1) + (CONC_2)(L_{22})(SIZE_2)$		
3	$SIZE_{AVG.} = (CONC_1)(L_{31})(SIZE_1) + (CONC_2)(L_{32})(SIZE_2) + (CONC_3)(L_{33})(SIZE_3)$		

$CONC_j$ = number density of particles in j-th ring

L_{ij} = path length through j-th ring at i-th measurement location

FIGURE 17. PRESSURE SWIRL ATOMIZER SPRAY STRUCTURE

toward the center. Thus the "average drop size" depends upon the measurement location and instrument type.

The Malvern laser-diffraction drop sizing instrument results in a line-of-sight average through the spray as shown in Figure 17, with measurements toward the outer part of the spray expected to be larger in average size and more uniform in size than measurements through the centerline. This is exactly the behavior observed, as shown in Figure 18 for a low flow rate ignition condition, in Figure 19 for a high flow rate ignition condition, and in Figure 20 for an idle condition. Figures 18, 19, and 20 are for a standard Navy distillate fuel (NDF). The average size is given by the SMD (Sauter mean diameter, or d_{32}), and the distribution width is given by the Rosin-Rammler N parameter, where larger values of N indicate narrower distributions and visa versa.

The most accurate description of the fuel spray drop-size distribution would be an average size and distribution function for each of the annular rings shown in Figure 17. Knowing the average size in each ring and the number density, the average size and distribution for the whole spray could be computed. As shown in the bottom of Figure 17, the measured line-of-sight values are a weighted average of the desired values. If measurements are made through several chords of the spray cone, a mathematical deconvolution procedure can be used to determine the average size in each ring. Such a deconvolution procedure has been developed by Hammond (23), and a corresponding computer model is now available at SwRI, with results for the high flow rate ignition condition shown in Figure 21. As expected, the actual drop size in the center of the spray is smaller than the measured line-of-sight average through the centerline (see Figure 17), while at the edges the actual and measured values converge. The weighted average SMD for the whole spray at this condition is 80 micrometers, while the measured line-of-sight value at the centerline is 31 micrometers. Thus, the measured line-of-sight centerline SMD which is traditionally reported is not necessarily a good measure of the SMD of the overall spray.

Most correlations for fuel sprays developed over the past ten years (e.g., References 21,24,25) are based on a laser-diffraction line-of-sight average through the centerline of the spray. It can be seen from the above data and Figure 17 that this value is weighted towards the average size in the inner part of the spray and, for pressure swirl atomizers, is considerably less than the average for the whole spray. In order to get a more

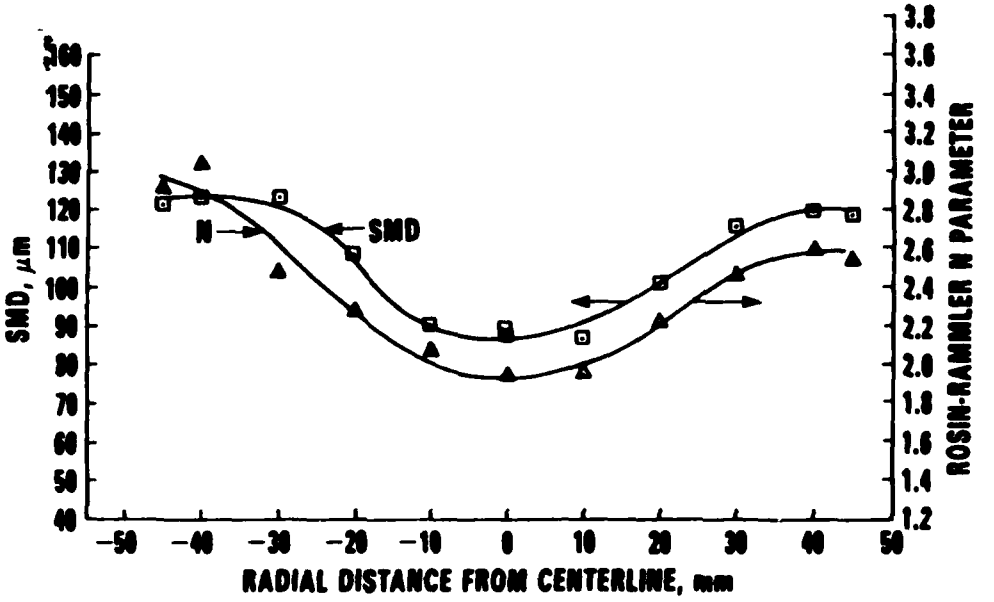

FIGURE 18. MEASURED SMD AND DISTRIBUTION WIDTH, T63 ATOMIZER, LOW-FLOW IGNITION CONDITION, NDF, T_f = 293K, ΔP = 296 kPa

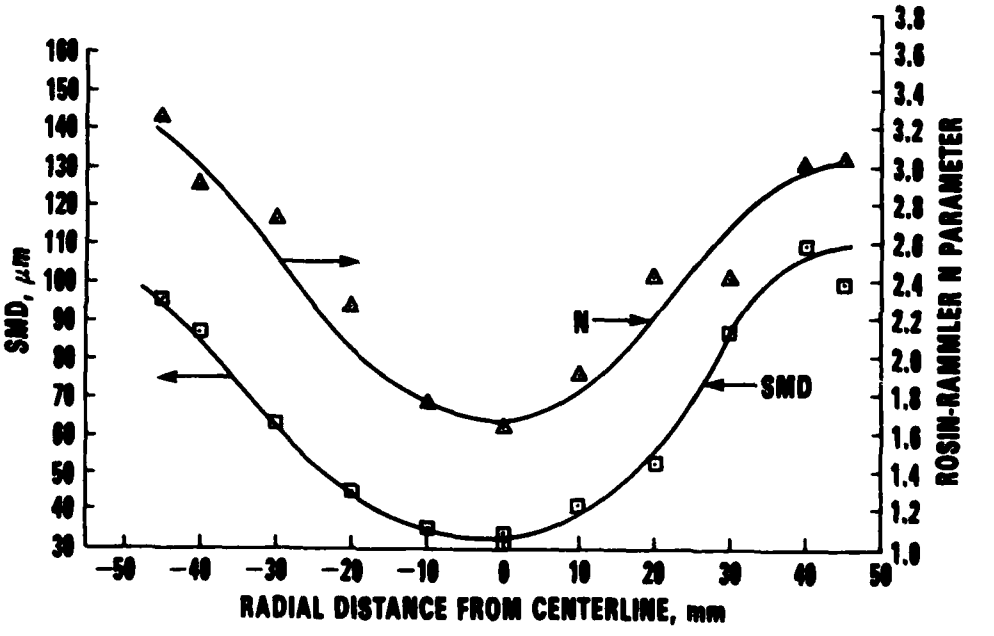

FIGURE 19. MEASURED SMD AND DISTRIBUTION WIDTH, T63 ATOMIZER, HIGH-FLOW IGNITION CONDITION, NDF, T_f = 293K, ΔP = 827 kPa

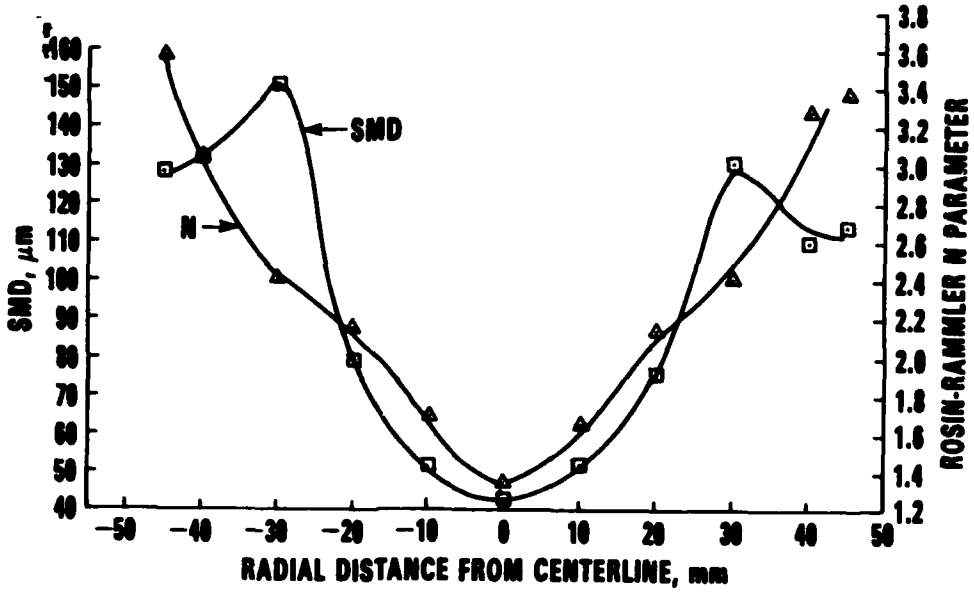

FIGURE 20. MEASURED SMD AND DISTRIBUTION WIDTH, T63 ATOMIZER, IDLE CONDITION, NDF, T_f = 291K, ΔP = 1310 kPa

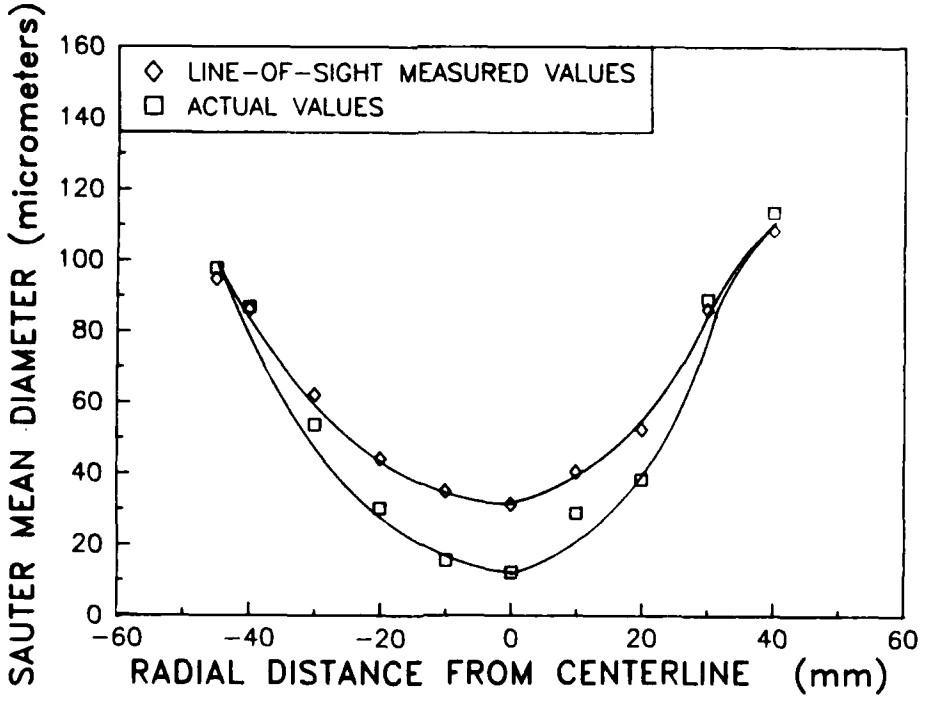

FIGURE 21. MEASURED LINE-OF-SIGHT AVERAGE SMDs COMPARED WITH ACTUAL VALUES, T63 ATOMIZER, HIGH-FLOW IGNITION CONDITION, NDF, T_f = 293K, ΔP = 827 kPa

representative average of the whole spray, measurements were made at each condition for each fuel through various chords of the spray from the centerline outward. However, due to an interruption of funding, time was not available to deconvolute the measured values and compute averages for the overall spray. Thus, measured line-of-sight averages through the centerline are reported here instead. This approach is consistent with current practice, but could be improved upon.

Fuel Effects—Fuel viscosity effects on atomization performance of the T63 nozzle are shown in Figure 22 for two different fuel flow rates spanning the minimum flows needed for ignition. That is, low viscosity fuels such as Jet A require fuel flow rates of about 3.1 mL/s (0.33 lbm/min) for ignition in the T63 combustor, while the high viscosity fuels such as HMGO require about 6.0 mL/s (0.7 lbm/min). Since these minimum flow rates for ignition were to be correlated with air velocity through the combustor, spark energy, and average drop size (SMD), it was necessary to predict the average drop size as a function of flow rate and fuel viscosity. The fuels tested included Fuel Nos. 1, 2, 3, 4, 5, 8, and 9 from Table 4. Note that the distillate fuels contaminated with 5- and 10-percent asphaltenes (Fuel Nos. 8 and 9 in Table 4) followed the same correlation for drop size versus viscosity as the other fuels. Therefore, the atomization of these contaminated fuels can be predicted simply from their viscosities. In Figure 22, these fuels had kinematic viscosities of 4.4 and 5.3 cSt.

Figure 22 illustrates an important feature of pressure swirl atomizers that has gone largely unrecognized in previous correlations for viscosity effects on atomization. At the lower flow rate of 3.12 mL/s, increases in viscosity cause large increases in SMD, while at a flow rate of 6.00 mL/s, the increase in viscosity has only a slight effect on atomization. The effect of viscosity on SMD is normally correlated in a form $SMD \sim \upsilon^{\alpha}$ where α is on the order of 0.16 [Jasuja (21)] to 0.25 [Rizk and Lefebvre (25)]. For the two curves shown in Figure 22, α varies from 0.472 at the lower flow rate to 0.100 at the higher flow rate. The T63 atomizer is a dual orifice pressure atomizer, with only the smaller primary nozzle used over the range of ignition conditions. At higher fuel flow rates, the larger secondary nozzle is also used, and the fuel effects at these higher flow rates are shown in Figure 23 for idle (11.0 mL/s or 1.23 lbm/min) and cruise (21.3 mL/s or 2.39 lbm/min) conditions. At these conditions, the viscosity effect is very pronounced with $\alpha = 0.731$ at idle and $\alpha = 1.070$ at cruise. Therefore, a significant conclusion is that the fuel effects on atomization can not be accurately predicted from generalized

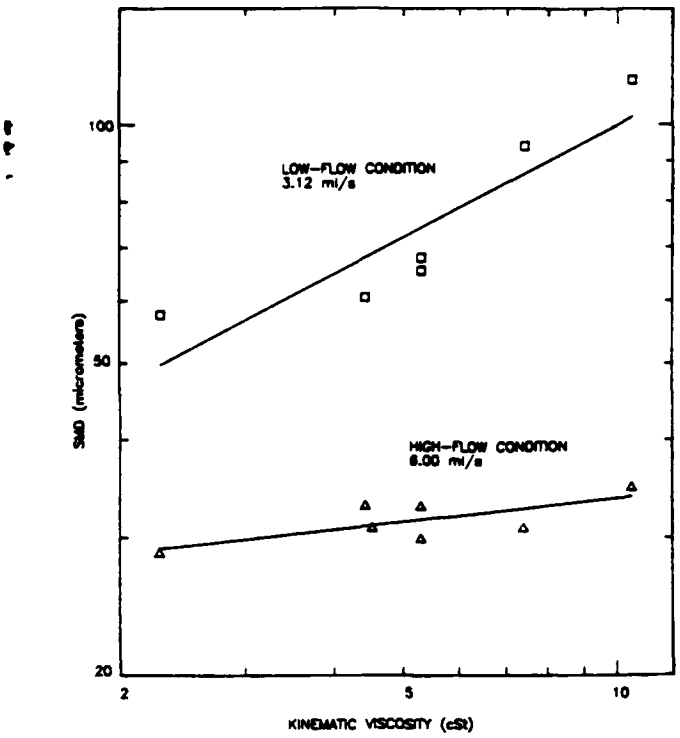

FIGURE 22. EFFECT OF FUEL VISCOSITY ON MEASURED CENTERLINE SMDs, T63 ATOMIZER, LOW-FLOW AND HIGH-FLOW IGNITION CONDITION

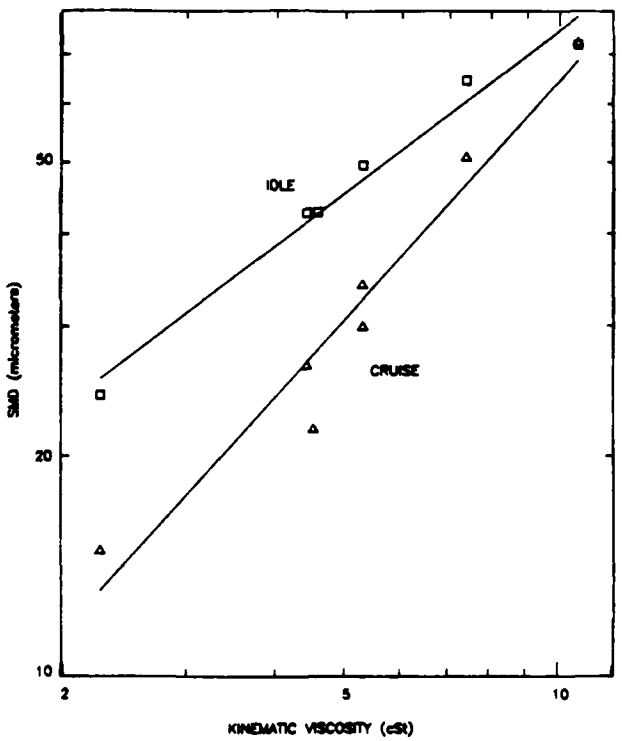

FIGURE 23. EFFECT OF FUEL VISCOSITY ON MEASURED CENTERLINE SMDs, T63 ATOMIZER, IDLE AND CRUISE CONDITIONS

equations developed from tests on "generic" fuel nozzles. Importantly, even for a given atomizer the viscosity effect on atomization varies at different fuel flow rates. Results of atomization tests for other atomizers for gas turbines within the Navy inventory are shown in Table 7. It can been seen that the fuel sensitivity varies, depending upon nozzle design, and that no single value of α is suitable for all atomizers at all conditions. Details of the tests on the first three atomizers in Table 6 (LM2500, DDA 501-K17, and TF40B) are given in Appendix A. The last four atomizers listed in Table 6 (T53 start, T53 main, T58 primary, and T76 start) were tested previously for the Naval Air Propulsion Center (Contract No. N00140-80-C-2269).

The results shown in Figure 22 indicated a flow rate dependent fuel viscosity effect which made it unreasonable for the limited data available to correlate the measured SMD with fuel flow rate and viscosity. However, the correlation of SMD with fuel flow rate and viscosity was needed in support of ignition tests already performed at SwRI as a part of this program. The interruption of funding on this program prevented further experimental data from being acquired. However, atomization tests on the same T63 atomizer with some of the same fuels were required for a Naval Air Propulsion Center program, and these more extensive data were used to correlate the SMDs for use in the ignition work carried out as another part of this project.

TABLE 7. DEPENDENCE OF SMD ON VISCOSITY FOR ATOMIZERS FROM SEVERAL GAS TURBINES IN THE NAVY INVENTORY
($SMD \sim \upsilon^{\alpha}$)

Atomizer	Condition	α
LM2500	Ignition	0.250
LM2500	Idle	0.267
DDA 501-K17	Ignition	0.390
DDA 501-K17	Idle	0.409
TF40B	Ignition	0.250
TF40B	Idle	0.267
T63	Ignition (low flow)	0.472
T63	Ignition (high flow)	0.100
T63	Idle	0.731
T63	Cruise	1.070
T53 Start	Ignition	0.089
T53 Main	Ignition	0.368
T58 Primary	Ignition	0.090
T76 Start	Ignition	-0.026

The fuels used for this portion of T63 atomization tests are described along with their physical properties (evaluated at the test temperature) in Table 3. They range in kinematic viscosity from less than 1 cSt for JP-4 to 28 cSt for cold (1°C) HMGO. Water was also used to independently vary surface tension from viscosity. Fuel flows were limited to those used for ignition and varied from about 0.75 to 6 g/s (0.64 to 5.1 mL/s or 0.10 to 0.79 lbm/min). Above 6 g/s, the secondary nozzle begins to flow and spray measurements are more difficult to interpret.

The first set of results covering the range of ignition mass flow rates are shown in Figure 24 for the fuels. Figure 25 is a similar plot for water and JP-4 which are the same viscosity, but the surface tension of water is three times that of JP-4. These curves illustrate that the atomization process undergoes a transition in the mass flow rate range used for ignition tests. This is the reason that different slopes were observed for the two different flow rates in Figure 22. This phenomena is not included in standard correlations for the atomization process, but Simmons (26) has observed this behavior and correlated it with the Weber number of the flow at the nozzle exit. The We number is defined as the ratio of the inertial force due to the air (which is proportional to the pressure equivalent of velocity multiplied by area) to the surface tension of the liquid. Simmons (26) shows that the Weber number may be expressed as,

$$We = \rho_a^2 \, \Delta P_F \, t_F \, / \, \rho_F \, \sigma \qquad (5)$$

where ρ_a = air density
ΔP_F = liquid pressure drop through nozzle
t_F = fuel film thickness leaving the lip of the nozzle
ρ_F = fuel density
σ = surface tension of fuel

Simmons (26) has shown that a transition in the atomization process occurs for Weber numbers on the order of unity, with the SMD being a much stronger function of flow rate for flows with Weber numbers of less than unity. This is qualitatively consistent with the results shown in Figures 24 and 25, where the lower Weber numbers occur at the lower fuel flow rates.

For the T63 atomizer, Equation 5 may be recast to predict the mass flow where the transition should occur, i.e., where $We \cong 1$.

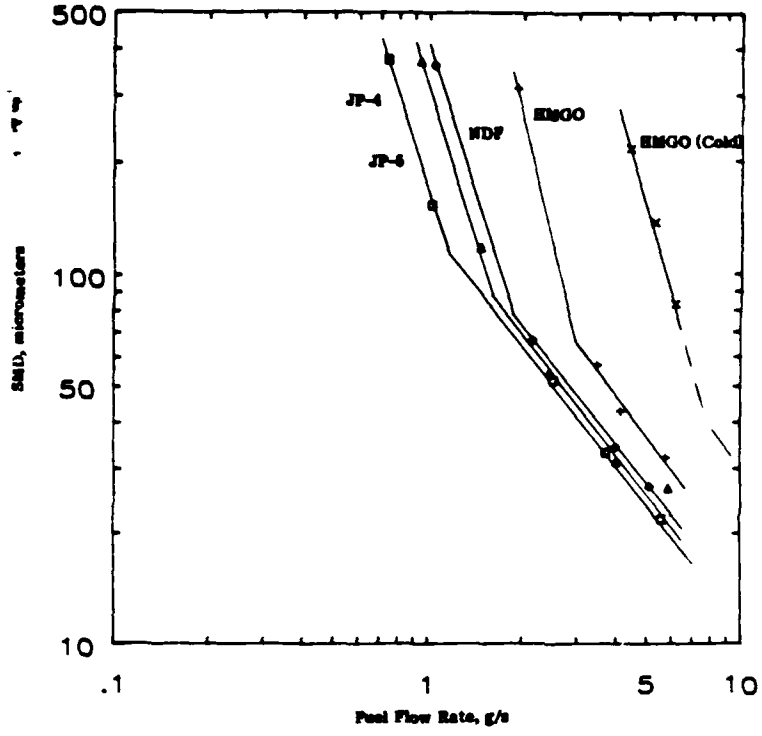

FIGURE 24. MEASURED SMDs AS A FUNCTION OF FUEL FLOW RATE FOR DIFFERENT FUELS, T63 ATOMIZER, IGNITION CONDITIONS

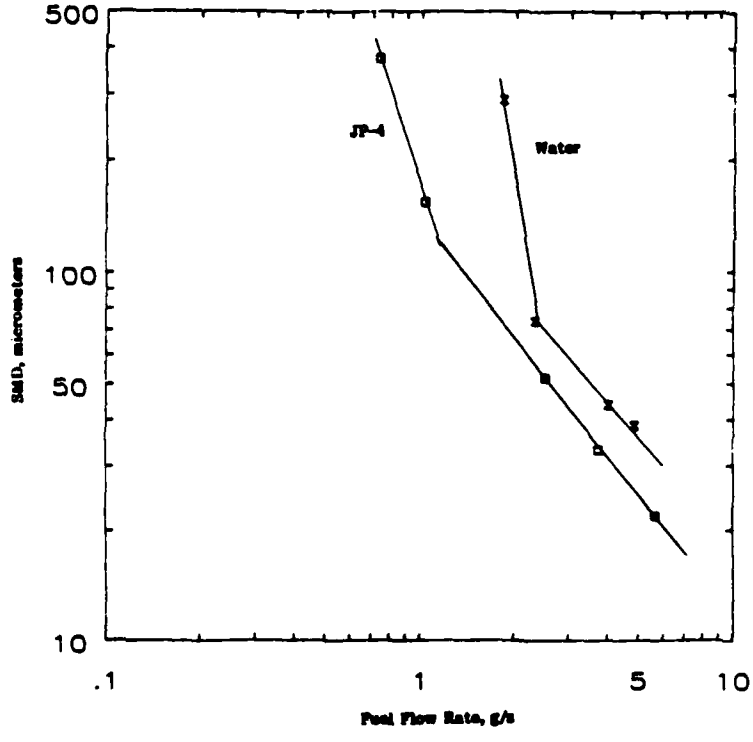

FIGURE 25. MEASURED CENTERLINE SMDs AS A FUNCTION OF FLOW RATE FOR JP-4 COMPARED TO WATER, T63 ATOMIZER, IGNITION CONDITIONS

$$W_F = 4.35 \times 10^{-2} (F_N \rho_F^{3/2} \sigma)^{1/2}$$

W_F = fuel mass flow, kg/s

F_N = nozzle flow number, kg/(s$\sqrt{Pa}$)

ρ_F = fuel density, kg/m^3

σ_F = surface tension, Nt/m

Thus, these predicted transition points may be compared with those of Figures 24 and 25 to verify that the phenomena observed here is the same one observed by Simmons:(26)

	Transition Point (g/s)	
Fuel	Predicted	Observed (Figs 24 and 25)
JP-4	2.5	1.2
JP-5	2.8	1.8
NDF	3.0	2.0
HMGO	3.3	3.0

The predicted transition points are only rough approximations based on the somewhat arbitrary criteria of We=1, but the behavior observed here is similar enough to that observed by Simmons (26) to attribute the change in slopes apparent in Figures 24 and 25 to the Weber number effect. The transition appears to have significance in terms of the ignition tests, as almost all of the successful ignitions were at fuel flow rates high enough for the transition to have occurred. The range of minimum flow rates required for successful ignition varied for each fuel depending on air flow through the combustor, but that range may be compared with the transition points in Figure 24:

Fuel	Observed Transition Pt. g/s (Fig 24)	Minimum Fuel Flow for Ignition (g/s)
JP-4	1.2	1.5-2.2
JP-5	1.8	2.0-2.8
NDF	2.0	2.3-3.9
HMGO	3.0	2.3-9.46

(Some of these ignition tests were a part of this program while others resulted from a Naval Air Propulsion Center program, Contract No. N00140-80-C-2269.)

It should also be noted that for all of the fuels, ignitions occurred under the most favorable air conditions only when the SMDs reached about 60 to 80 micrometers. The more viscous fuels required higher fuel pressures and higher fuel flow rates to achieve these drop sizes, but the SMD range was similar for all fuels.

A slight complication arose in interpreting the atomization data when it was found that the air flow occurring through the nozzle at ignition conditions had a minor effect on the atomization. The atomizer is described as a pure hydraulic pressure atomizer, but some air is forced through the nozzle by the pressure drop across the combustor can, and this appears to have an effect on atomization, as shown in Figure 26. The air pressure drop across the nozzle was measured to be about 154 Pa (0.62 in. H_2O) at an air flow of 0.09 kg/s (0.2 lbm/s), and 772 Pa (3.1 in. H_2O) at an air flow of 0.27 kg/s (0.6 lbm/s). These air flow rates represent the extremes over which ignition tests were performed.

The atomization measurements were repeated for all liquids in Table 3 except water, with two different air flow rates corresponding to the pressure drops of 154 and 772 Pa as discussed above. Since successful ignitions seemed to be restricted to those fuel mass flow rates high enough for the nozzle transition to have occurred, these atomization tests were limited to those flow rates above the transition point. The results for the lower air pressure drop are shown in Figure 27 and for the higher air pressure drop in Figure 28.

The atomization results in Figures 27 and 28 were correlated with mass flow rates and fuel properties to develop equations to predict the SMDs over the whole range of conditions at which ignition tests were performed.

A multiple-variable linear regression analysis was used to relate the dependent variable SMD to the independent variables. Independent variables which were tested for significance to the correlation included fuel mass flow rate, pressure drop across the nozzle, fuel viscosity, surface tension, and density. Fuel mass flow rate is proportional to the square root of pressure drop, so either variable, but not both, could be used in the correlation. Fuel density was not significant. For petroleum fuels, viscosity and surface tension are correlated, and viscosity provides a significant correlation with SMD while surface tension is insignificant. If water had been included in the data in Figures 27 and 28, then surface tension would be a significant variable, in that, compared with

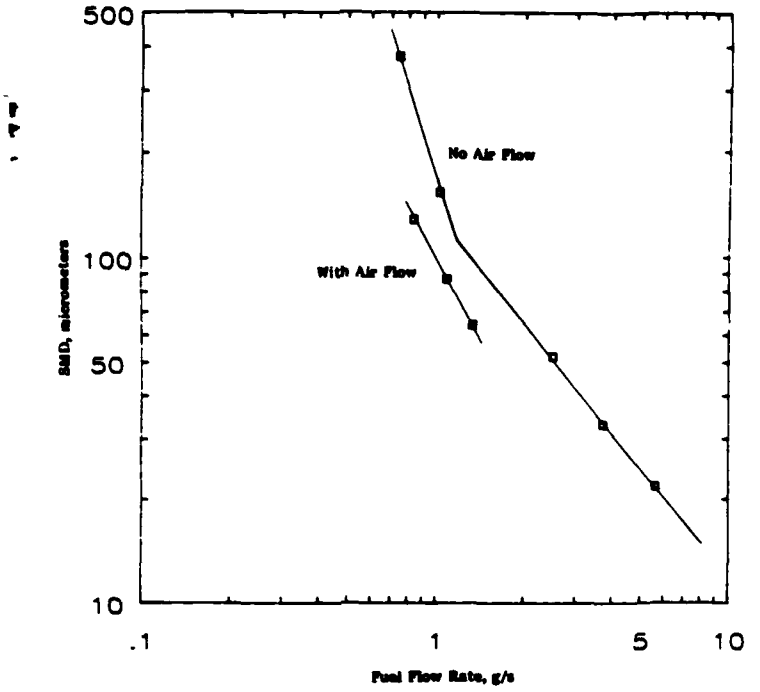

FIGURE 26. EFFECT OF AIR FLOW ON ATOMIZATION, T63 ATOMIZER, JP-4 FUEL

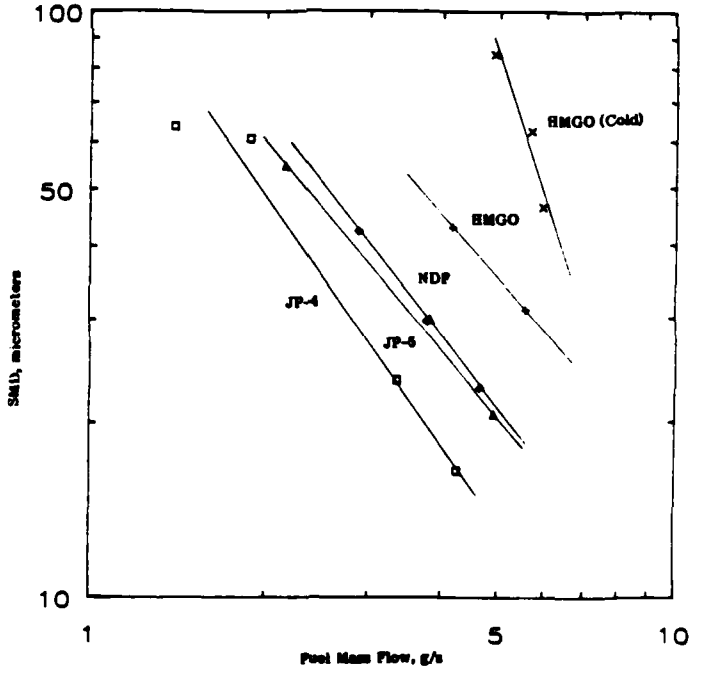

FIGURE 27. MEASURED CENTERLINE SMDs AS A FUNCTION OF FUEL FLOW RATE FOR DIFFERENT FUELS, T63 ATOMIZER WITH LOW AIR FLOW, ΔP_A = 154 kPa, IGNITION CONDITIONS

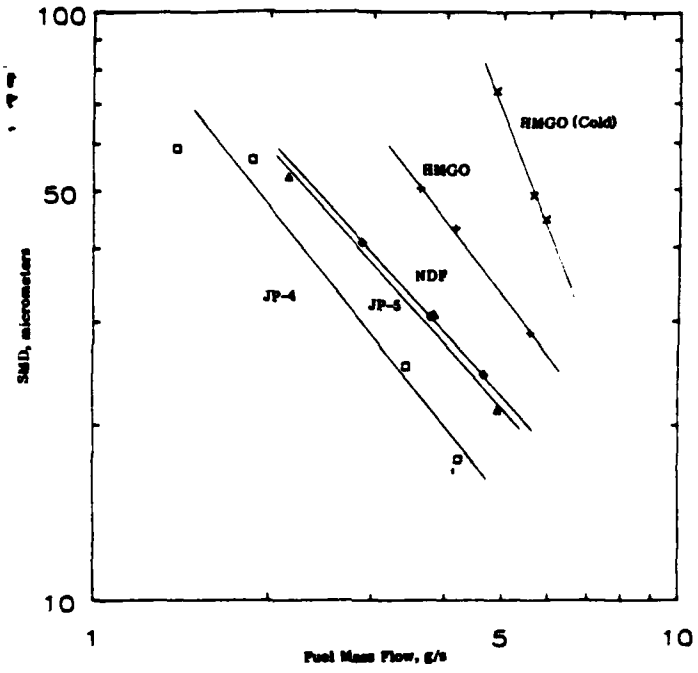

FIGURE 28. MEASURED CENTERLINE SMDs AS A FUNCTION OF FUEL FLOW RATE FOR DIFFERENT FUELS, T63 ATOMIZER WITH HIGH AIR FLOW, ΔP_A = 772 Pa, IGNITION CONDITIONS

petroleum fluids, water has a very high surface tension and low viscosity. After selecting out the significant variables, the following correlations were obtained:

Low air flow case (ΔP_a= 154 Pa, or 0.62 in H_2O):

$$SMD = 112.6\, \upsilon^{0.399}\, W^{-1.22} \quad (r^2 = 84.1)$$

$$SMD = 459.0\, \upsilon^{0.287}\, \Delta P^{-0.500} \quad (r^2 = 87.2)$$

High air flow case (ΔP_a= 772 Pa, or 3.1 in H_2O):

$$SMD = 99.7\, \upsilon^{0.334}\, W^{-1.09} \quad (r^2 = 85.4)$$

$$SMD = 345.5\, \upsilon^{0.233}\, \Delta P^{-0.445} \quad (r^2 = 88.8)$$

where, υ = kinematic viscosity, cSt

W = fuel mass flow rate, g/s

ΔP = fuel pressure drop across nozzle, kPa

Although the correlation with nozzle pressure drop shows a slightly better correlation coefficient and is a more common form of the equation, the correlations with mass flow

were used to estimate the SMDs for the ignition tests, because fuel mass flow rather than pressure drop was monitored for those tests. Ignition tests were performed at three air flow rates - the low and high cases listed above and an intermediate case. The SMDs for the intermediate case were estimated as the average of the low-air and high-air cases.

C. Flame Radiation and Exhaust Smoke

Soot formation in gas turbine engines is observed in the form of exhaust smoke and increased combustion chamber liner temperature, i.e., radiant heat transfer from incandescent carbon particles.(27,28) The flame radiation intensity is a function of the gas temperature and the flame emissivity which depends on soot concentration. Exhaust smoke is that which remains after about 98 percent (29) of the soot is oxidized in the secondary and quench zones of the combustor; these oxidation rates are dependent solely on combustor operating conditions, such as burner inlet temperature, and not on fuel properties.

The radiative component of combustor liner temperature has been found (30) to correlate most consistently with hydrogen-carbon ratio of the fuel. For a typical engine such as the J79, increased liner temperature due to a reduction in fuel hydrogen content from 14.5 to 12 percent will curtail the cycle life by 65 percent.(31)

The correlation of flame radiation and exhaust smoke with H/C atom ratio has been found to be valid for distillate fuels ranging from unleaded gasoline to diesel fuel marine.(2) The results of previous studies in laboratory flames (32) and in gas turbine engines (32) have shown that soot formation is a gas phase phenomenon. There is no firm evidence that carbon particulate formation via liquid-phase pyrolysis of fuel droplets plays an important role in the soot-forming process in gas turbine engines. However, the correlations of flame radiation and exhaust smoke with H/C atom ratio have not been confirmed for middle distillate fuels containing heavy residual oil components such as asphalts. Recent work by Marrone, et al. (33) on the combustion history and coking of free and suspended droplets of a residual oil has shown that coke particles form within the final 9 percent of the droplet burning period and the mass of the coke particle is about 3 percent of the mass of the initial residual oil droplet. Changing the temperature history of a droplet by varying the initial droplet size between 260 to 570 micrometers or

by diluting the residual oil with a lower viscosity No. 2 fuel oil did not affect the mass fraction of the residual oil in the initial droplet which was converted to coke. Based on the work of Marrone, et al. (33), it would be expected that the formation of coke in droplet combustion would add substantially to the soot yield in a gas turbine combustor.

The results of the present work indicate that the soot production rates of fuels containing asphalts is not increased above that predicted by the hydrogen content of the fuel. Figures 29 and 30 show the respective correlations of flame radiation index and exhaust smoke index with H/C atom ratio. The indices of flame radiation and exhaust smoke are relative values obtained by normalizing the data to the reference fuel. The actual data obtained in the present study may be found in Appendix B. In addition to data on the reference fuel and the 25 test fuels in Table 4, some data on conventional aviation fuels from a previous study (2,30) are shown as a comparison; the straight lines in Figures 29 and 30 are least squares fits of the conventional aviation fuels data. The results show that the flame radiation and exhaust smoke from the 25 test fuels appear to correlate with H/C atom ratio in about the same way as typical jet fuels. However, instead of being on the high side, as expected from the droplet burning studies of Marrone, et al. (33), the values of radiation and smoke are somewhat lower than those measured using jet fuels. One possible explanation for this is that the test fuels evaporate and burn more slowly because of their high molecular weight components. If combustion occurs more gradually, i.e., the light fuel components burn well in advance of the heavy fuel components, the flame temperature is lower because of the reduced heat release rate. This may explain the lower radiation and smoke since soot formation is strongly dependent on flame temperature.(5)

Figures 31 through 34 give a more detailed description of the effects of asphalts and slurry oil on the flame radiation and exhaust smoke measured at full power. It is apparent that these heavy residual oil components have a negligible effect on the radiation and smoke, and there is little difference caused by the composition of the asphalt material. If anything, Fuel Nos. 25 and 26 containing slurry oil produced slightly higher levels of radiation and smoke than the asphalts, but this can be attributed to the lower hydrogen contents of those fuels. It is concluded that the radiation and smoke produced by fuels contaminated with heavy residual oil components correlate with H/C atom ratio in the same as conventional jet fuels.

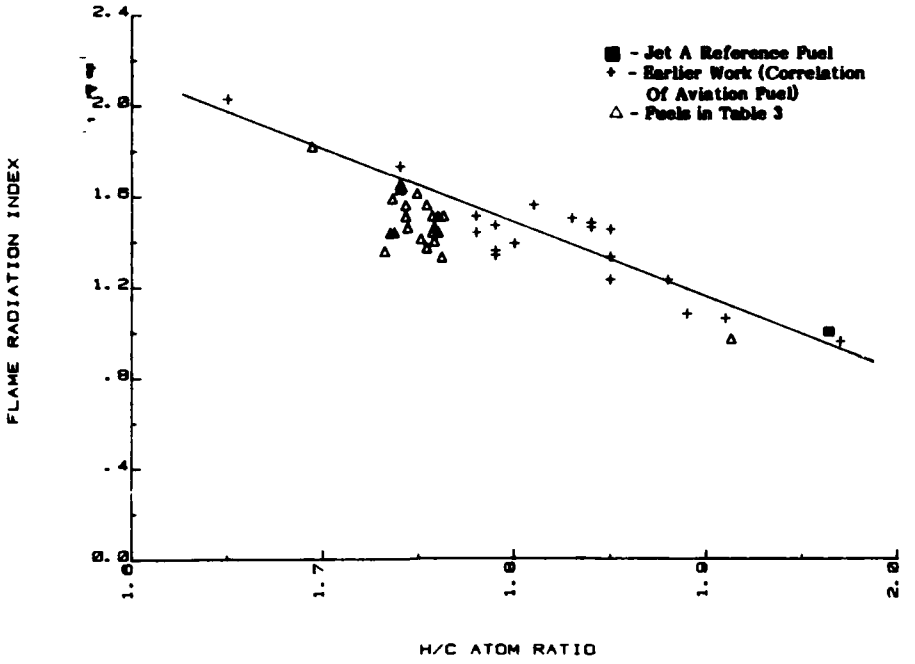

FIGURE 29. CORRELATION OF FLAME RADIATION INDEX WITH H/C ATOM RATIO

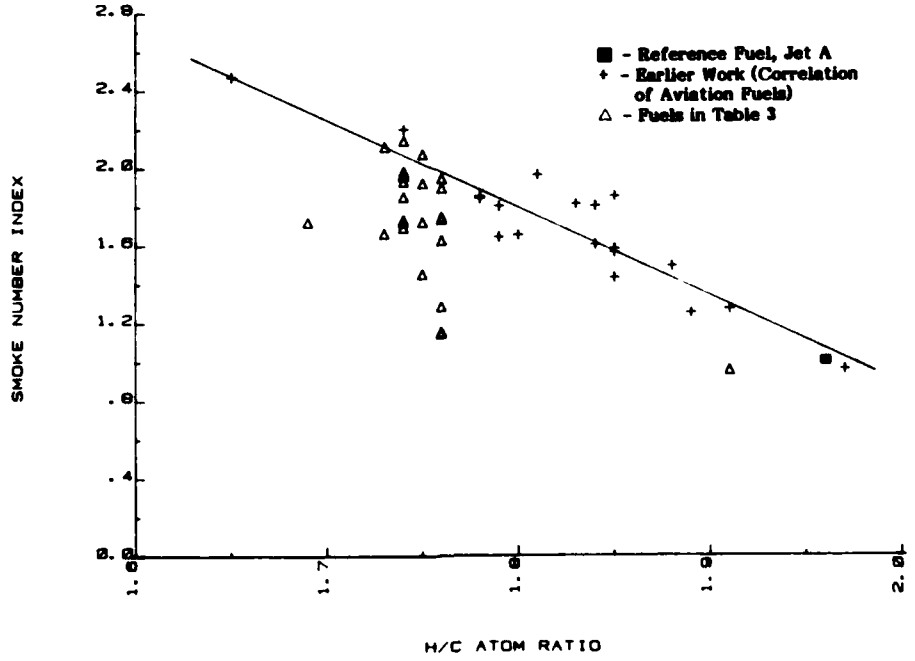

FIGURE 30. CORRELATION OF EXHAUST SMOKE INDEX WITH H/C ATOM RATIO

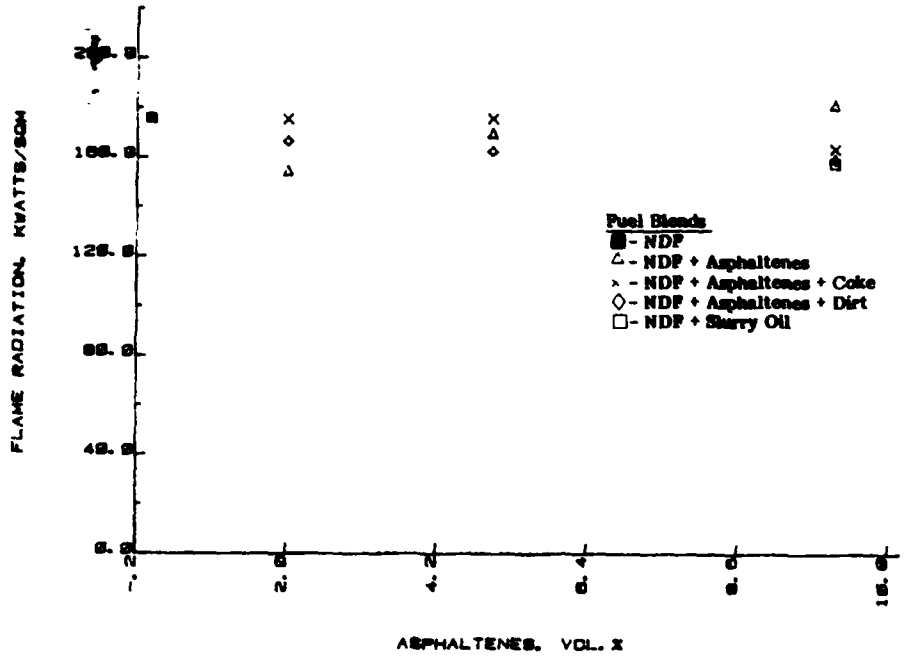

FIGURE 31. THE EFFECT OF ASPHALTS (INCLUDING SLURRY OIL) BLENDED WITH NDF ON FLAME RADIATION MEASURED AT FULL POWER

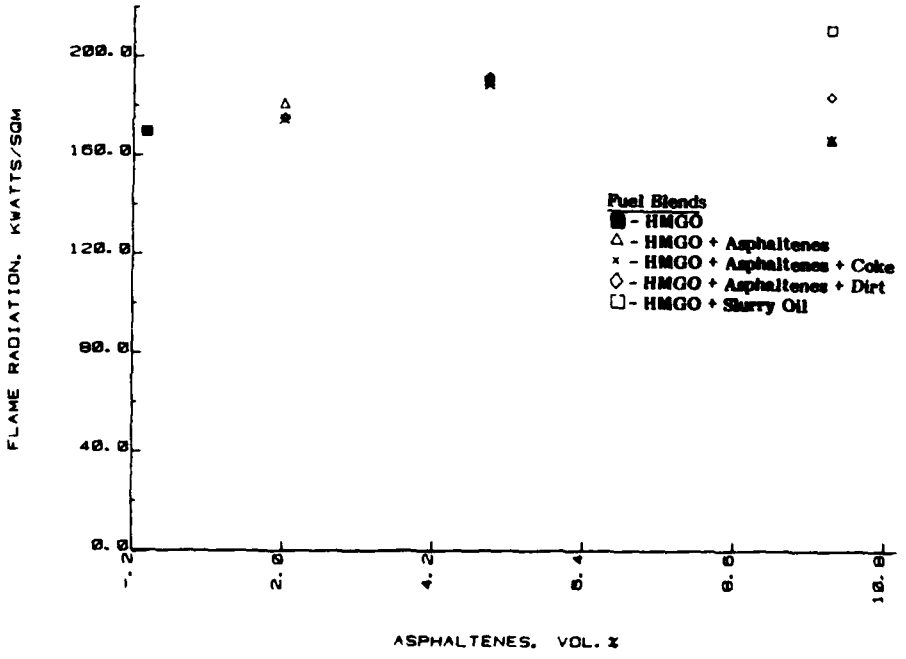

FIGURE 32. THE EFFECT OF ASPHALTS (INCLUDING SLURRY OIL) BLENDED WITH HMGO ON FLAME RADIATION MEASURED AT FULL POWER

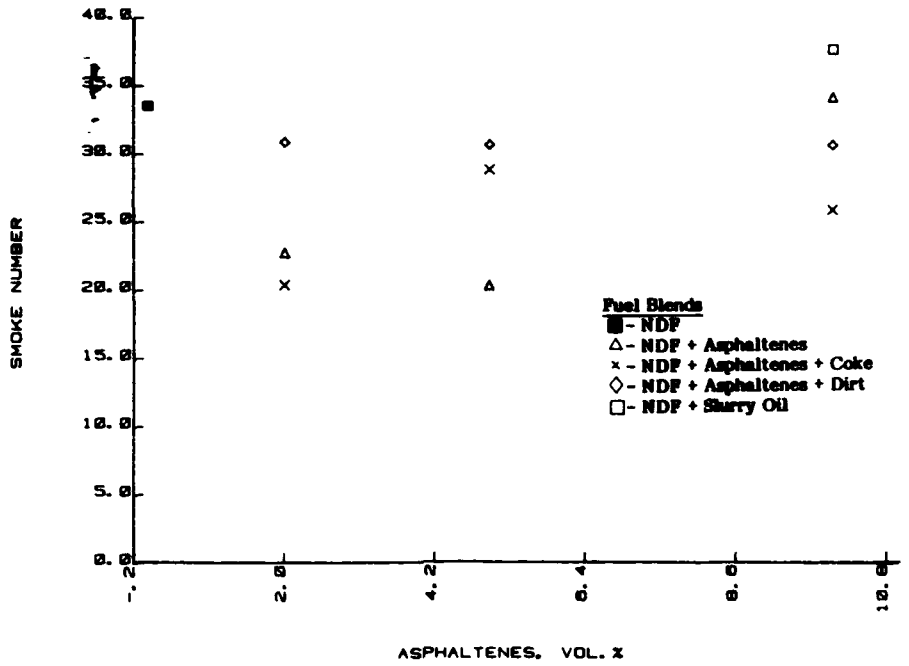

FIGURE 33. THE EFFECT OF ASPHALTS (INCLUDING SLURRY OIL) BLENDED WITH NDF ON EXHAUST SMOKE MEASURED AT FULL POWER

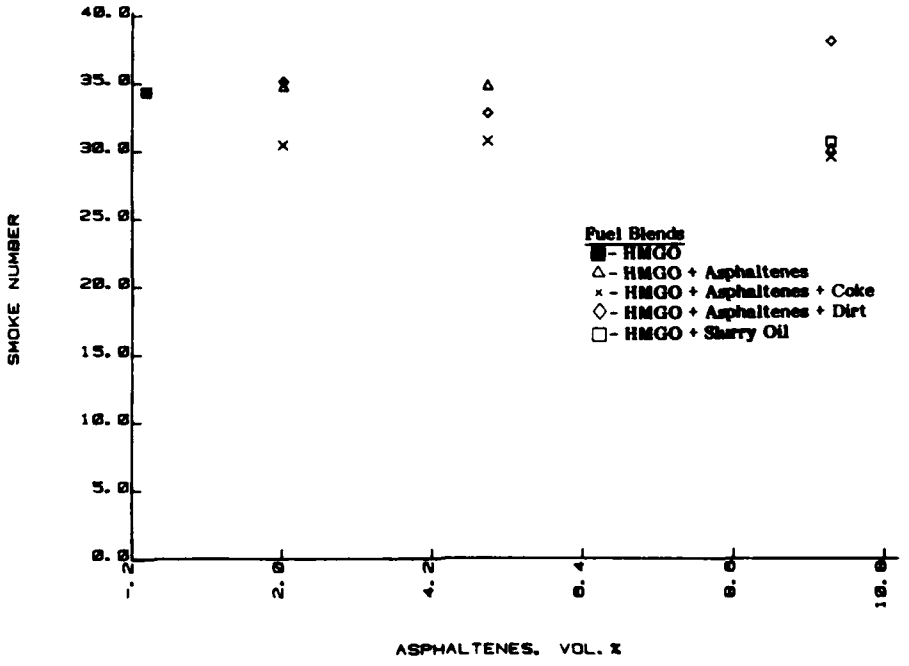

FIGURE 34. THE EFFECT OF ASPHALTS (INCLUDING SLURRY OIL) BLENDED WITH HMGO ON EXHAUST SMOKE MEASURED AT FULL POWER

D. Liner Temperature

When the flame radiation in the combustor rises, the liner temperature generally increases in the region of the primary zone, dome, and sidewall (see Figure 1). Liner temperature measurements were made on all the test fuels at the four power conditions described in Table 1. Measurements at full power on Fuel Nos. 1 through 5 showed that surface temperatures in the region of the primary zone were from 20 to 40K greater than the burner inlet air temperature. Smaller differences were observed at the lower power conditions. Part of this increase in surface temperature was no doubt due to radiative heat loading. In comparing the liner temperature measurements on Fuel Nos. 1 through 5 it was not possible to resolve any significant differences. The measurements indicated that flame radiation intensity at the liner surface was about the same for both the reference fuel and test Fuel Nos. 2 through 5. Fuel Nos. 2 through 5 should have resulted in higher liner temperatures because of their lower hydrogen contents. However, this effect was not observed.

Measurements on test Fuel Nos. 6 through 26 containing the various asphalts and the slurry oil showed that liner temperatures in the region of the dome decreased in comparison to the neat fuel; at the sidewall of the primary zone, the temperatures were actually lower than the burner inlet air temperature by as much as 30°C. Of course, this result seemed to be unreasonable and suggested that the liner thermocouples were malfunctioning. Subsequent tests with neat Jet A, NDF, and HMGO showed normal behavior, i.e., the liner temperatures were all greater than the burner inlet air temperature. It was concluded that the unusually low liner temperatures obtained with Fuel Nos. 6 through 26 containing asphalt and slurry oil were real. Upon inspection of the liner after examining the combustion performance of these fuels, it was found that substantial deposition had occurred on the dome and sidewall of the primary zone. This suggested that the liner temperature decreased because fuel droplets composed mainly of heavy components adhered to the walls and evaporated, leaving a deposit. The evaporation of fuel components at the wall appeared to act as a heat sink which cooled the surface. In accordance with this elucidation, the observed decreases in liner temperature tended to increase as the concentration of asphalt or slurry oil in the fuel was raised.

E. Gaseous Emissions and Combustion Efficiency

The general patterns of the exhaust emissions followed expected trends: total hydrocarbons (THC) and CO were highest at low power conditions due to lower burner inlet temperatures and poorer mixing, while NO_x increased with power because of the increase in primary zone flame temperature, a combination of higher inlet air temperature and fuel/air ratio.

The combustion performance data on gaseous emissions and combustion efficiency may be found in Appendix C. The effect of power on the THC emissions index, the CO emissions index, and the combustion efficiency of Fuel Nos. 1 through 5 is shown in Figures 35 through 37, respectively. The NO_x emissions are not shown because they were essentially independent of the fuel properties. It is apparent that the THC and CO emissions are the highest for HMGO and the lowest for NDF and the reference fuel Jet A. Gaseous emissions increase and combustion efficiency decreases as the concentration of HMGO in NDF is increased. Although the differences in gaseous emissions and combustion efficiency are substantial at the idle condition, they are much smaller at the higher power conditions. This was also found for the fuels containing asphalts and slurry oil. Gas turbine engines used for Naval applications are generally operated at 60 percent of full power. For a vessel at sea, the main concern would be the combustion efficiency; a small increase in gaseous emissions would not seem to be a problem.

The THC emissions index for Fuel Nos. 7 through 26 measured at the 10 percent of full power (idle) condition are shown in Figures 38 and 39. Here the THC emissions index is plotted against the concentration of the heavy oil component that was blended with NDF and HMGO.

In general, the heavy oils, asphalts and the slurry oil, increase the THC emissions index. However, there seemed to be some exception to this in Fuel Nos. 19 through 24 which contained dirt. The dirt in these blends was originally added to the asphalt in the form of metal oxides of silicon, aluminum, and iron. Fuel impurities such as iron have been known to have catalytic effects on the oxidation of soot. However, the exhaust smoke did not seem to be perturbed by the presence of dirt in the fuel. Fuel Nos. 13 through 18 containing high resin asphalt with coke also tended to give lower THC levels than Fuel Nos. 7 through 12 with the low resin asphalt. Fuel Nos. 25 and 26 containing

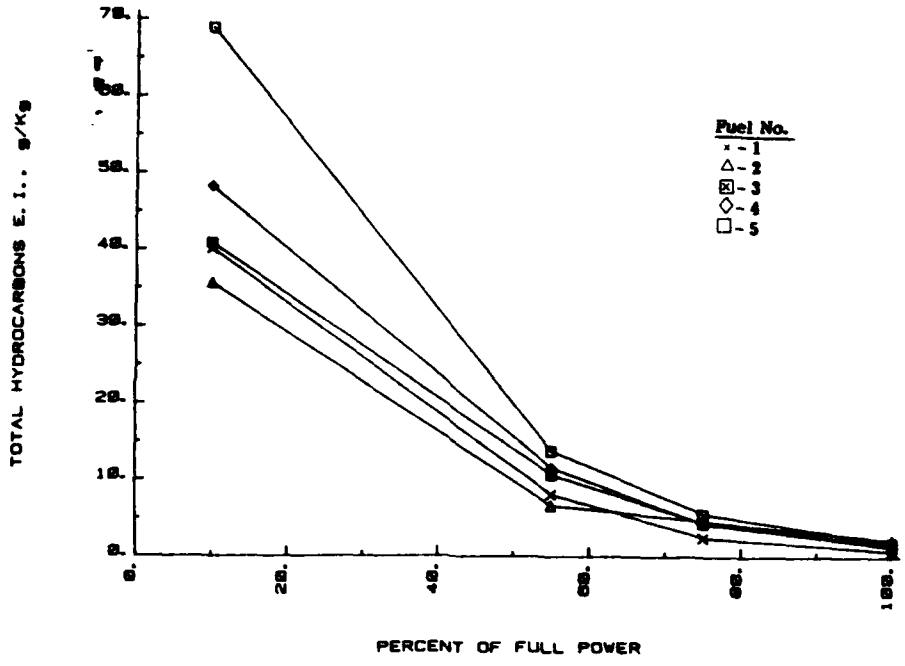

FIGURE 35. THE EFFECT OF ENGINE POWER ON THE TOTAL HYDROCARBONS EMISSIONS INDEX FOR FUEL NOS. 1 THROUGH 5

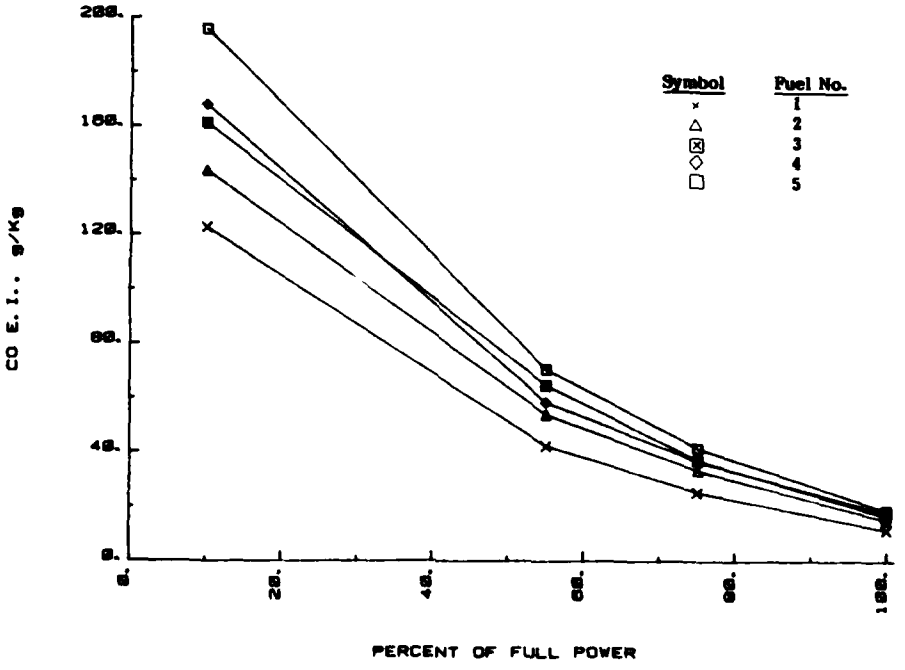

FIGURE 36. THE EFFECT OF ENGINE POWER ON THE CO EMISSIONS INDEX FOR FUEL NOS. 1 THROUGH 5

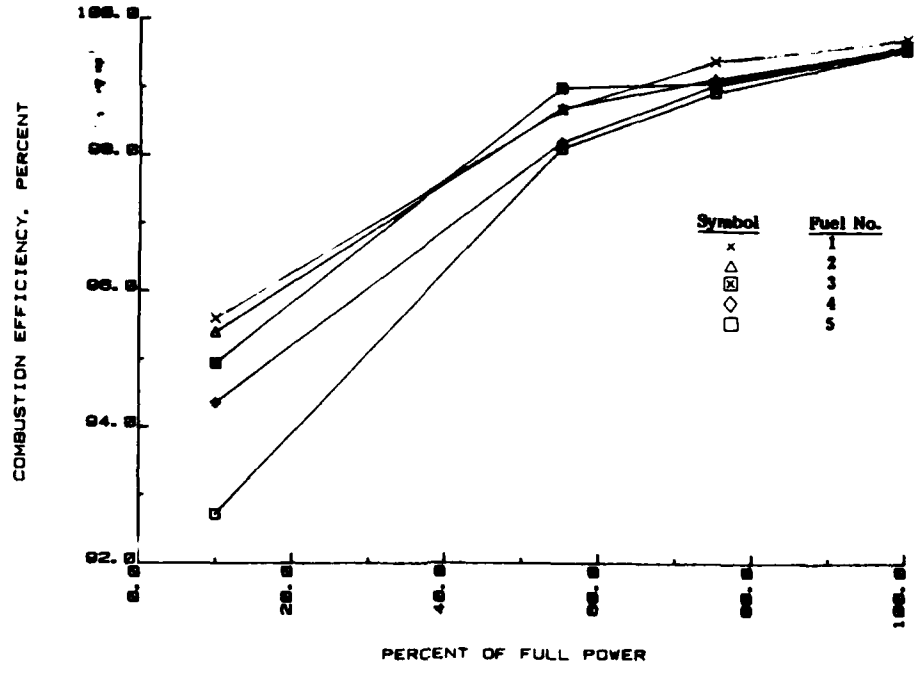

FIGURE 37. THE EFFECT OF ENGINE POWER ON THE COMBUSTION EFFICIENCY OF FUEL NOS. 1 THROUGH 5

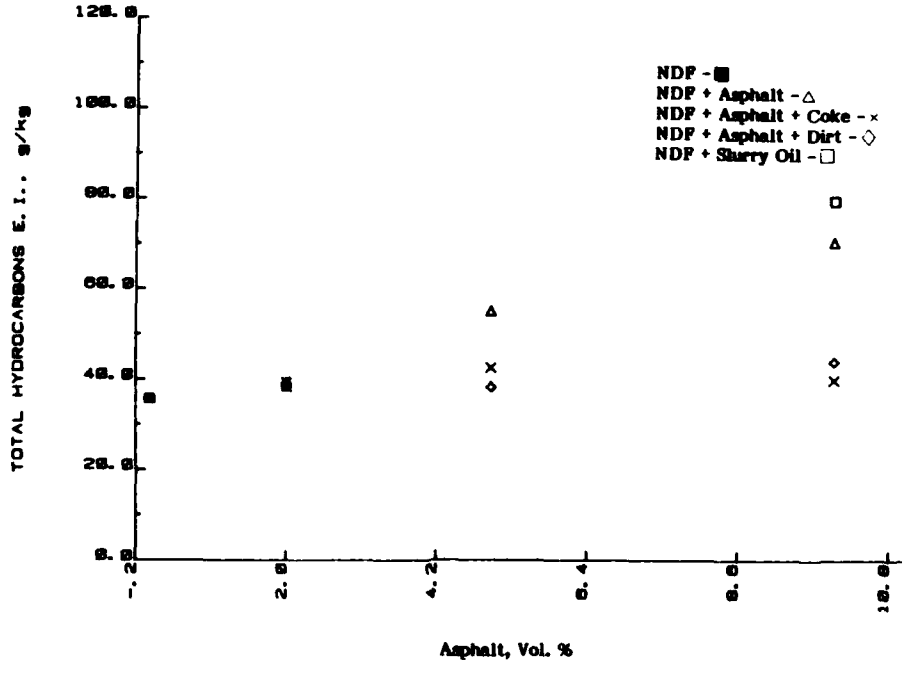

FIGURE 38. THE EFFECT OF ASPHALTS AND SLURRY OIL BLENDED WITH NDF ON THE TOTAL HYDROCARBONS EMISSIONS INDEX MEASURED AT 10 PERCENT OF FULL POWER

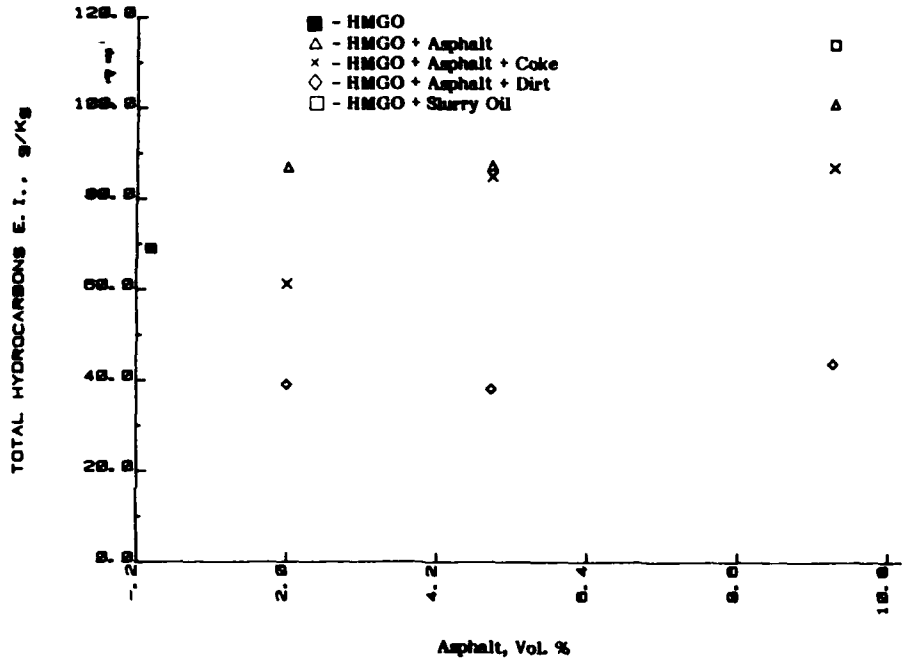

FIGURE 39. THE EFFECT OF ASPHALTS AND SLURRY OIL BLENDED WITH HMGO ON THE TOTAL HYDROCARBONS EMISSIONS INDEX MEASURED AT 10 PERCENT OF FULL POWER

10-percent slurry oil with catalytic fines had the highest THC emissions. This was probably due to the fact that the slurry oil had a higher pour point (-13°C) than the asphalt (-26°C) which indicated that it was a higher molecular weight material. Fuel droplets of the slurry oil would evaporate slower than the other fuels, and this would result in higher hydrocarbon emissions.

Figures 40 and 41 show the effect of the heavy oil component on the CO emissions index measured at the 10 percent of full power condition. The results show a general increasing trend of the CO emissions index with higher concentrations of the heavy oil component. However, there is too much scatter in the data to discern any differences in the CO emissions from the fuel groups 7 through 12, 13 through 18, and 19 through 24, containing asphalts and 25 and 26 containing slurry oil with catalytic fines.

The combustion efficiencies at the 10 percent of full power condition for Fuel Nos. 7 through 26 are shown in Figures 42 and 43. The results show that the combustion efficiency tends to decrease as the concentration of the heavy oil (asphalt) component in the fuel is inceased. The differences in the combustion efficiencies among the fuels

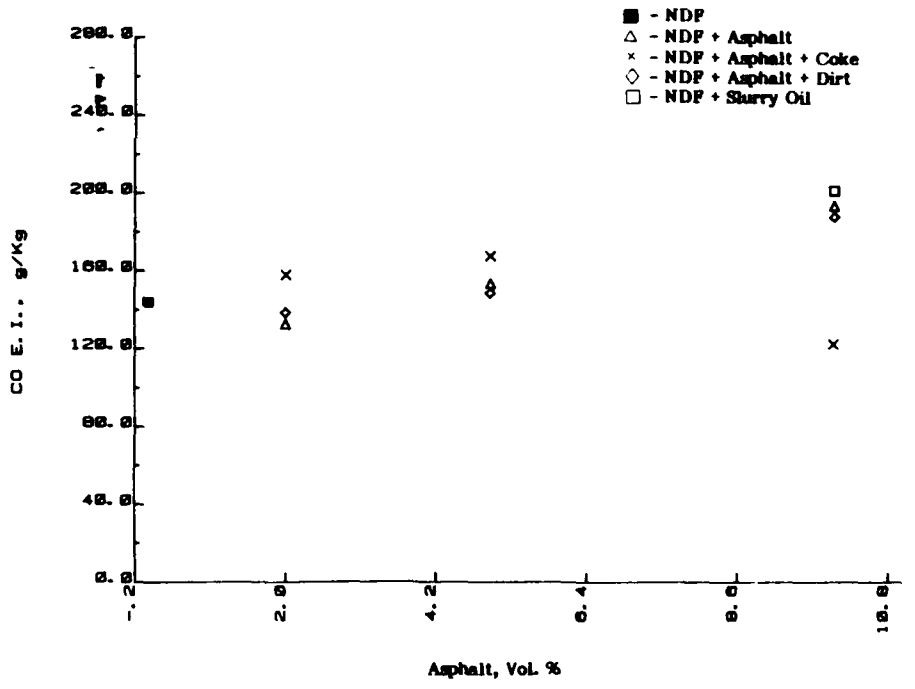

FIGURE 40. THE EFFECT OF ASPHALTS AND SLURRY OIL BLENDED WITH NDF ON THE CO EMISSION INDEX MEASURED AT 10 PERCENT OF FULL POWER

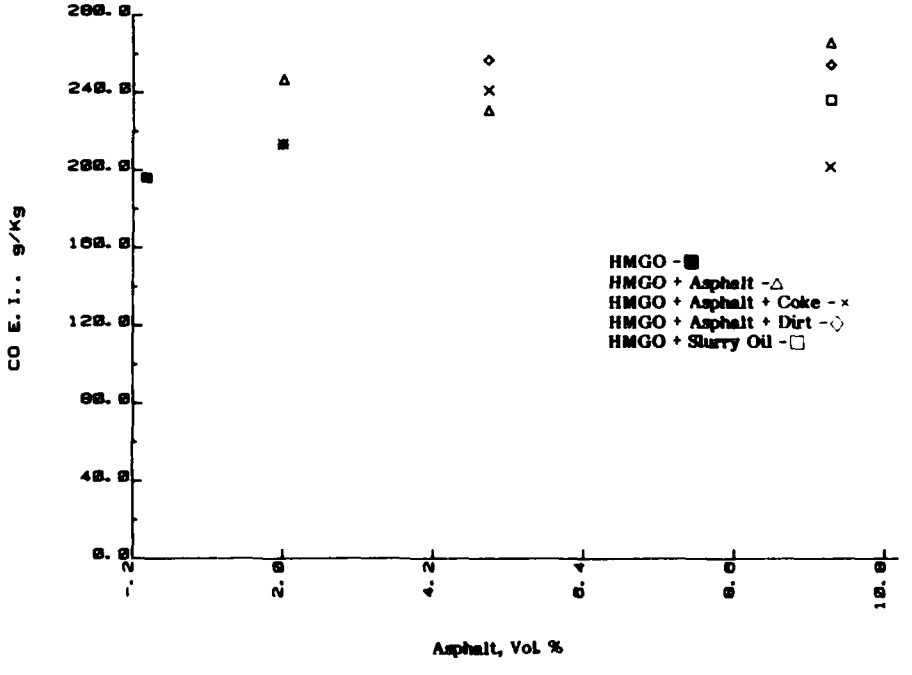

FIGURE 41. THE EFFECT OF ASPHALTS AND SLURRY OIL BLENDED WITH HMGO ON THE CO EMISSIONS INDEX MEASURED AT 10 PERCENT OF FULL POWER

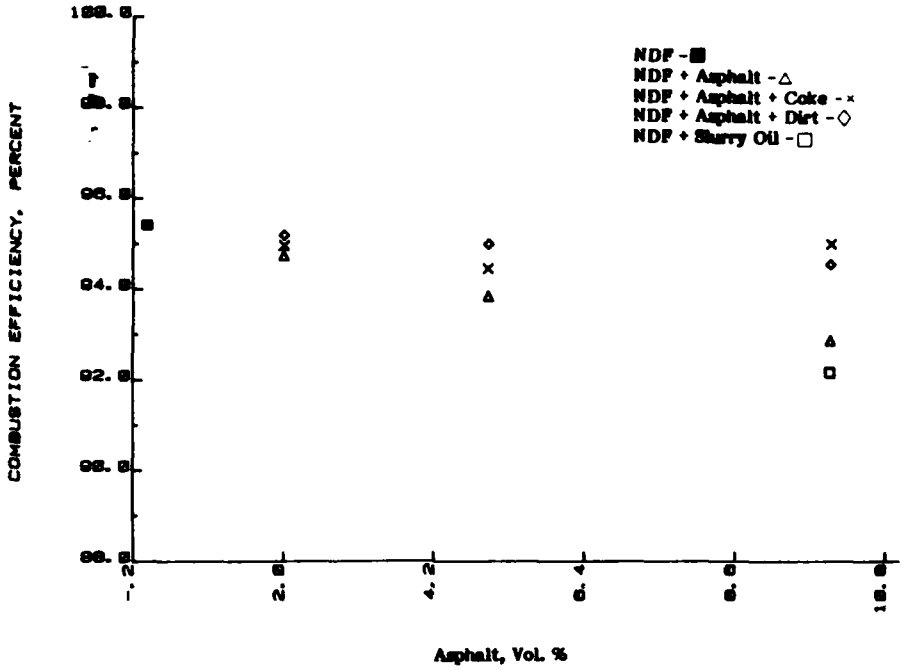

FIGURE 42. THE EFFECT OF ASPHALTS AND SLURRY OIL BLENDED WITH NDF ON THE COMBUSTION EFFICIENCY MEASURED AT 10 PERCENT OF FULL POWER

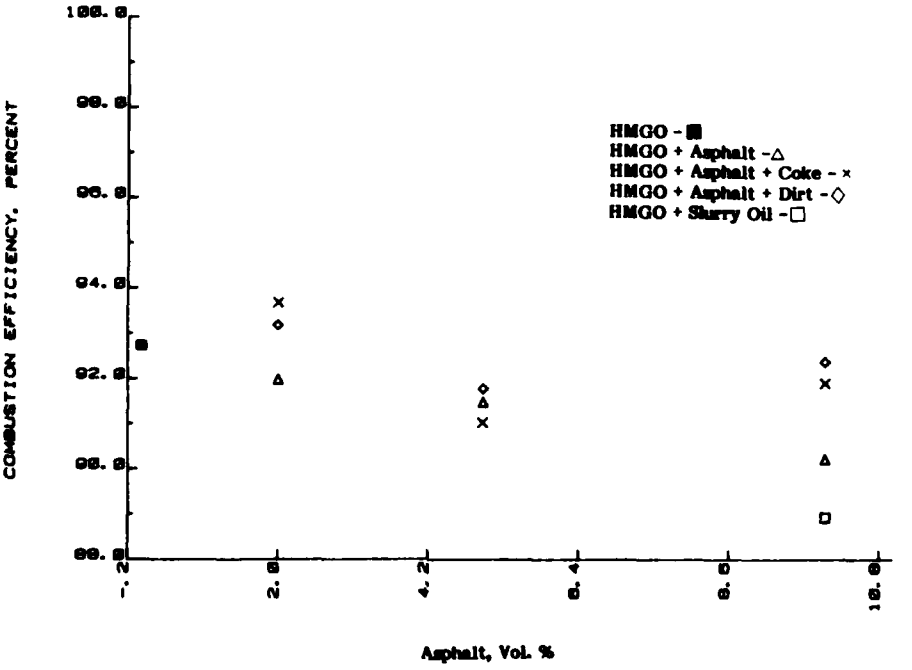

FIGURE 43. THE EFFECT OF ASPHALTS AND SLURRY OIL BLENDED WITH HMGO ON THE COMBUSTION EFFICIENCY MEASURED AT 10 PERCENT OF FULL POWER

appear to parallel the THC emissions. Fuels containing dirt and coke appear to have somewhat higher combustion efficiencies than the other fuels. Fuel Nos. 25 and 26 containing the slurry oil with catalytic fines have the lowest combustion efficiency. As mentioned before, this is because the slurry oil appears to be a less volatile and higher molecular weight material.

F. Deposit Formation

Due to the nature of the fuel contaminants tested in this work, it was expected that deposit formation in the combustor would be of concern. It appeared highly probable that the residual components of the test fuels would not evaporate completely in the combustion zone and would instead be carried by turbulent air movement to the relatively cool wall where they would adhere to the surface.

Figure 44 shows that neat NDF and HMGO form slightly more soot on the combustor walls than Jet A, but there is no indication that this light soot on the dome and primary zone sidewall would build up to an extent that it would cause a combustion performance problem. However, Figures 45 and 46 which compare neat NDF and neat HMGO with Fuel Nos. 7 through 12, i.e., NDF and HMGO each containing 2-, 5-, and 10-percent low resin asphalt, show that the asphalt contaminant causes significant deposit formation. Similar results were obtained from Fuel Nos. 13 through 24 containing asphalt with high resins and dirt. The deposit formations produced by Fuel Nos. 25 and 26 containing slurry oil with catalytic fines were also similar to those in Figures 45 and 46 obtained from the fuels containing low resin asphalts.

It is important to realize that fuel blends containing only 2 percent of the asphalt cause significant deposit buildup on the dome and primary zone sidewall. Increasing the concentration of asphalt in the fuel to 5 and 10 percent continues to increase the deposit buildup, but the increased rate of buildup appears to be less than proportional to the increase in asphalt concentration.

The deposits formed from both the asphalts and slurry oil contaminants had similar appearance. The deposits were hard and crisp, but they also had the characteristics of a plastic material in that they would bend appreciably before breaking. At the edges of air inlet holes in the combustor, the deposits would take the form of outcrops extending as far as 1.6 cm into the combustion volume.

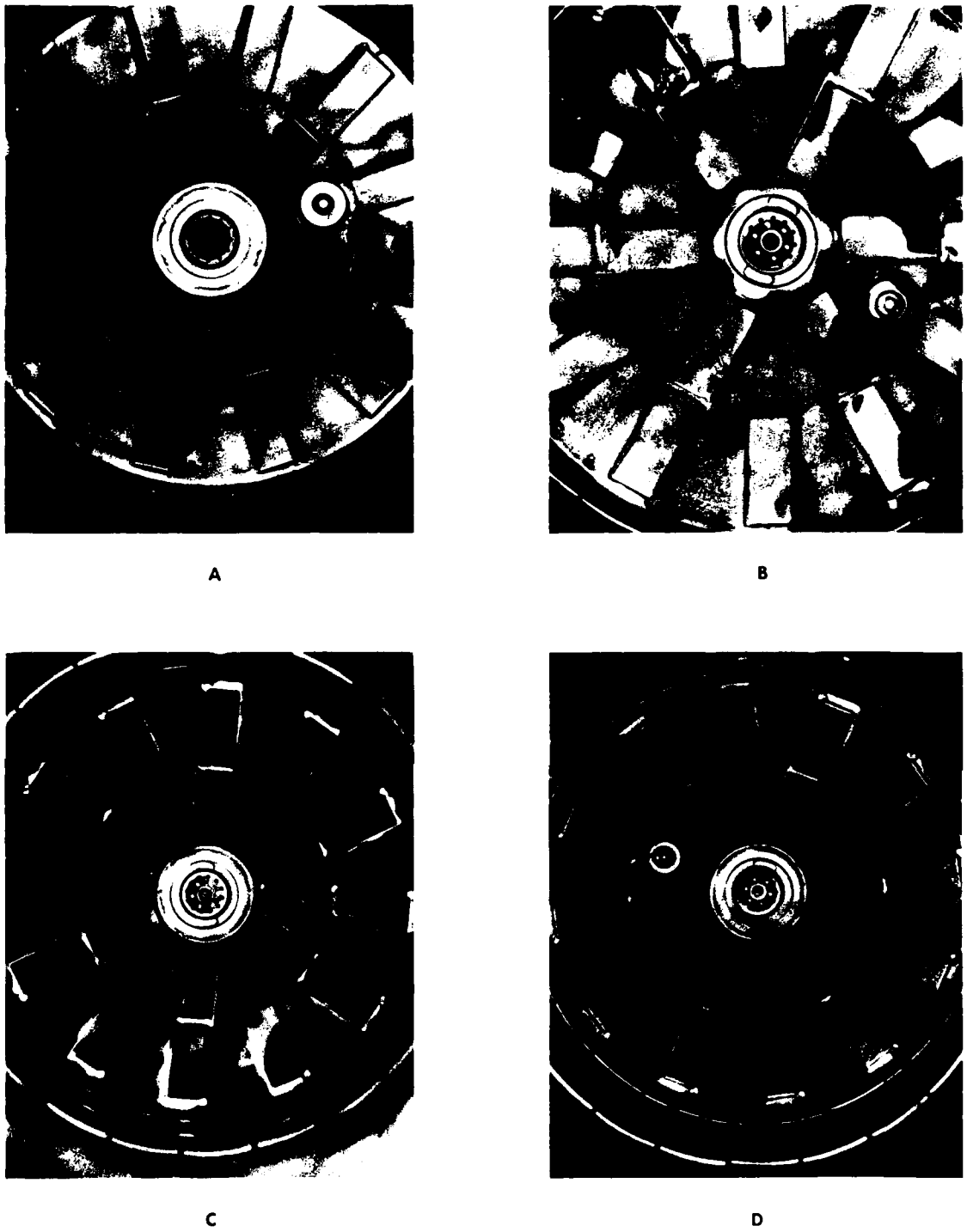

FIGURE 44. DEPOSIT FORMATIONS FROM JET A, NDF, AND HMGO PRODUCED IN 120-MINUTE TEST PROCEDURE
(A-Clean Liner; B-Burning Jet A; C-Burning NDF; D-Burning HMGO)

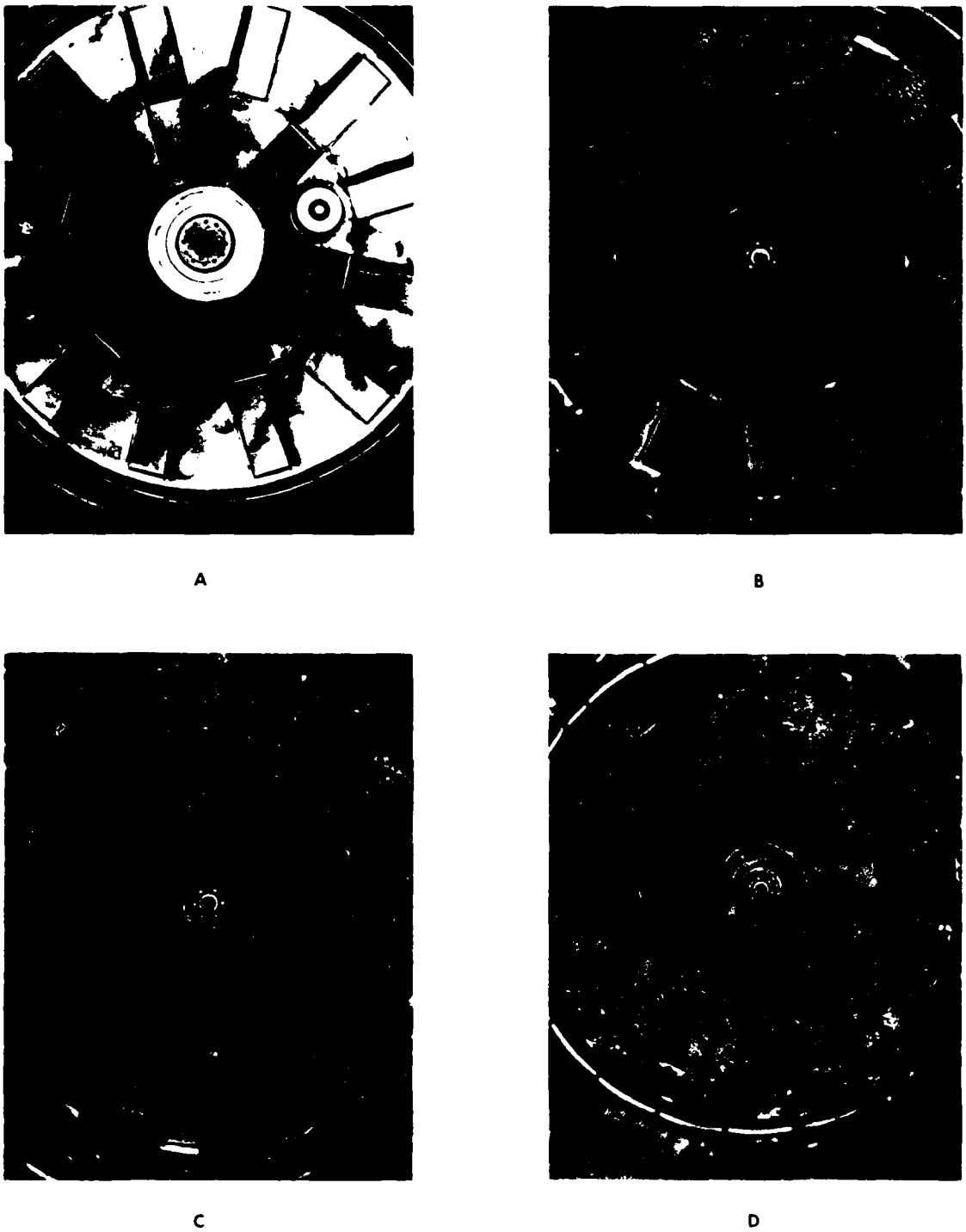

FIGURE 45. DEPOSIT FORMATIONS FROM NDF, NDF + 2-, 5-, AND 10-PERCENT ASPHALT PRODUCED IN 120-MINUTE TEST PROCEDURE
(A-Burning Neat NDF; B-Burning NDF + 2-Percent Asphalt; C-Burning NDF + 5-Percent Asphalt; D-Burning NDF + 10-Percent Asphalt)

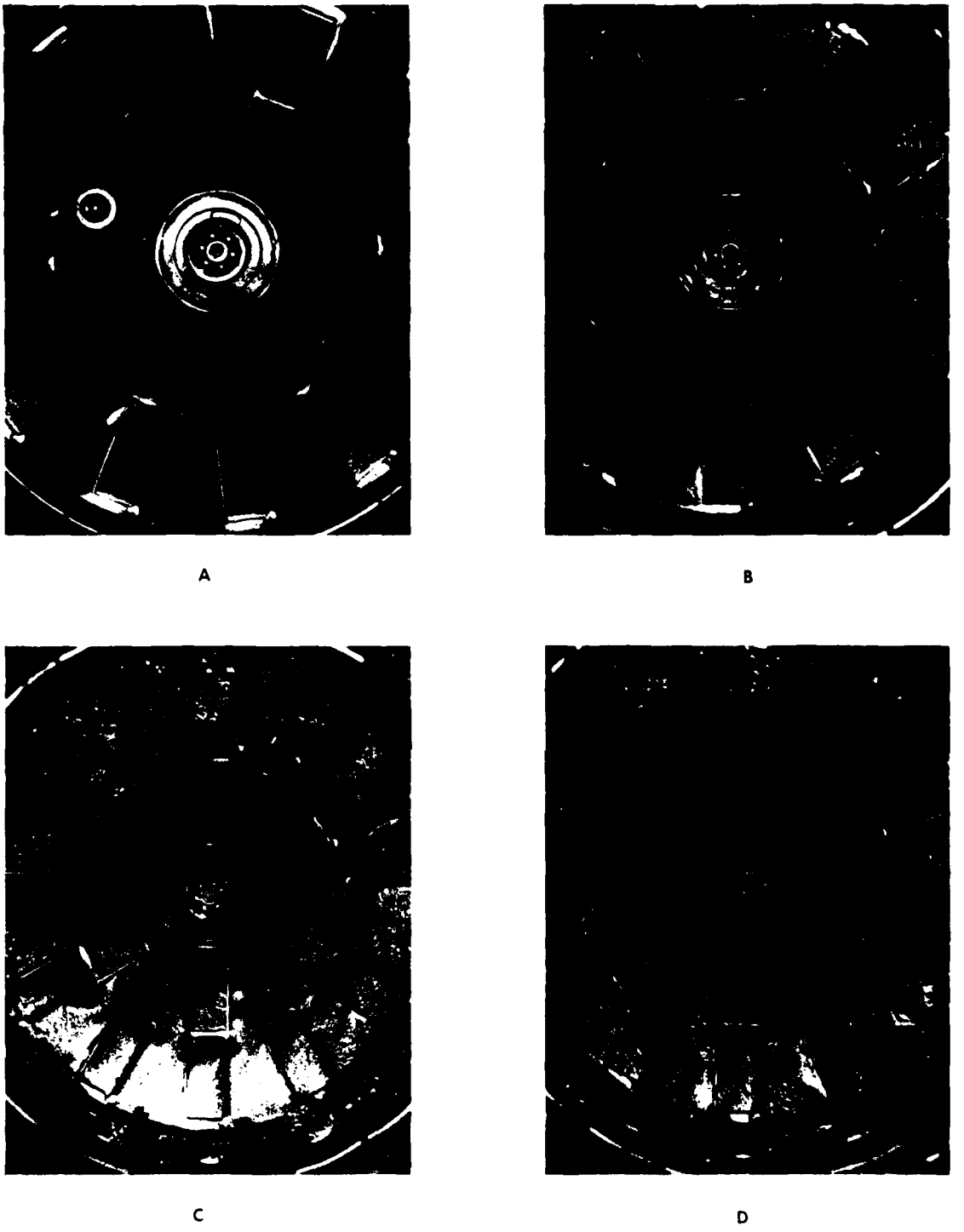

FIGURE 46. DEPOSIT FORMATIONS FROM HMGO, HMGO + 2-, 5-, AND 10-PERCENT ASPHALT PRODUCED IN 120-MINUTE TEST PROCEDURE
(A-Burning Neat HMGO; B-Burning HMGO + 2-Percent Asphalt, C-Burning HMGO + 5-Percent Asphalt; D-Burning HMGO + 10-Percent Asphalt)

Deposits formed from the low resin asphalt containing Fuel Nos. 7 through 12 were examined using thermogravimetric analysis and carbon/hydrogen analysis. The hydrogen contents of the deposits ranged from 5.7 to 7.5 percent, which is considerably less than the hydrogen content (12.3 percent) of the low resin asphalt blending stock. The deposits from Fuel Nos. 7 and 10 containing 2-percent asphalt had slightly lower hydrogen contents than the deposits from Fuel Nos. 9 and 12 with 10-percent asphalt. It seems reasonable to assume that deposits produced from fuels low in asphalt content would tend to loose volatile hydrocarbons to a greater extent than fuels with high asphalt contents, because the rate of deposit buildup on the surface is slower. Also, there is more time to evaporate hydrocarbons before new layers of deposit form. Since the volatile hydrocarbons are more hydrogen rich than the hard coke in the deposits, the hydrogen content of a deposit formed from a low asphalt fuel is expected to be slightly lower than that from a high asphalt fuel.

The carbon contents of the deposits from Fuel Nos. 7 through 12 ranged from 79 to 83 percent. This is somewhat lower than the 86.3-percent carbon content found in the asphalt blending stock. The combined carbon and hydrogen contents of the deposits range from 85 to 90 percent of the total weight. The remaining 10 to 15 percent was not determined, but it probably consists of sulfur and oxygen. It is well-known that sulfur concentrates in engine deposits (34), and oxygenates form in hydrocarbons when they are exposed to oxygen at high temperatures.(35)

The thermogram in Figure 47 shows that the low resin asphalt blending stock consists of three components, a volatile oil that evaporates between 50° and 210°C, a less volatile fraction that evaporates between 300° and 510°C, and a relatively non-volatile fraction that evaporates (or sublimes) between 520° and 1000°C. The three fractions starting with the most volatile account for 47, 44, and 9 percent of the total weight, respectively. The most volatile fraction (47 percent) appears to be a light oil or middle distillate constituent similar to a diesel fuel. The intermediate volatile fraction (44 percent) appears to be the asphaltenes, resins, and some other high molecular weight hydrocarbons. Note the combined asphalts and resins determined by the method of Strieter (13) account for only about 22 percent of the asphalt weight. The least volatile fraction (9 percent) resembles the carbon residue which was determined by ASTM Method D 524 to be 9.22 percent (see Table 5).

In comparing the thermogram of the low resin asphalt blending stock (see Figure 47) to that of a typical deposit, it is evident in Figure 48 that the volatile fraction is

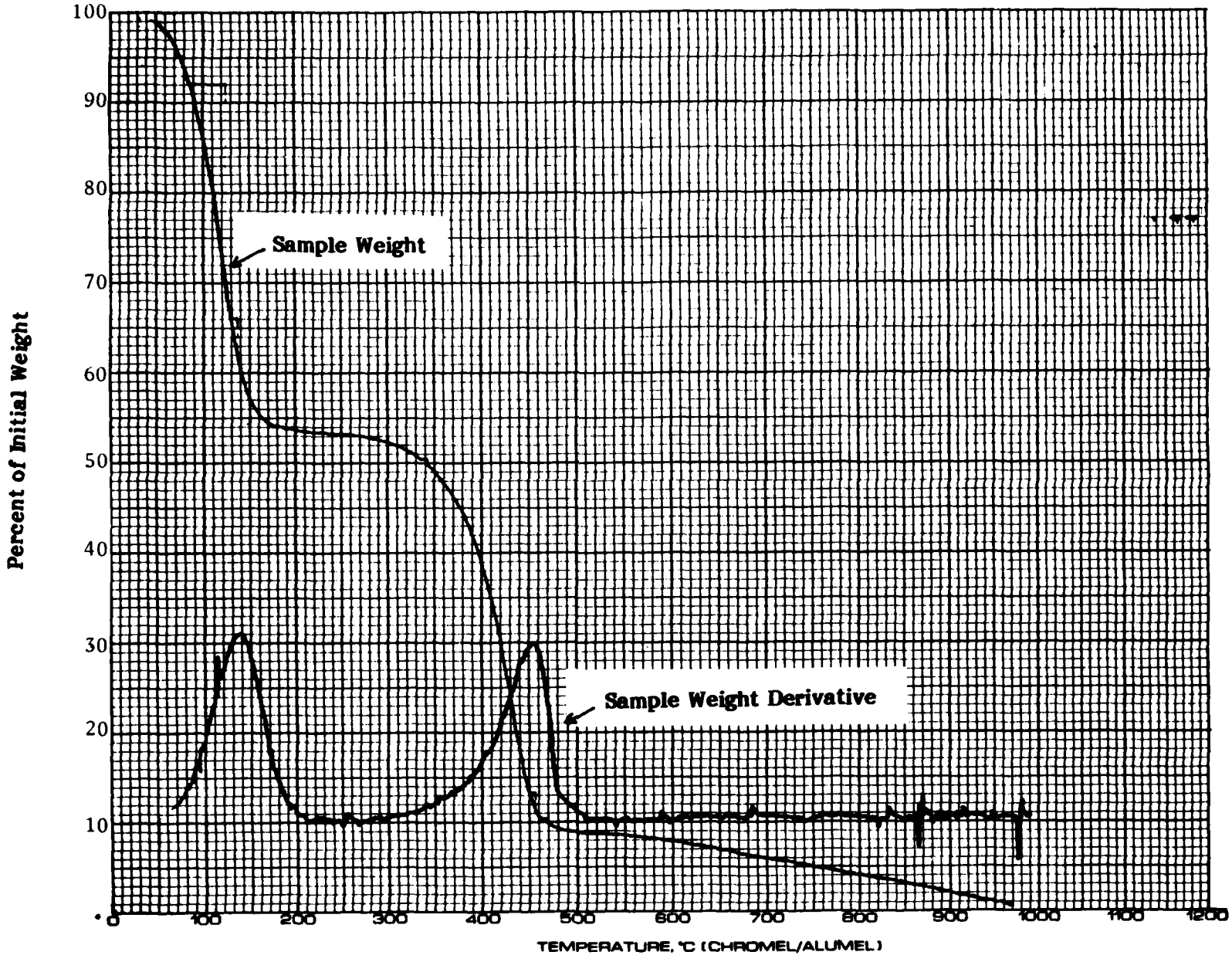

FIGURE 47. THERMOGRAVIMETRIC ANALYSIS OF LOW RESIN ASPHALT BLENDING STOCK R_1 (SEE TABLE 3)

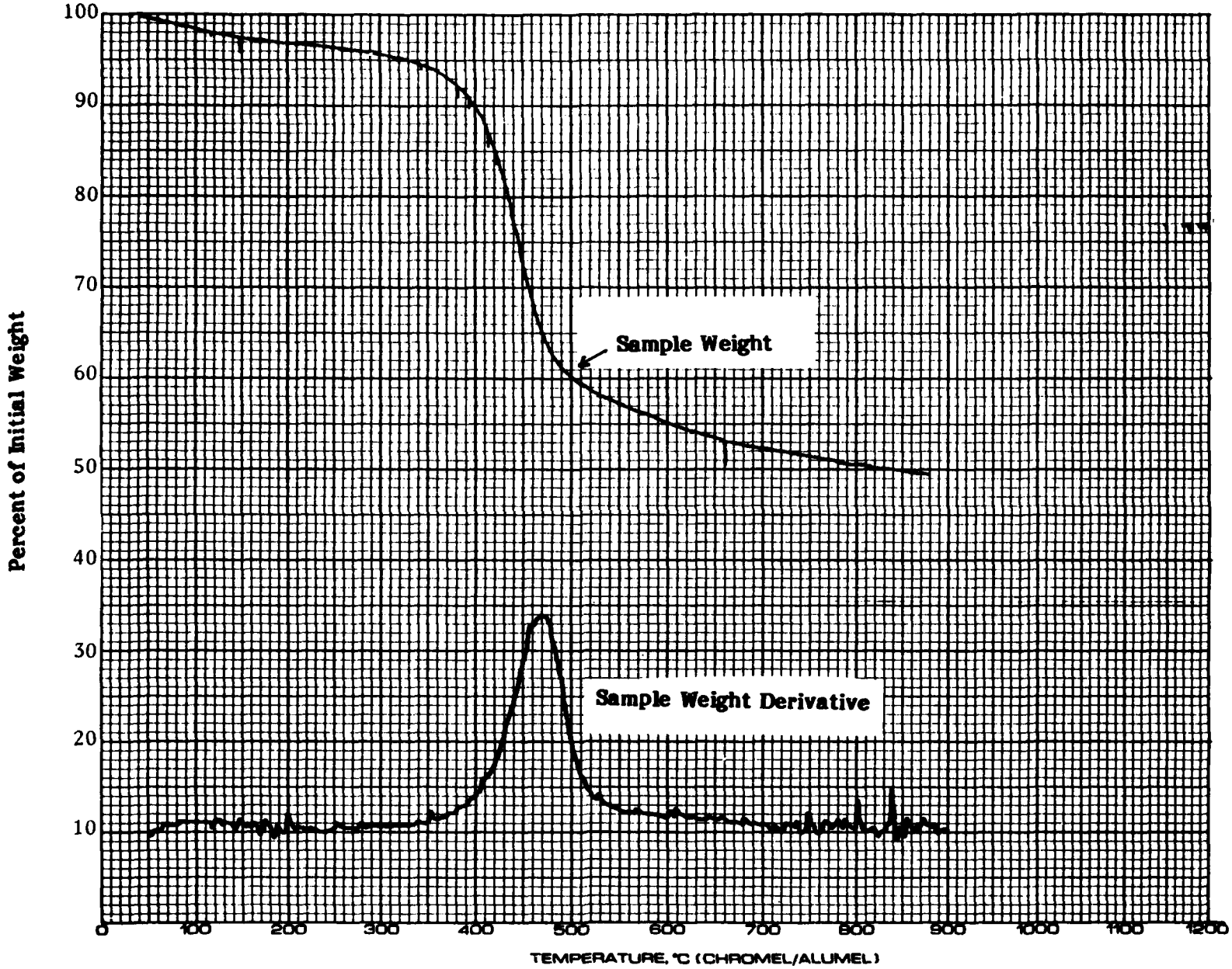

FIGURE 48. THERMOGRAVIMETRIC ANALYSIS OF COMBUSTOR DEPOSIT FORMED FROM FUEL NO. 8 (NDF + 5-PERCENT ASPHALT)

completely absent, but a significant portion of the intermediate asphalt fraction is still present in the deposit. The thermogram also shows that the relatively non-volatile carbon residue fraction from the asphalt material is even less volatile in the deposit and has appeared to have undergone considerable coking. It seems reasonable to conclude that the deposits were formed from the asphaltenes, resins, and carbon residue in the asphalt blending stock. It should be remembered from the test fuels section L that resins are classified in two categories of low and high molecular weight. The carbon residue is a material resembling coke and could be regarded as a high molecular weight resin constituent.

Deposit Burn-Off—In addition to characterizing the deposits according to their origin and composition, it was important in this program to investigate possible means of removing deposits once fixed on the combustor surface. Experiments were carried out to determine the possibilities of burning off the deposits by operating the engine on neat NDF or perhaps a lighter distillate such as JP-5.

Combustor tests were performed to determine the rate of deposit buildup with Fuel No. 9 (NDF plus 10-percent asphalt) and also the rates of deposit burnoff with neat NDF and JP-5. These tests were carried out at 55 percent of full power, which was assumed to be within the power range used for gas turbine engines used to generate electric power for Navy vessels.

Figure 49 shows the buildup of deposits caused by Fuel No. 9 (NDF plus 10-percent asphalt) and the burnoff when the combustor is operated on neat NDF and JP-5. For each data point in Figure 49, the combustor was disassembled and the liner was weighed. Special care was taken to reassemble the combustor so as not to disturb the deposit on the liner surface. The results show that in only 2 hours of operation, Fuel No. 9 (NDF plus 10-percent asphalt) caused appreciable deposit buildup. Switching to neat NDF was effective in burning off about 33 percent of the deposit in 1 hour of operation. Continued operation with neat NDF for 8 more hours had very little effect on the deposit. Finally, operation of the combustor on JP-5 for 2 hours reduced the deposit an additional 25 percent.

Figure 50 shows the results of two experiments: the buildup of deposit formed by Fuel No. 9 over a 6-hour period; and the deposit burnoff when the fuel is changed to JP-5 after two hours of buildup from Fuel No. 9.

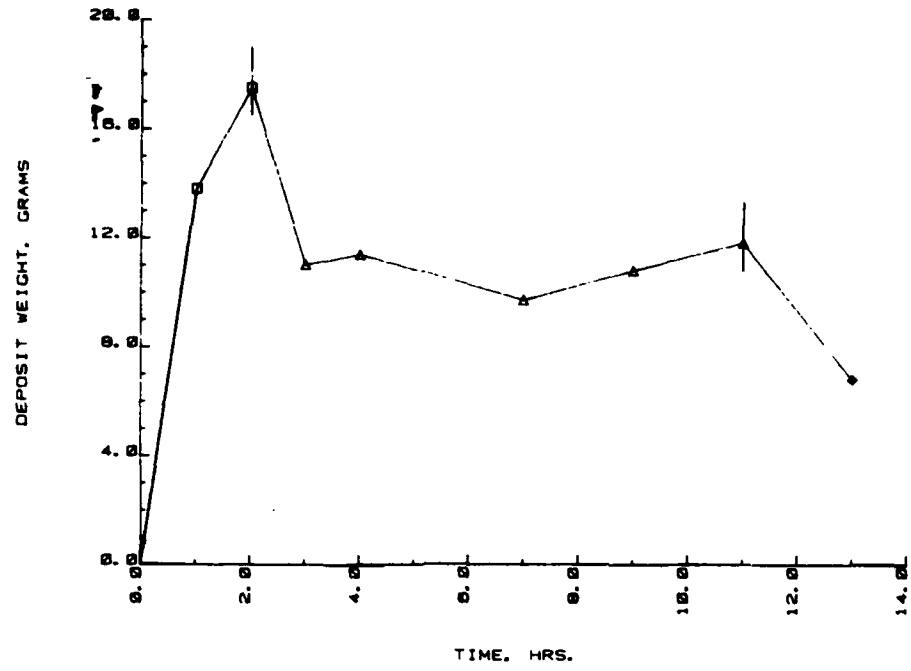

FIGURE 49. DEPOSIT PRODUCTION FROM FUEL NO. 9 (NDF + 10-PERCENT ASPHALT) -□; BURN-OFF WITH NEAT NDF-△; AND JP-5-◇

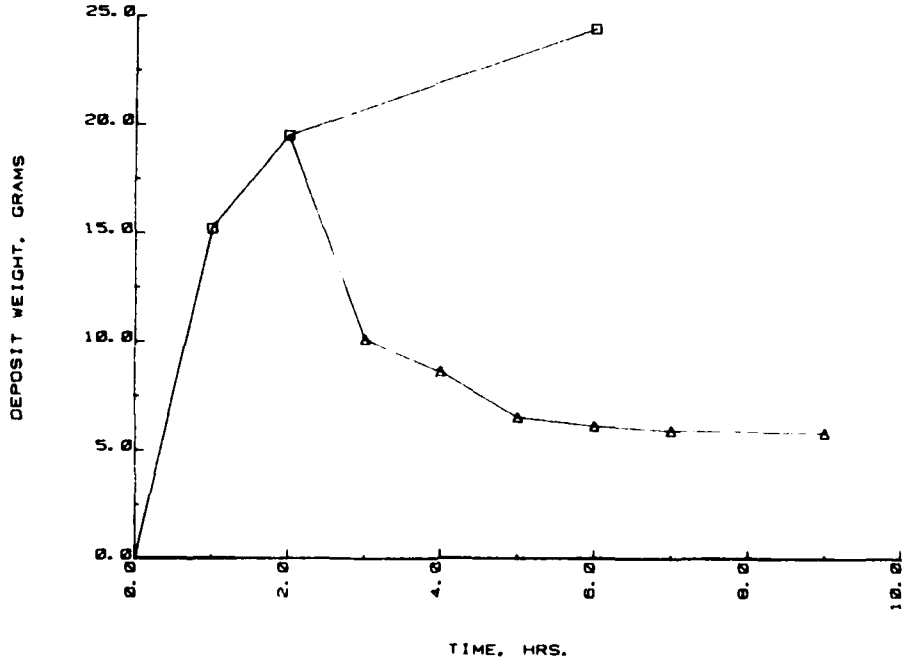

FIGURE 50. DEPOSIT FORMATION FROM FUEL NO. 9 (NDF + 10-PERCENT ASPHALT)-□; BURN-OFF BY JP-5-△

The results show that deposit buildup from Fuel No. 9 is very rapid in the first few hours of operation. The rate of deposit buildup decreased as the operation time increased. The data indicate that the rate may eventually approach zero. The rate of buildup appears to decrease with operation time because the surface area of deposit formations increase and gain more exposure to the hot combustion gases. After significant deposit outcrops have formed on the liner wall, the deposit material makes more contact with the combustion volume, and oxidation occurs there more easily than it would at the liner surface. Thus, the process of deposit oxidation tends to counterbalance the formation process.

When the fuel is changed to JP-5, the deposit is reduced substantially (approximately 47 percent) in 1 hour. A significant rate of deposit burnoff continues for about 5 hours until about 65 percent is burned off. After 6 hours, the rate of burnoff is very low, which indicates that the last 35 percent of the deposit might be very difficult to remove. However, the deposit remaining on the surface after 6 hours of operation did not seem to have any deleterious effect on the combustion performance. For example, the pattern factor and gaseous emissions were the same as they would be using a clean liner. Figure 51 shows photographs of the dome of the liner after: (a) 2 hours of operation on Fuel No. 9, (b) followed by 1 hour on JP-5, (c) and a total of 5 hours on JP-5. It is seen that significant deposit removal occurred in critical areas such as the fuel atomizer and spark igniter. It is concluded from these results that contaminated diesel fuels could be used in gas turbine power plants for limited durations and still be restored to near normal operation by using JP-5 to burn off deposits.

Fuel Temperature--It was important in this study not only to examine possible ways of removing deposits formed from contaminated diesel fuels, but to also investigate methods of preventing the formation of deposits. Since deposits appear to be formed because of incomplete fuel droplet evaporation, it was proposed that raising the fuel temperature would result in enhanced atomization and fuel vaporization. This would preclude the impingement of incompletely vaporized fuel droplets on the surface of the liner.

Combustion tests of 2-hour duration were carried out to measure the deposit-forming rates of Fuel Nos. 8 and 9, i.e., NDF containing 5- and 10-percent asphalt, at fuel inlet temperatures of approximately 80°F (26°C) and 170°F (77°C). At a fuel temperature of 80°F, Fuel Nos. 8 and 9 formed about the same weights of deposit. In one test, Fuel

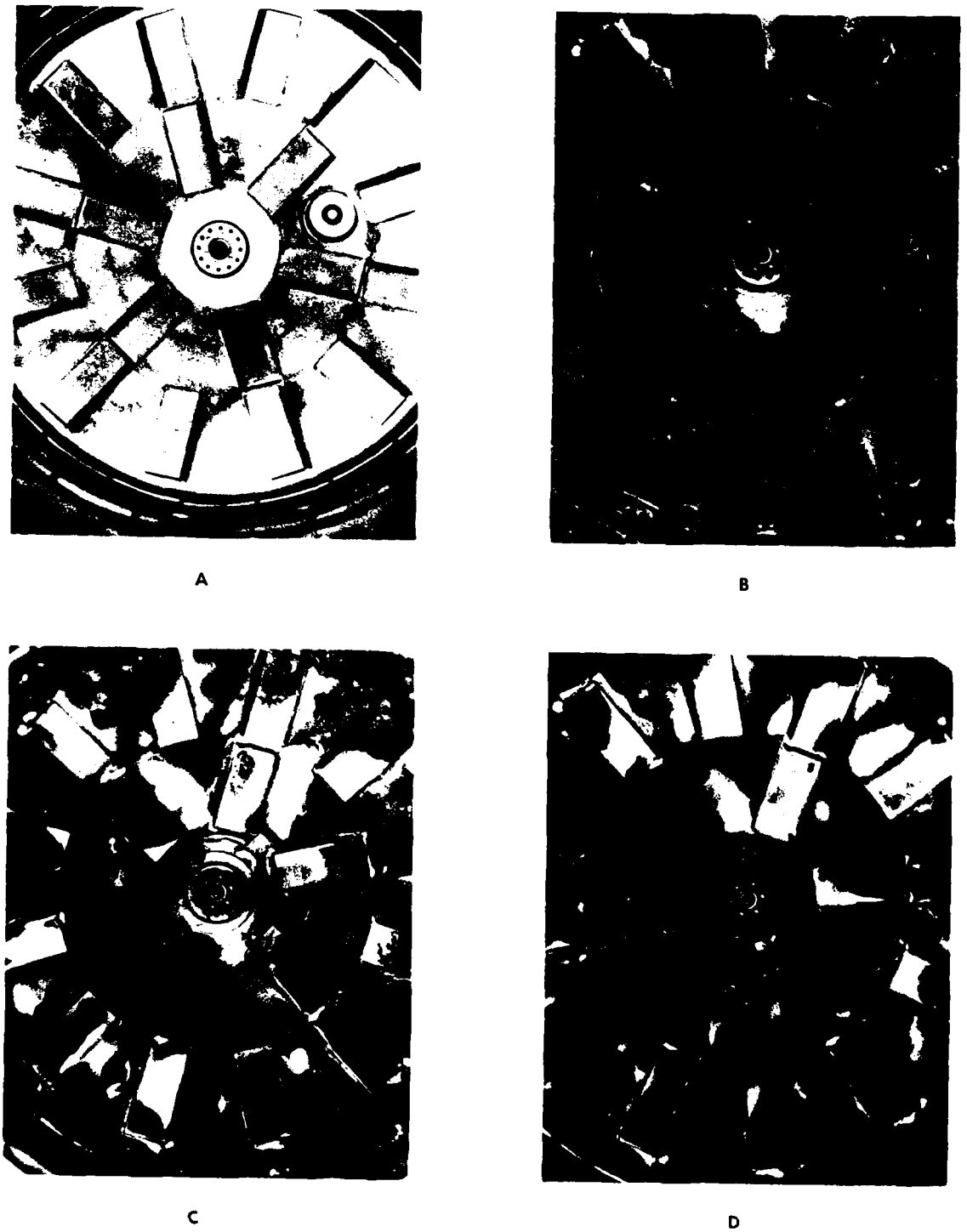

FIGURE 51. DEPOSIT FORMATION FROM FUEL NO. 9 (NDF + 10-PERCENT ASPHALT) AND BURN-OFF WITH JP-5
(A-Clean Liner; B-2-Hours Operation on Fuel No. 9 Followed by C-1-Hour Operation on JP-5; D-Total of 5 Hours Operation on JP-5)

No. 8 produced 17.5 and 19.5 grams in two separate tests. In combustor tests conducted at fuel inlet temperatures of 170°F, Fuel No. 8 produced 15.0 grams of deposit and Fuel No. 9 produced 17.1 grams. The results show that there is some beneficial effect of increasing the fuel inlet temperature. Comparison of photographs show that deposits formed on the fuel atomizer are significantly reduced when the fuel is heated. There was considerable clogging of the peripheral air holes in the atomizer when 80°F fuel was used. The air holes were entirely clear when the inlet fuel temperature was raised to 170°F. It is concluded that deposit formation can be reduced somewhat by increasing the evaporation rate of the fuel. As discussed earlier in section B, the rate of fuel vaporization is largely controlled by the initial droplet size. The fuel properties that affect droplet size are viscosity and surface tension. These properties are strongly dependent on the fuel temperature. On the other hand, the benefits of improving the atomization process by raising the fuel temperature or perhaps changing the atomizer are not very substantial and probably are not of practical importance.

IV. SUMMARY AND CONCLUSIONS

The following conclusions are drawn from the results of the ignition tests.

- Cold start ignition tests were performed on NDF and HMGO, blends of NDF and HMGO, blends of NDF and asphaltic contaminants, and a Jet A reference fuel for a total of nine fuels.

- A wide range of operating conditions was examined. Burner inlet temperatures ranged from 238 to 300K, reference velocities ranged from 4 to 16 m/sec, and fuel temperatures ranged from 267 to 300K.

- Cold start ignition tests carried out at a constant fuel temperature of about 300K showed that all the test fuels would ignite at burner inlet air temperatures down to 239K. Ignition occurred most easily at low reference velocities, about 5 m/sec.

- The fuel/air ratio required for ignition was strongly dependent on the fuel temperature and only weakly dependent on the burner inlet temperature. This supported the concept that ignition depends more strongly on atomization than on evaporation of the fuel.

- The ignitability of the test fuels was most dependent on their viscosity. It was found that a viscosity of 10 cSt was an upper limit if ignition is to be possible at burner inlet temperatures down to 238K (-31°F). The fuel temperatures for the 10 cSt viscosities of NDF and HMGO are 267K (22°F) and 298K (77°F), respectively.

- The ignition data were analyzed using the characteristic time model developed by Peters and Mellor.(17) Correlations of the characteristic times were obtained by using Sauter mean droplet size diameters (SMD) calculated from the empirical equation of Jasuja (21) and by using measured SMDs of sprays from the T63 atomizer. Both of the characteristic time model correlations using the two different sources for the SMD had high correlation coefficients ($R \simeq 0.9$). However, since the correlations were very different in intercept and slope, it was reasoned that the correlation based on the measured SMD should be used for predictions of ignitability of fuels in the T63 combustor. It was hoped that the use of measured SMDs would provide a superior correlation of the data. Unfortunately, since this was not found, future studies will have to address other aspects of the characteristic time model.

The following conclusions are drawn from the results of the droplet size measurements.

- The effect of fuel viscosity on atomization quality as measured by the SMD varies with nozzle design, and even with fuel flow rate for a given nozzle design.

- Of the four atomizers tested in this program, the fuel sensitivities, ranging from most sensitive to least, were in the following order: T63, DDA 501-K17, LM2500, and TF40B.

- The atomization quality of the distillate fuels contaminated with up to 10-percent asphalts (as high as tested) was comparable to uncontaminated fuels of similar viscosity. Thus, their atomization could be predicted simply from their viscosity, without any unusual behavior attributed to the presence of the very "heavy" contaminants.

- Atomization quality of fuels more viscous than NDF could be made equivalent to that of NDF by heating the fuels to an equivalent viscosity.

- Ignition for the T63 combustor required an average drop size (SMD) of about 60 to 80 micrometers at the lowest air flows, relatively independent of the fuel type. However, achieving this 60 to 80 micrometer drop size required significantly higher fuel flow rates and pressure drops with the more viscous fuels. Higher air flows required slightly smaller drop sizes for successful ignition.

- The T63 atomizer undergoes a transition in atomization behavior in the fuel flow range used for ignition. At fuel flow rates lower than the transition point, the drop sizes are too large for ignition. The transition point is related to a Weber number effect, and higher flow rates are required to reach the transition point for the more viscous fuels. This transition behavior is expected for all pressure swirl atomizers; however, except for the T63 atomizer the other three (DDA 501-K17, LM2500, and TF40B) were not tested to specifically identify such behavior.

- All four atomizers tested showed large radial variations in average drop size, with the smallest drops toward the centerline of the spray cone. The traditional measurement method for characterizing sprays by using laser-diffraction line-of-sight averages through the centerline results in an average weighted by the average size in the central core of the atomizer. For pressure swirl atomizers, this measured value is smaller than a true average value for the overall spray.

The following conclusions are drawn from the results of the flame radiation, liner temperature, and exhaust smoke measurements.

- The results show that the flame radiation and exhaust smoke from the 25 test fuels correlate with H/C atom ratio in essentially the same way as typical middle distillate jet fuels.

- The heavy residual oil components, asphalts and slurry oil with catalytic fines, which were blended with NDF and HMGO had a negligible effect on the flame radiation and exhaust smoke. This was due to the fact that the heavy components had hydrogen contents that were approximately the same as the base fuels NDF and HMGO.

- Liner temperatures on the dome and primary zone sidewall of the combustor were slightly higher for NDF, HMGO and blends thereof than for the reference fuel, Jet A. This was apparently due to the higher flame radiation from the test fuels.

- When fuel blends containing the heavy residual oil components were burned in the combustor, the liner temperatures were much lower than those of the neat base fuels. In fact, in several instances the liner temperatures of the dome and primary zone sidewall were lower than the burner inlet air temperature. This was attributed to deposition of fuel/asphalt mixtures on the liner surface followed by the evaporation of the lighter fuel components, thus lowering the surface temperature.

The following conclusions are drawn from the results of the gaseous emissions and combustion efficiency.

- The general patterns of the exhaust emissions and combustion efficiency followed expected trends. The total hydrocarbons (THC) and CO were highest at low power conditions, while the NO_x and combustion efficiency both increased with power.

- HMGO produced the highest THC and CO emissions. The THC and CO emissions decreased and the combustion efficiency increased as the concentration of HMGO in NDF decreased. The THC and CO emissions and combustion efficiencies were approximately the same for NDF and the reference fuel Jet A.

- The NO_x emissions were essentially independent of fuel properties.

- In general, the heavy residual oil components moderately increased the THC and CO emissions and reduced the combustion efficiency. However, there were some exceptions to this which indicated that the heavy residual oil components containing high resins (coke) and high ash (dirt) tended to lower the THC emissions and raise the combustion efficiency.

The following conclusions are drawn from the results on deposit formation in the liner.

- The blends of neat NDF and HMGO formed negligible deposits; they formed only slightly more soot on the dome and primary zone sidewall than the reference fuel, Jet A.

- All of the test fuels containing heavy residual oil constituents caused significant deposit formation on the dome and primary zone sidewall of the combustor.

- The deposit buildup increased as the concentration of heavy residual oil constituent was increased in the test fuel. However, the buildup was substantially less than in proportion to the concentration of heavy residual oil constituent.

- Thermogravimetric analysis showed that the deposits consisted of volatile and non-volatile fractions. The volatile fraction seemed to correspond to the asphaltenes and low molecular weight resins in the heavy residual oil component of the test fuel. The non-volatile fraction appeared to correspond to the carbon residue or high molecular weight resin in the heavy residual oil component.

- Substantial burnoff of deposits formed from contaminated fuels may be obtained by switching to a neat middle distillate. Neat NDF was effective in burning off some of the deposit; neat JP-5 was much more effective than NDF and would burnoff as much as 65 percent of the deposits in about 6 hours of operation.

- Raising the fuel temperature reduced the rate of deposit formation from contaminated fuels. However, this method of preventing deposit formation is only partial and should not be considered as a practical approach.

V. LIST OF REFERENCES

1. Lefebvre, A.H., "Gas Turbine Combustor Design Problems," Hemisphere Publishing Corporation, Washington, New York, and London, p. 39, 1980.
2. Moses, C.A., and Naegeli, D.W, "Fuel Property Effects on Combustor Performance," Final Report No. MED114, March, 1980.
3. Dodge, L.G., Naegeli, D.W., and Moses, C.A., "Fuel Property Effects on Flame Radiation in Aircraft Turbine Combustors," Presented at the 1980 Spring Meeting of the Western States Section/The Combustion Institute, 1980.
4. Naegeli, D.W., Dodge, L.G., and Moses, C.A., "Sooting Tendency of Fuels Containing Polycyclic Aromatics in a Research Combustor," Journal of Energy, 7 (2), p. 168, 1983.
5. Naegeli, D.W., Dodge, L.G., and Moses, C.A., "Effect of Flame Temperature and Fuel Composition on Soot Formation in Gas Turbine Combustors," Combustion Science and Technology, 35, p. 117, 1983.
6. Champagne, D.L., "Standard Measurement of Aircraft Turbine Engine Exhaust Smoke," ASME 71-GT-88, 1971.
7. Troth, D.L., Verdouw, A.J., and Verkamp, F.J., "Investigation of Aircraft Gas Turbine Combustor Having Low Mass Emissions," USAAMRDL Technical Report 73-G, Eustis Directorate, U.S. Army Air Mobility Research and Development Laboratory, Ft. Eustis, VA, April 1973.
8. Dodge, L.G., "Calibration of the Malvern Particle Sizer," Applied Optics, 23, p. 2415, 1984.
9. Dodge, L.G., "Change of Calibration of Diffraction-Based Particle Sizers in Dense Sprays," Optical Engineering, 23, p. 626, 1984.
10. Felton, P.G., Hamidi, A.A., and Aigal, A.K., "Multiple Scattering Effects on Particle Sizing by Laser Diffraction," Report No. 413HIC, August 1984.
11. Allen, T., Particle Size Measurement, 3rd Ed., Chapman and Hall, New York, p. 139, 1981.

12. Hardin, M.C., "Calculation of Combustion Efficiency and Fuel-Air Ratio from Exhaust Gas Analysis," Technical Data Report RN73-48, Detroit Diesel Allison Division, General Motor Corporation, Indianapolis, IN, 27 July 1973.

13. Streiter, O.G., "Method for Determining the Components of Asphalts and Crude Oils," Journal of Research NBS, Vol. 26, Research Paper RP1387, May, 1941.

14. Peters, J.E., and Mellor, A.M., "A Spark Ignition Model for Liquid Fuel Sprays Applied to Gas Turbine Engines," Journal of Energy, 6 (4), p. 272, 1982.

15. Peters, J.E., and Mellor, A.M., "Characteristic Time Ignition Model Extended to An Annular Gas Turbine Combustor," Journal of Energy, 6 (6), p. 439, 1982.

16. Ballal, D.R., and Lefebvre, A.H., "A General Model of Spark Ignition for Gaseous and Liquid Fuel-Air Mixtures," pp. 1737-1746, 18th Symposium (International) on Combustion, The Combustion Institute, Pittsburgh, PA, 1981.

17. Peters, J.E., and Mellor, A.M., "An Ignition Model for Quiescent Fuel Sprays," Combustion and Flame, 38, p. 65, 1980.

18. Leonard, P.A., Peters, J.E., and Mellor, A.M., "AGT-1500 Combustor and Fuel Effects Modeling," USARO Final Technical Report, Contract No. DAAG29-79-C-0169.

19. Plee, S.L., and Mellor, A.M., "Characteristic Time Correlation for Lean Blow Off of Bluff-Body-Stabilized Flames," Combustion and Flame, 35, p. 61, 1979.

20. Fenn, J.B., "Lean Flammability Limit and Minimum Spark Ignition Energy," Industrial Engineering Chemistry, 43, p. 2865, 1951.

21. Jasuja, A.K., "Atomization of Crude and Residual Fuel Oils," ASME Paper No. 78-GT-83.

22. Naegeli, D.W., Moses, C.A., and Mellor, A.M., "Preliminary Correlation of Fuel Effects on Ignitability for Gas Turbine Engines," ASME 83-JPGC-GT-8.

23. Hammond, D.C., Jr., "Deconvolution Technique for Line-of-Sight Optical Scattering Measurements in Axisymmetric Sprays," Applied Optics, 20, pp. 493-499, 1981.

24. Rizk, N.K., and Lefebvre, A.H., "Influence of Airblast Atomizer Design Features on Mean Drop Size," AIAA 82-1073, 1982.

25. Rizk, N.K., and Lefebvre, A.H., "Spray Characteristics of Simplex Swirl Atomizers,: presented at the Central States Section/The Combustion Institute, Paper CSS/CI83-19, 1982.

26. Simmons, H.C., and Harding, C.F., "Some Effects of Using Water as a Test Fluid in Fuel Nozzle Spray Analysis," ASME 80-GT-90, 1980.

27. Shirmer, R.M., and Quigg, H.T., "High Pressure Combustor Studies of Flame Radiation as Related to Hydrocarbon Structure," Phillip Petroleum Company, Report No. 3952-65R.

28. Lefebvre, A.H., "Progress and Problems in Gas Turbine Combustion," 10th Symposium (International) on Combustion," University of Cambridge, England, 1964.

29. Colket, M.B., Stefucza, J.M., Peters, J.E., and Mellor, A.M., "Radiation and Smoke From Gas Turbine Flames, Part II; Fuel Effects on Performance," Purdue University, Report No. PURDU-CL-77-01.

30. Naegeli, D.W., and Moses, C.A., "Effects of Fuel Properties on Soot Formation in Turbine Combustion," SAE Paper No. 781026.

31. Gleason, C.C., and Bahr, D.W., "Fuel Property Effects on Life Characteristics of Aircraft Turbine Engine Combustors," ASME 80-GT-55, 1980.

32. Glassman, I., Combustion, Academic Press, New York, San Francisco, and London, pp. 240-249.

33. Marrone, N.J., Kennedy, I.M., and Dryer, F.L., "Coke Formation in the Combustion of Isolated Heavy Oil Droplets," Presented at the 1983 Fall Meeting of the Western States Section/The Combustion Institute, 1983.

34. Vere, R.A., "Aviation Fuel Thermal Stability Measurements," Presented at the Conference on Long-Term Storage Stabilities of Liquid Fuels, Edited by Nahum Por, The Israel Institute of Petroleum and Energy, Tel Aviv, Israel, December 1983.

35. Mayo, F.R., Richardson, H., and Mayorga, G.D., "The Chemistry of Jet Turbine Fuel Deposits and Their Precursors," Presented before the Division of Petroleum Chemistry, Inc./American Chemical Society, Philadelphia Meeting, April 1975.

APPENDIX A

SPRAY CHARACTERIZATION OF THE LM2500, 501-K17, AND TF40B FUEL NOZZLES

LIST OF ILLUSTRATIONS

LIST OF TABLES

SPRAY CHARACTERIZATION OF THE LM2500, 501-K17, AND TF40B FUEL NOZZLES

INTRODUCTION

The main body of this report provides an analysis of the effects of alternative fuels to the standard Naval distillate fuel (NDF) on gas turbine combustor performance using a T63 combustor available at SwRI. The T63 combustor tests were extensive and included combustion efficiency, deposit formation, ignition, and other performance parameters. Included in these tests were measurements of the atomization quality of the T63 fuel nozzles on seven different fuels, which were used to help correlate the ignition test results. In addition to the tests with the T63 hardware, detailed atomization tests were conducted on atomizers from three different gas turbines in the Navy ship inventory, the LM2500, 501-K17, and TF40B. The atomization tests on these three atomizers are discussed in this Appendix. The results of these atomization tests may be combined with models such as the charcteristic-time model for ignition to predict fuel effects on ignition for these engines. These atomization data could also be used in more complex three-dimensional fluid flow and combustion models to predict other aspects of combustor performance such as deposit formation, emissions, or efficiency.

The performance of gas turbine combustors depends strongly on fuel atomization, particularly in the areas of ignition, low-power efficiency, soot formation, and gaseous emissions. Atomization is typically degraded by alternative or emergency fuels which are higher in viscosity and surface tension than the standard specification fuels. However, the sensitivity of combustors to fuel changes varies considerably, and atomization is a key parameter for combustion sensitivity. In order to estimate the sensitivity of gas turbines in the Naval ship inventory to changes in physical properties of the fuels, atomization tests were conducted with nozzles from an LM2500, a 501-K17, and a TF40B with seven fuels spanning a range of kinematic viscositities from about 1 to 10 cSt, and a range of surface tensions from about 25 to 31 dynes/cm.

The General Electric Co. (GE) LM2500 gas turbine engine is the main propulsion system for some ships in the destroyer and frigate classes. The LM2500 is a single-spool free-power turbine engine rated at 21500 hp (Navy) maximum continuous, and is

a derivative of the TF39 and CF6-6. The combustor is full annular type, while the atomizer is a dual-orifice pressure-swirl type, with thirty atomizers per engine. The atomizer tested was P/N 14481A.

The DDA 501-K17 is used to drive 2000 kW electrical generators. It is a single-spool free-power turbine engine rated at 3001 hp (Navy) maximum continuous, and is a derivative of the T56. The combustor is a can-annular reverse flow type with 6 dual-orifice hybrid air-blast/pressure-swirl atomizers per engine. Three different types of fuel atomizers have been used for this combustor. The first type was a single-entry nozzle with an internal flow divider. The single-entry nozzle suffered from fuel coking after shutdown, and was replaced by a dual-entry nozzle with an external flow-divider valve. This nozzle, manufactured by Rochester Products Div. of GM, features a quick-drain system which resolved the internal coking, but it suffers from coking on the outside of the nozzle during startup or shutdown. A second generation dual-entry nozzle, manufactured by Parker-Hannifin Corp., is currently being introduced into the 501-K17 fleet. No atomizers of the last type are currently available for testing, so the first-generation dual-entry nozzle was used for these tests. The atomizer tested was P/N 6899300.

The AVCO Lycoming TF40B is used for both lift and propulsion on the LCAC (Landing Craft Air Cushion). The engine is a single-spool free-power turbine rated at 3205 hp (Navy) maximum continuous, and is a derivative of the T55. The combustor is a reverse flow annular type, while the atomizer is a dual-orifice hybrid air-blast/pressure-swirl atomizer.

APPROACH: Experimental Facilities and Methods

Atomization measurements have been conducted for fuel nozzles from three types of gas turbine engines in the Navy ship inventory - the LM2500, 501-K17, and TF40B. Seven fuels were included in the atomization tests, and included numbers 2, 3, 4, 5, 8, and 9 from Table 4 (in the main body of the text). Additionally, aircraft fuel system calibration fluid (MIL-C-7024 Type II) was included, because it is an industry standard for fuel system and atomization tests. The physical properties of fuels are important to atomization, and these properties are given in Table A-1 for the fuels tested. These fuels include five that span the kinematic viscosity range of about 1 to

TABLE A-1. PHYSICAL PROPERTIES OF FUELS USED IN ATOMIZATION TESTS FOR LM2500, 501-K17, AND TF40B

Fuel No. From Table 4	Fuel Type	Specific Gravity	Kinematic Viscosity @ 40°C cSt	Kinematic Viscosity @ 20°C cSt	Kinematic Viscosity @ 0°C cSt	Surface Tension @ 23°C dynes/cm
-	Calibration Fluid (MIL-C-7024II)	0.770	0.96	1.25	1.72	24.95
2	NDF	0.8484	2.75	4.32	7.90	28.67
3	Blend 1	0.8565	3.42	5.69	11.00	29.15
4	Blend 2	0.8670	4.76	8.42	18.50	29.52
5	HMGO	0.8756	6.25	12.03	28.52	31.40
8	NDF +5% Resid.	0.8513	3.09	4.82	9.01	28.67
9	NDF +10% Resid.	0.8543	3.46		10.53	28.41

10 cSt, and two that represent standard NDF contaminated with 5 and 10 percent residuals. Attempts were made to test these atomizers at fuel flow rates for ignition, idle, and an intermediate power condition. These lower power conditions, particularly ignition, are usually more sensitive to atomization quality. Further, the flow rates for these atomizers are so high at higher power conditions that the sprays are too opaque to characterize with any optical instruments. In fact, even at the idle condition, the sprays from the LM2500 and 501-K17 were so dense that they required special procedures to correct for the multiple scattering of the laser beam. The high attenuation problem has been studied at this laboratory and is discussed in more detail in the body of the main report under "APPROACH, Section I, Droplet Size Measurement." The correction procedure used was developed by Felton, et al.(A-1)* In order to obtain drop-size data at higher fuel flow rates, other experimental approaches must be employed. These approaches might include use of the Aerometrics phase/doppler drop-sizing instrument and/or physically blocking successive parts of the spray. Combining measurements of different parts of the spray into overall averages is discussed by Dodge, et al.(A-2)

The overall spray structure resembles that shown in Figure A-1, and the comments in Section B of the Results are an appropriate description of the spray development, and the sampling process of the laser-diffraction drop-sizing instrument. Measurements of drop-size distribution were performed for each nozzle, fuel, and flow rate combination at a single axial location, 51 mm (2 in.) downstream of the tip, for several different radial chords from the centerline to the edge of the spray. These measurements through different chords correspond roughly to those indicated in Figure A-1, and were performed to better determine the overall spray characteristics. As mentioned in the main body of the report (RESULTS AND DISCUSSION, Section B, Droplet Size Measurements), measurements through various chords of the spray may be used along with a deconvolution computer program to convert the line-of-sight averaged drop-size data into drop-size data for each of the annular rings as shown in Figure A-1. The measurements taken for these atomizers were not spaced closely enough to perform a reliable deconvolution. Depending upon the inhomogeneity of the spray, measurements through about 10 chords from the centerline to the edge are required, while approximately 4 were recorded for these tests. However, the data

* Underscored numbers in parentheses refer to the list of references at the end of this appendix.

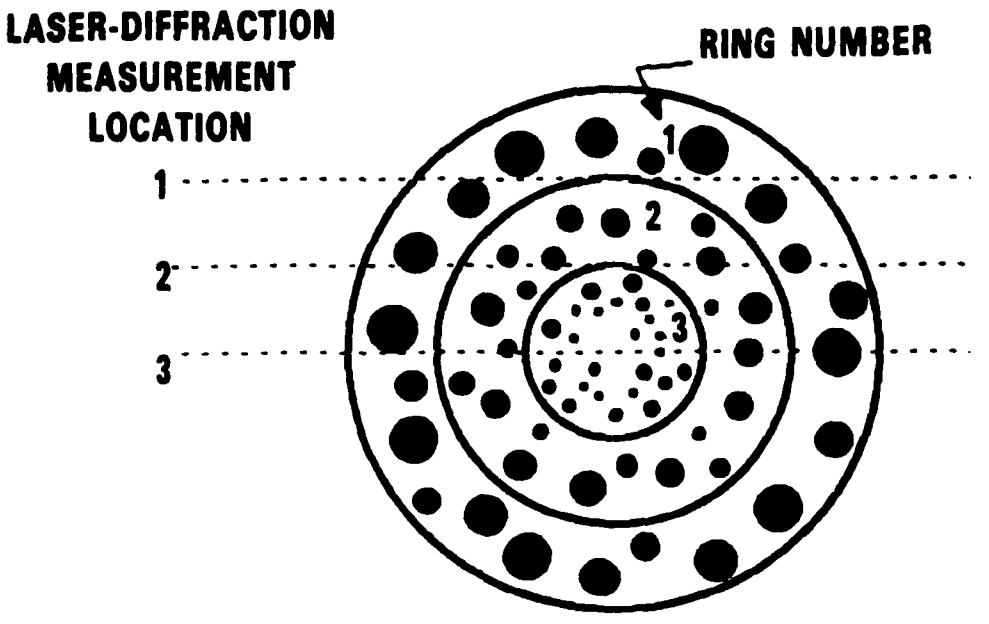

LINE-OF-SIGHT MEASURED VALUES

MEAS. LOCATION		INCREASING MEAS. AVG. SIZE	INCREASING MEAS. WIDTH OF DIST.
1	$SIZE_{AVG.} = SIZE_1$	↑	↓
2	$SIZE_{AVG.} = (CONC_1)(L_{21})(SIZE_1) + (CONC_2)(L_{22})(SIZE_2)$		
3	$SIZE_{AVG.} = (CONC_1)(L_{31})(SIZE_1) + (CONC_2)(L_{32})(SIZE_2) + (CONC_3)(L_{33})(SIZE_3)$		

$CONC_j$ = number density of particles in j-th ring

L_{ij} = path length through j-th ring at i-th measurement location

FIGURE A-1. PRESSURE SWIRL ATOMIZER SPRAY STRUCTURE

recorded do show the trends through the spray, with the smaller drops toward the center and the larger drops towards the edge.

The experimental apparatus was described in the main body of the report, under APPROACH, Section L, Droplet Size Measurement. Drop size data were obtained with a Malvern Model 2200 Particle Sizer, calibrated as previously described. For these tests, the laser power was degraded, resulting in a lower signal-to-noise ratio than normal for this instrument. The replacement laser did not arrive until tests were complete. All measurements were performed at atomospheric pressure and temperature in a spray chamber of square cross-section 30 cm on a side and 76 cm long, with air pulled through the chamber at a velocity of about 2.1 m/s by an explosion-proof exhaust fan.

For the majority of tests, fuel temperatures were maintained at 300 ± 3 K (80 ± 5°F). This simulates the temperatures of day tanks on shipboard which are maintained at about 300 K (80°F) to 306 K (90°F). A second set of measurements were performed with fuels more viscous than NDF heated to a temperature sufficient to reduce their viscosity to that of NDF at 300 K (80°F). The purpose of heating the fuels was to determine if the atomization quality of NDF could be duplicated by heating the fuels. The fuel temperatures required are shown in Table A-2 and Figure A-2.

TABLE A-2. FUEL TEMPERATURE REQUIREMENTS TO REDUCE FUEL VISCOSITY TO THAT OF NDF AT 26.7°C (299.9K or 80.0°F), OR 3.65 cSt

Blend #1	38°C	311K	100°F
Blend #2	50°C	323K	122°F
HMGO	62°C	335K	144°F
NDF + 5% Asphaltenes	32°C	305K	89°F
NDF + 10% Asphaltenes	37°C	310K	98°F

The fuel-flow rate/pressure-drop combinations used to test the three nozzles varied somewhat because the LM2500 atomizer has an internal flow-divider valve, while the 501-K17 and TF40B atomizers have an external flow-divider valve. All three of the atomizers tested were dual-orifice atomizers (e.g., primary and secondary or pilot and main), and the flow-divider valve determines the relative amount of fuel

AD-A173 747 COMBUSTION PERFORMANCE OF CONTAMINATED MARINE DIESEL FUELS IN A T63 GAS T (U) SOUTHWEST RESEARCH INST SAN ANTONIO TX BELVOIR FUELS AND LUBR D W NAEGELI ET AL 2/2

UNCLASSIFIED DEC 85 BFLRF-208 DAAK70-85-C-0007 F/G 21/4 NL

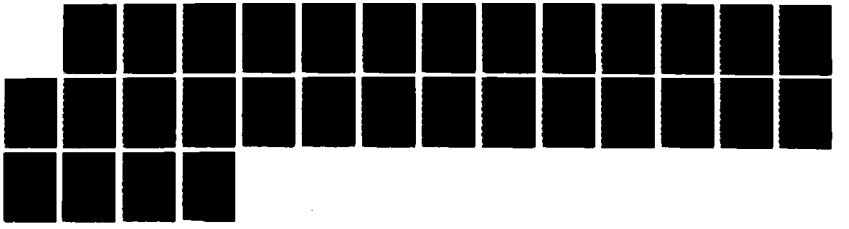

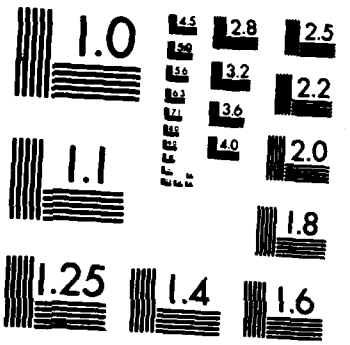

CROCOPY RESOLUTION TEST CHART
NATIONAL BUREAU OF STANDARDS-1963-A

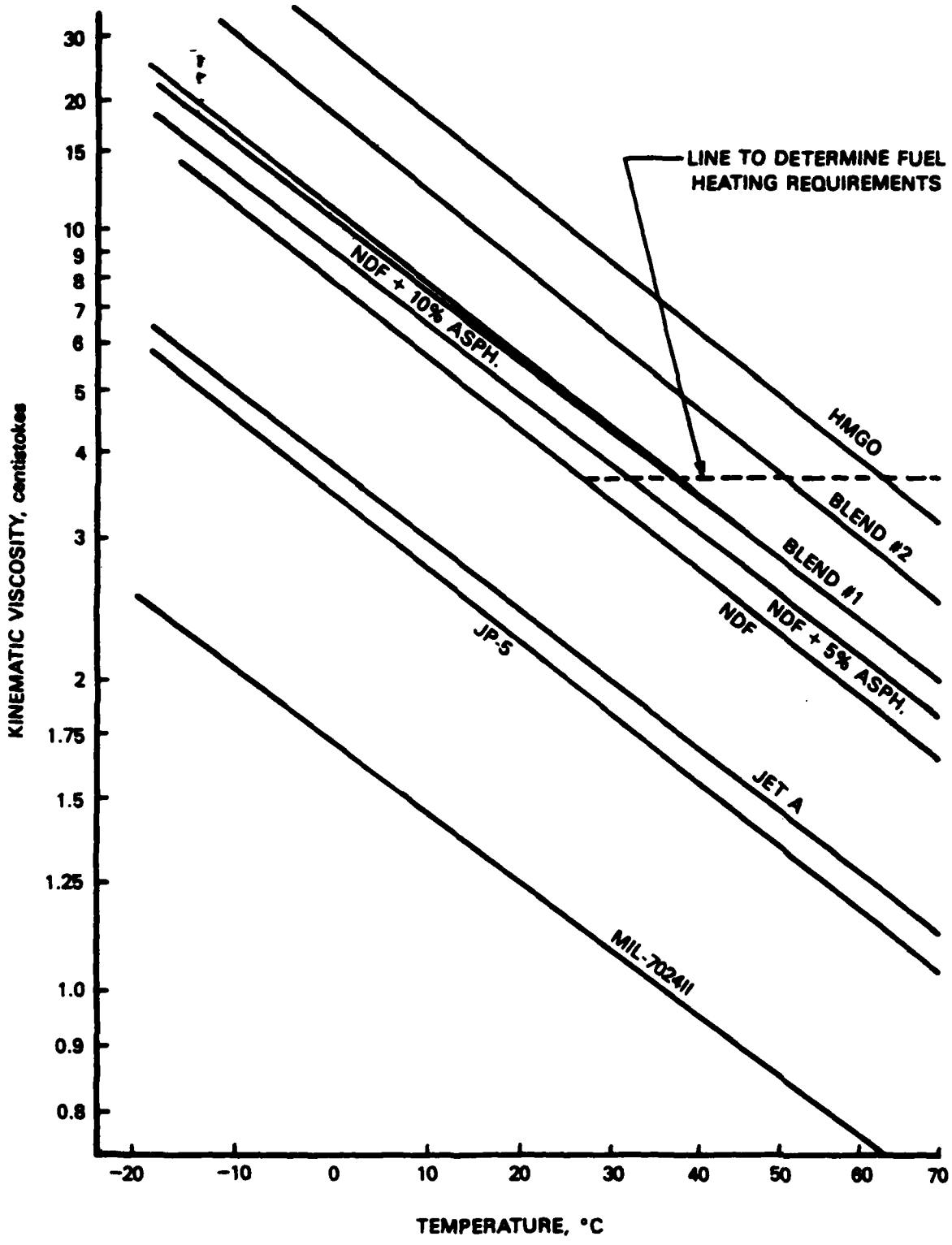

FIGURE A-2. EFFECT OF FUEL TEMPERATURE ON KINEMATIC VISCOSITY

delivered to each of the two orifices. For atomizers with only one fuel inlet, such as the LM2500, the flow-divider valve is internal to the nozzle, while atomizers with two fuel inlets, such as the 501-K17 and TF40B, perform the flow split external to the atomizer. In testing atomizers for fuel effects on spray quality, any one of three quantities may be kept constant - fuel pressure drop, mass flow rate, or volume flow rate. Because of fuel viscosity and density differences, the other two quantities must vary.

Since the flow-divider valve is sensitive to pressure, the LM2500 atomizer was tested at the same pressure drop for each fuel at a given condition and the volume flow rate was measured for each fuel. The pressure drop required to supply the fuel flow rate at ignition, idle, and an intermediate power condition were determined using M1L-F-16884H Navy Distillate fuel.

For the atomizers with external flow-divider valves (501-K17 and TF40B), the fuel supply line was connected to a tee which delivered fuel directly to the primary (or pilot) orifice, and the other side of the tee was connected through a valve to the secondary (or main). With the valve to the secondary closed, the fuel pressures required to deliver the primary fuel flow rate at the ignition, idle, and an intermediate power condition were determined using M1L-F-16884H Navy Distillate fuel. Then for each fuel tested the appropriate fuel pressure determined for M1L-F-16884H was set, and the valve to the secondary was adjusted to deliver the total (primary plus secondary) volume fuel flow required at a given condition.

The test matrix for all three atomizers is given in Table A-3.

RESULTS OF ATOMIZATION TESTS

Spray Structure and Radial Profiles

All three atomizers (LM2500, 501-K17, and TF40B) produced sprays similar in structure to that shown in Figure A-1, that is, approximately axially symmetric with the larger drops around the periphery of the spray. This structure is evident in Figures A-3 through A-7 which show the measured line-of-sight averaged Sauter mean diameter (SMD) from the centerline radially outward. Because of funding limitations,

TABLE A-3. TEST MATRIX FOR FUEL ATOMIZERS FOR LM2500, 501-K17, AND TF40B

(All Flow Rates are Per Individual Fuel Nozzle)

	Ignition	Idle	Intermediate Power
LM2500			
Fuel flow rate, lbm/hr	21.7	28.3	141.9
ml/min	193.	253.	1265.
ΔP, psid	88.	190.	417.
kPa (differential)	607.	1310.	2875.
501-K17 (dual entry)			
P/N 6899300			
Fuel flow rate, lbm/hr	62.5	144.2	*
ml/min	557.	1286.	*
Fuel flow rate, pilot only			
lbm/hr	36.8	37.8	*
ml/min	328.	337.	*
ΔP, psid	160.	165.	
kPa (differential)	1103.	1138.	
TF40B			50%MCP
Fuel flowrate, lbm/hr	5.4	12.5	47.1
ml/min	48.	111.	420.
Fuel flow rate, primary only			
lbm/hr	5.4	8.4	4.8
ml/min	48.	75.	43.
ΔP, primary, psid	82.	205.	65.
kPa (differential)	565.	1413.	448
ΔP, secondary, psid	0.	0.2	18.5
kPa (differential)	0.	1.4	128.
ΔP, air, inches H_2O	1.9	26.5	84.4
mmH_2O	49.	674.	2145.
psid	.07	.96	3.05

*Flow rates are too high for reliable drop-size measurements.

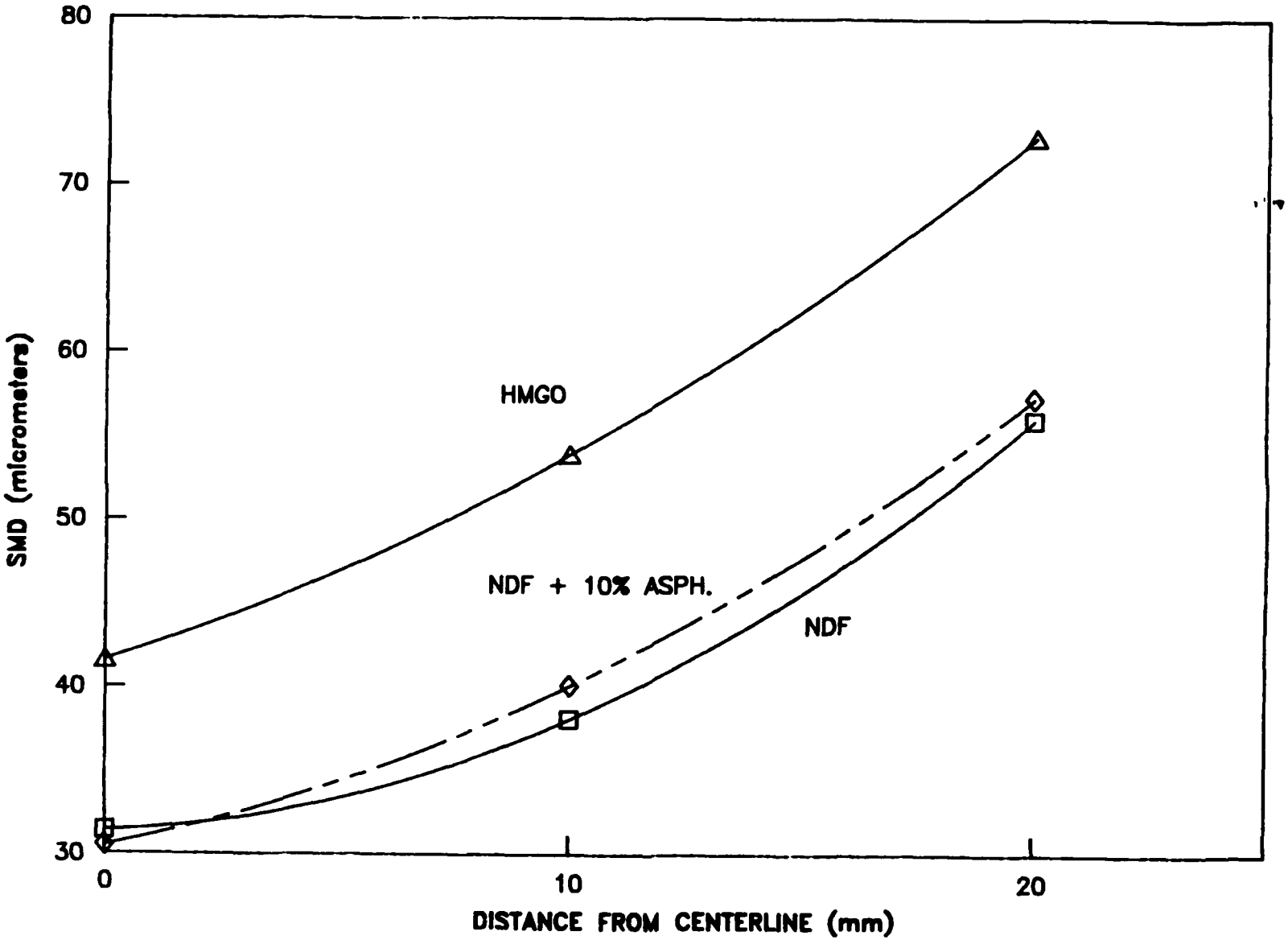

FIGURE A-3. MEASURED SMD AS A FUNCTION OF RADIAL LOCATION, LM2500 ATOMIZER AT IGNITION CONDITION, 51 MM AXIAL LOCATION

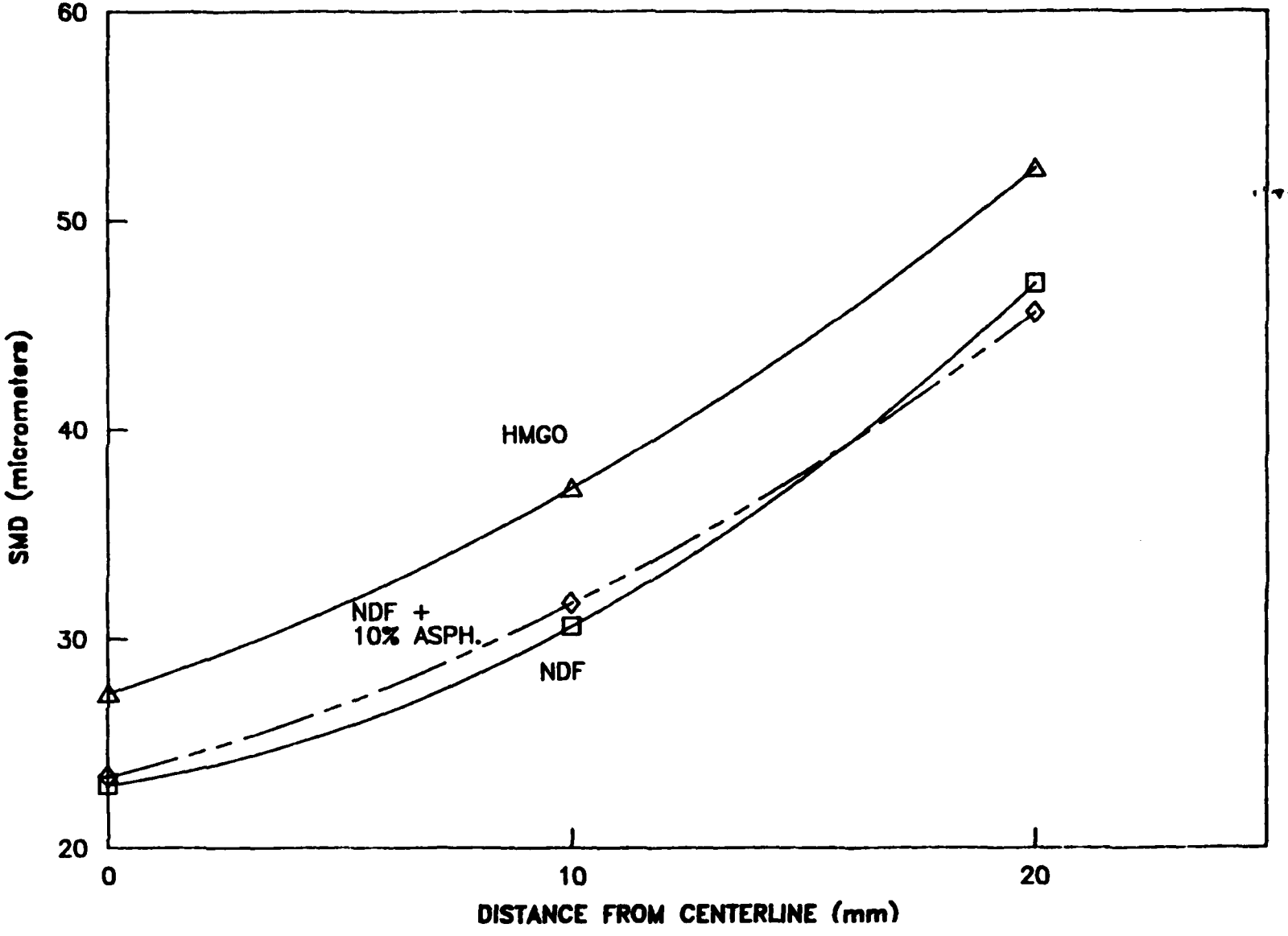

FIGURE A-4. MEASURED SMD AS A FUNCTION OF RADIAL LOCATION, LM2500 ATOMIZER AT IDLE CONDITION, 51 MM AXIAL LOCATION

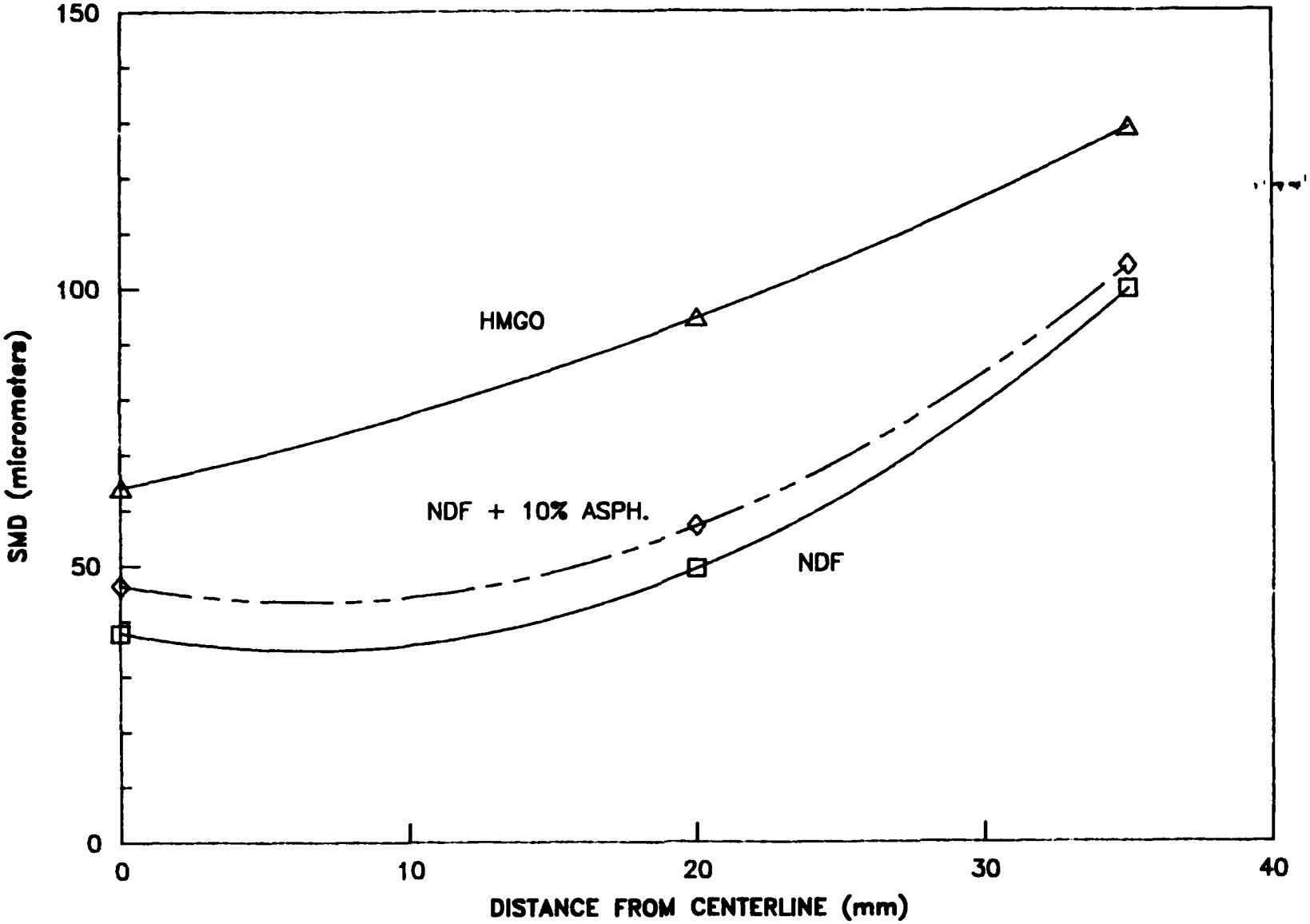

FIGURE A-5. MEASURED SMD AS A FUNCTION OF RADIAL LOCATION, 501-K17 ATOMIZER AT IGNITION CONDITION, 51 MM AXIAL LOCATION

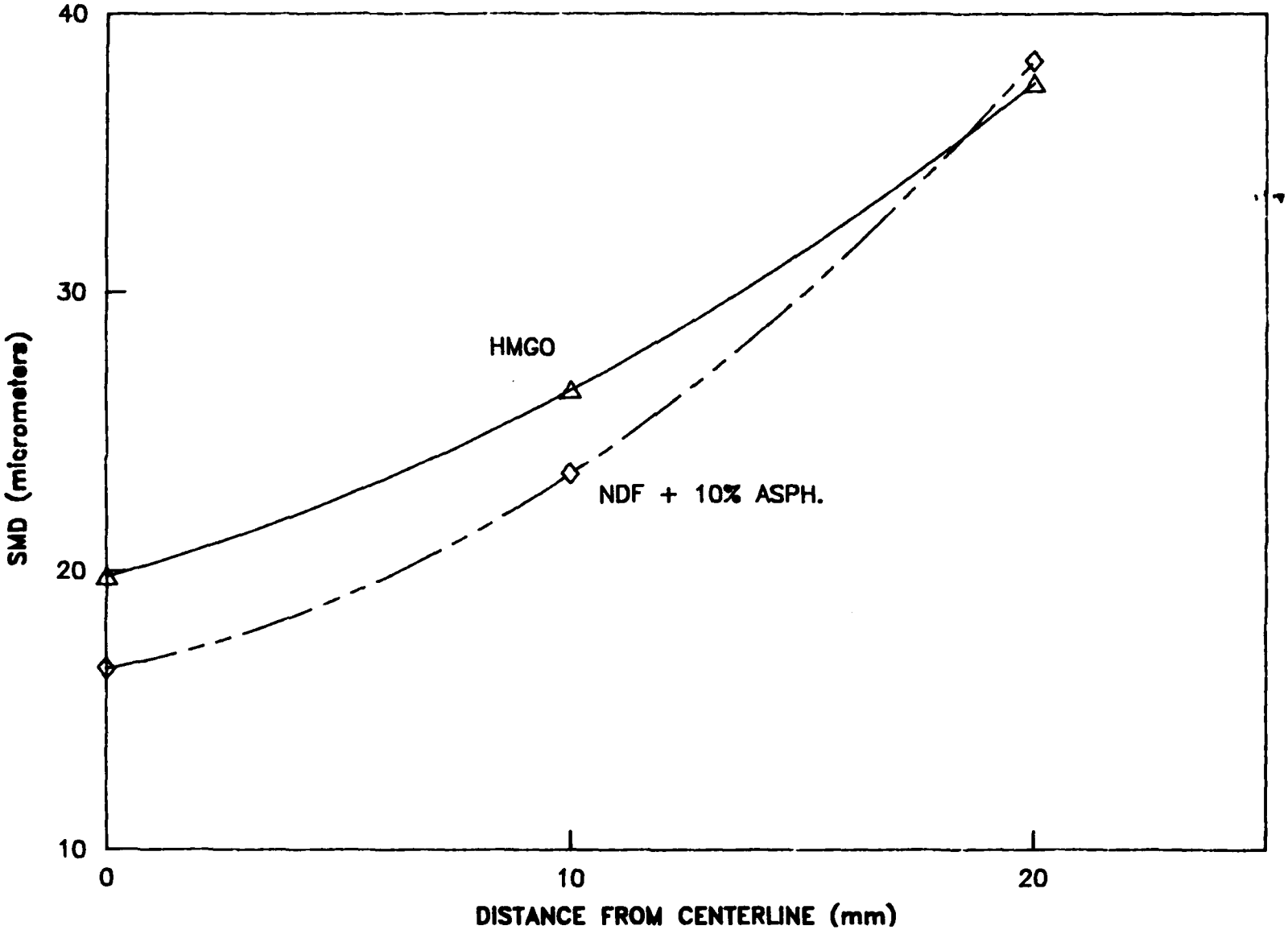

FIGURE A-6. MEASURED SMD AS A FUNCTION OF RADIAL LOCATION, TF40B ATOMIZER AT IDLE CONDITION, 51 MM AXIAL LOCATION

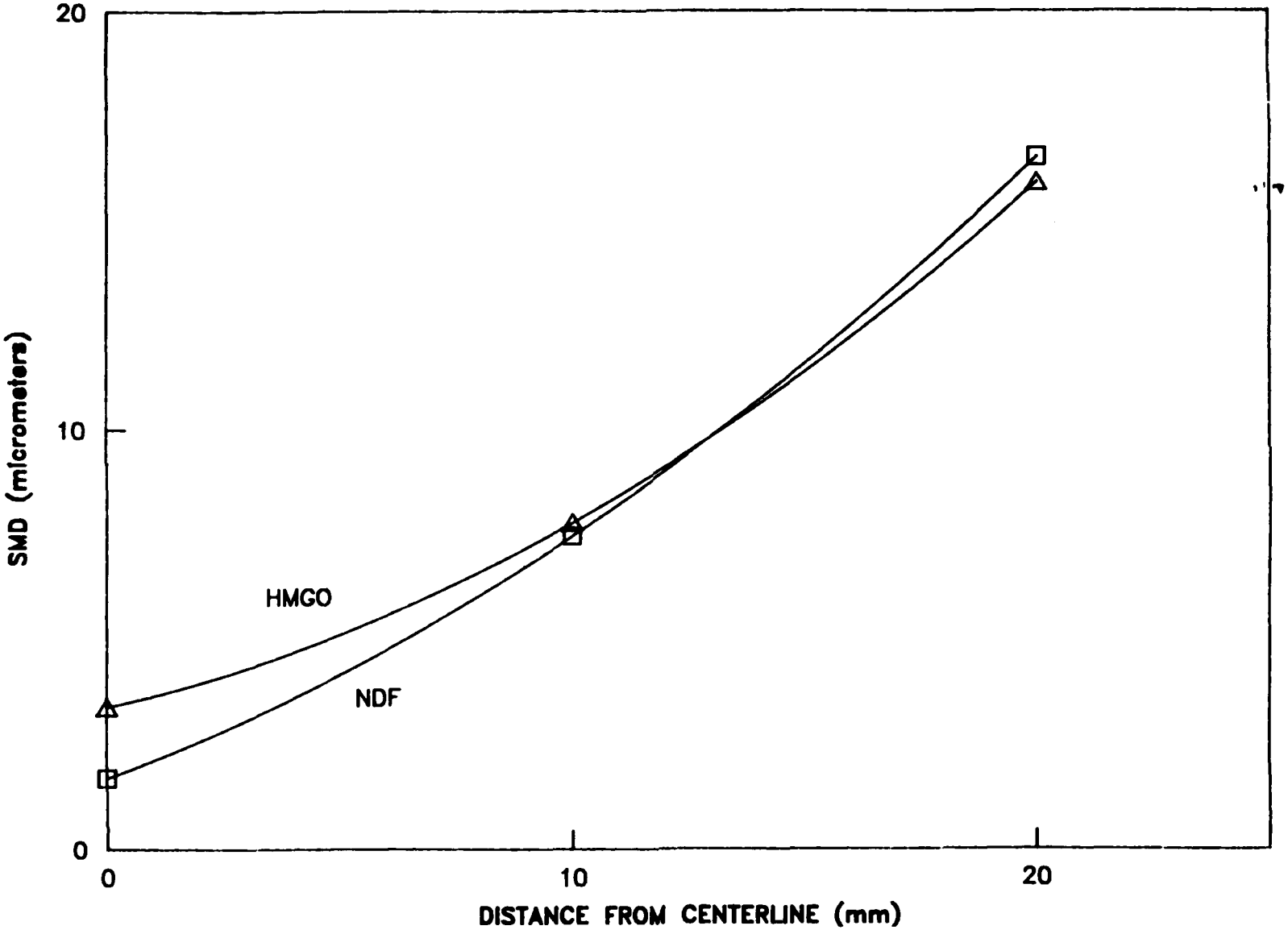

FIGURE A-7. MEASURED SMD AS A FUNCTION OF RADIAL LOCATION, TF40B ATOMIZER AT INTERMEDIATE POWER CONDITION, 51 MM AXIAL LOCATION

not all of the radial data were reduced, but data through the centerline and two other locations radially outward from the centerline are shown in each figure for two or three of the fuels.

Radial profiles for the LM2500 at an axial distance of 51 mm (2 in.) are shown in Figure A-3 for the ignition condition and in Figure A-4 for the idle condition. The spray density was too high (greater than 97 percent opacity) at intermediate power for reliable data reduction, even using the correction procedure for dense sprays.(A-1) Drop-size data for NDF, NDF contaminated by 10 percent asphaltenes (representing contamination by residuals), and HMGO all show similar trends of increased drop sizes towards the periphery of the spray. The more viscous HMGO produces the largest drop sizes, while the contaminated NDF shows only slightly degraded atomization relative to straight NDF.

A radial profile (at an axial distance of 51 mm) for the 501-K17 at the ignition condition (Figure A-5) shows similar trends to the data for the LM2500. The drop sizes for the 501-K17 are somewhat larger reflecting the higher fuel flows in that atomizer. Again the contaminated NDF shows slightly larger drop sizes than NDF, while the HMGO is significantly higher.

A radial profile for the TF40B at idle is shown in Figure A-6 and at intermediate power in Figure A-7. Trends of SMD versus radial distance are similar to the other atomizers, except that the drop sizes at intermediate power, where the air-blast effect becomes important, are extremely small and fuel properties are relatively unimportant for atomization.

Fuel Effects on Atomization

The effects of fuel properties on atomization were determined from measurements through the centerline of the atomizers, at an axial distance of 51 mm (2.0 in.) from the nozzle tips. The effect of fuel viscosity on atomization quality as measured by the centerline SMD is shown for the LM2500 atomizer in Figure A-8. The format of this figure is ln (SMD) versus ln (viscosity), with the straight line correlation representing an equation of the form

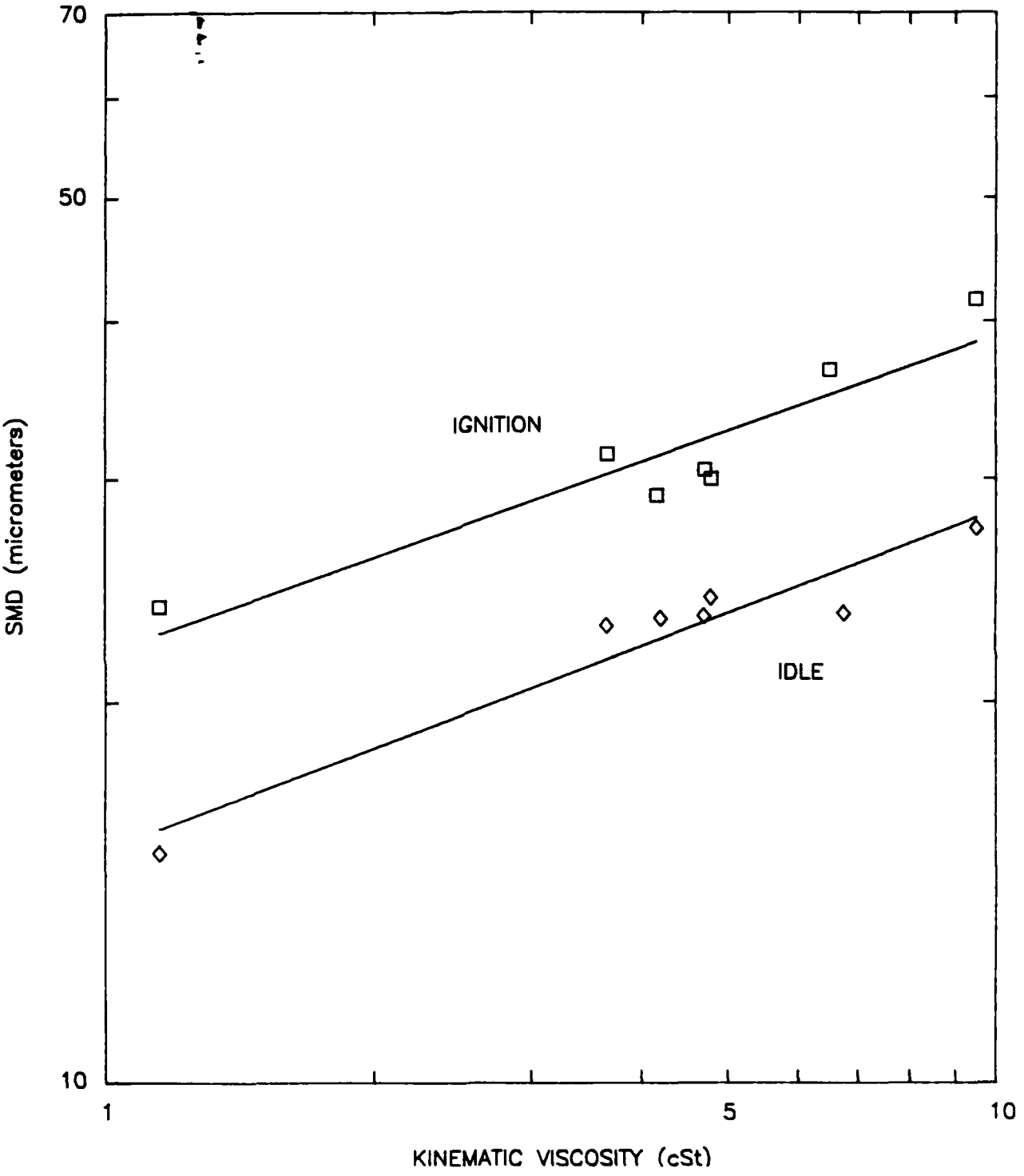

FIGURE A-8. EFFECT OF FUEL KINEMATIC VISCOSITY ON MEASURED CENTERLINE SMD FOR LM2500 ATOMIZER, 51 MM AXIAL LOCATION

$$\ln (SMD) = \alpha \ln (viscosity) + c \quad \text{(A-1)}$$

or

$$SMD = C_o \nu^{\alpha} \quad \text{(A-2)}$$

where α is the slope of the line and ν is the kinematic viscosity. Thus, α represents the fuel sensitivity for the atomization process. Typical values of α reported in the literature range from 0.16 to 0.25. Several conclusions may be drawn from Figure A-8. First, the data can be correlated reasonably well with an equation of the above form. Second, the value of α, which is 0.250 for ignition and 0.267 for idle, is similar for the two conditions tested and is in the expected range. Third, the two fuels contaminated with 5 and 10 percent asphaltenes (to represent contamination by residuals), which have kinematic viscosities of about 4.2 and 4.7 cSt, follow the same correlation as the other fuels. This implies that for soluble contaminants, the atomization quality (for at least this atomizer) can be predicted from the viscosity of the fuel, even though the contaminant is a mixture of very viscous asphaltenes.

A similar plot of ln (SMD) versus ln (viscosity) for the 501-K17 atomizer is shown in Figure A-9. As compared with Figure A-8 for the LM2500 atomizer, the slope is much steeper indicating a significantly greater fuel sensitivity. In fact, the value of α in Eq. (A-2) is 0.390 for ignition and 0.409 for idle. These tests were performed without air flow through the swirler valves around the nozzle which might affect atomization and fuel sensitivity. An air flow schedule was not available at the time of these tests. Typically at ignition conditions the air flow through an externally mixing atomizer is not significant, but at idle it may be significant.

The fuel sensitivity for the TF40B atomizer is shown in Figure A-10. At ignition conditions the value of the fuel sensitivity, α, is 0.231 which is typical of pressure swirl atomizers. However, at idle the internal-mixing airblast effect is significant and the drop sizes are reduced considerably, and the fuel sensitivity is much reduced to a value for α of 0.057. At the intermediate power condition, the SMD's are below 5 micrometers for all fuels, which is on the extreme low end of the instrument's range. Thus, the measured values have considerable uncertainty. For drop sizes this small, evaporation is extremely rapid, and fuel effects on atomization are relatively unimportant.

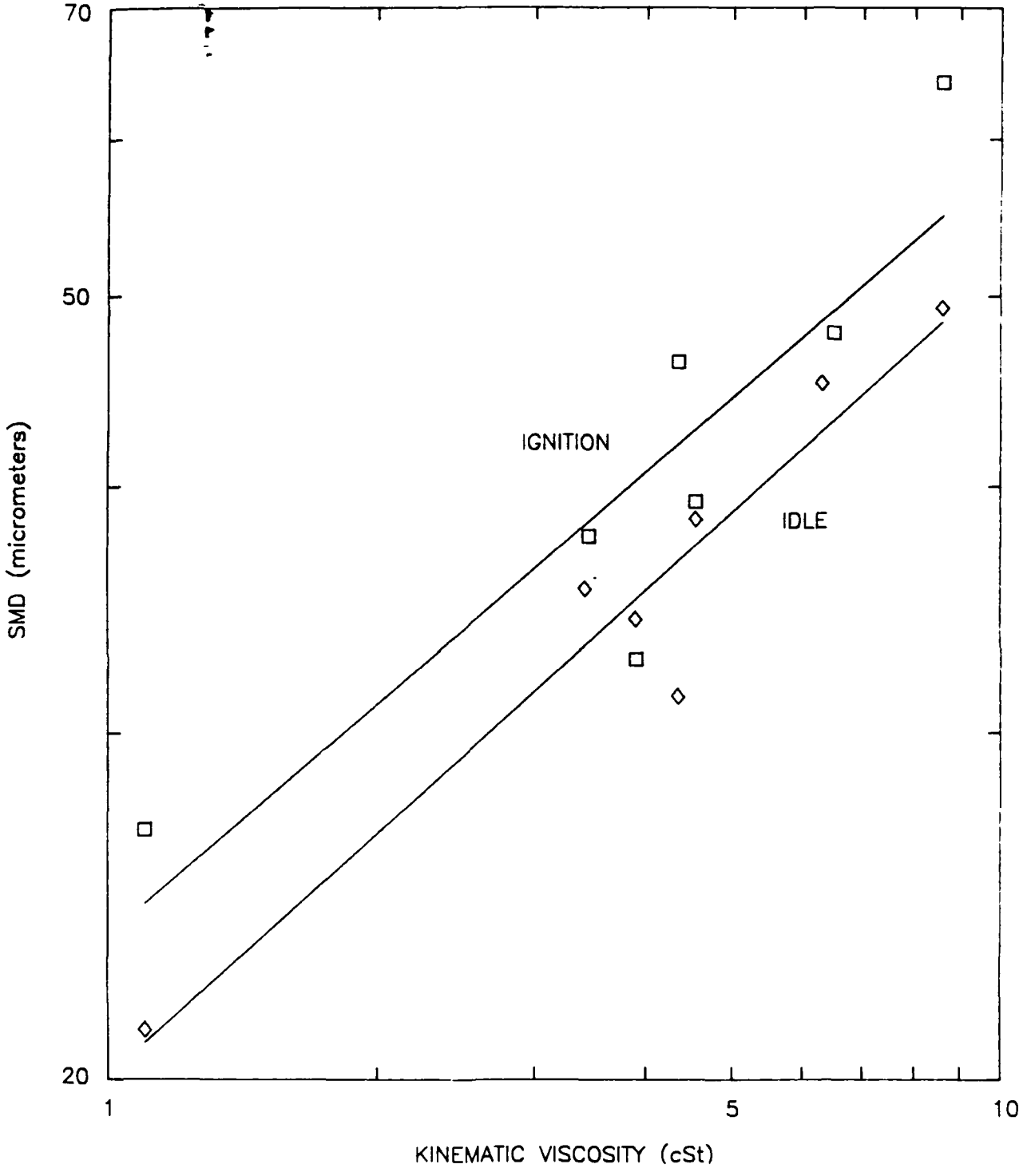

FIGURE A-9. EFFECT OF FUEL KINEMATIC VISCOSITY ON MEASURED CENTERLINE SMD FOR 501-K17 ATOMIZER, 51 MM AXIAL LOCATION

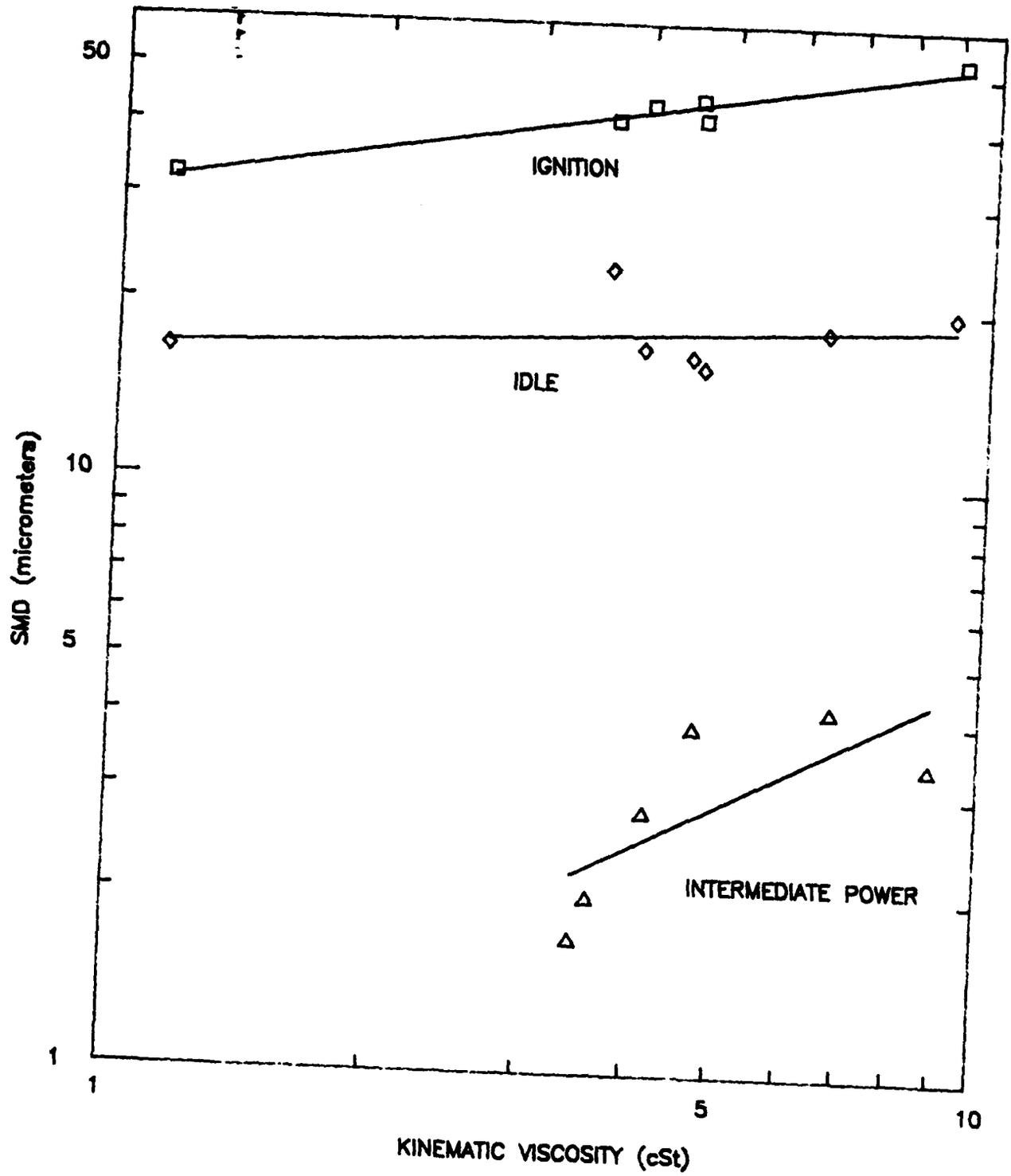

FIGURE A-10. EFFECT OF FUEL KINEMATIC VISCOSITY ON MEASURED CENTERLINE SMD FOR TF40B ATOMIZER, 51 MM AXIAL LOCATION

These fuel effects are summarized in Table A-4 which includes results for the three atomizers discussed above, the T63 atomizer discussed in the main text of this report, and four other atomizers tested previously for the Naval Air Propulsion Center. Included in Table A-4 is the value of α, the fuel sensitivity, as defined in Eq. A-2. Examination of Table A-4 leads to several conclusions. No single value of α is suitable for all atomizers. In fact, at different flow conditions, a given atomizer can have very different fuel sensitivities. Existing fuel spray correlations generally ignore this variation in fuel sensitivity, resulting in significant errors in predicting fuel-related effects on gas turbine combustor performance. The fuel sensitivity of the TF40B atomizer is significantly reduced when the airblast effect becomes important, in agreement with the lower fuel viscosity sensitivity generally reported for airblast atomizers.

TABLE A-4. DEPENDENCE OF SMD ON VISCOSITY FOR ATOMIZERS FROM SEVERAL GAS TURBINES IN THE NAVY INVENTORY
$(SMD \sim \gamma^{\alpha})$

Atomizer	Condition	α
LM2500	Ignition	0.250
LM2500	Idle	0.267
501-K17	Ignition	0.390
501-K17	Idle	0.409
TF40B	Ignition	0.231
TF40B	Idle	0.057
T63	Ignition (low flow)	0.472
T63	Ignition (high flow)	0.100
T63	Idle	0.731
T63	Cruise	1.070
T53 Start	Ignition	0.089
T53 Main	Ignition	0.368
T58 Primary	Ignition	0.090
T76 Start	Ignition	-0.026

Elevated Fuel Temperature Atomization Tests

The degraded atomization of the other fuels relative to NDF was attributed to their higher viscosity. Atomization tests were performed with the more viscous fuels heated to temperatures sufficient to reduce their viscosity to that of NDF at 300K (80°F) (see Table A-2 and Figure A-2), to see if equivalent atomization performance could be obtained. This may not always be a practical solution for two reasons. First,

in some systems, the fuels are heated significantly by pumping so that the temperature is very different from the storage temperature. Second, heating the fuels can increase thermal stability and coking problems. However, the question remains, "Could the atomization performance of NDF be duplicated by more viscous fuels through fuel heating?" The results shown in Table A-5 indicated that the answer is "Yes." That is, if the viscosity of any heavier fuel is reduced to that of NDF at the atomizer, then the atomization is equivalent to that of NDF. There is some scatter in the data in Table A-5 due to poor laser performance and temperature gradients in the atomizers, but basically the atomization performance of NDF was duplicated by the other fuels.

TABLE A-5. EFFECT OF INCREASED FUEL TEMPERATURE ON ATOMIZATION

Atomizer	Condition	Fuel No. in Tables 4 and A-1	Fuel	Fuel Temp. (K)	Fuel Temp. (°F)	Kinematic Viscosity (cSt)	SMD (μm)
LM2500	Ignition	2	NDF	300	80	3.65	31.4
		3	Blend 1	312	101	3.60	30.9
		4	Blend 2	322	120	3.80	27.2
		5	HMGO	336	145	3.60	28.3
		8	NDF+5% Resid.	304	88	3.65	27.0
		9	NDF+10% Resid.	309	97	3.70	30.5
LM2500	Idle	2	NDF	300	80	3.65	23.0
		3	Blend 1	312	102	3.55	21.5
		4	Blend 2	323	122	3.70	23.1
		5	HMGO	334	141	3.65	17.2
		8	NDF+5% Resid.	305	89	3.62	22.1
		9	NDF+10% Resid.	310	98	3.65	22.4
501-K17	Ignition	2	NDF	302	84	3.45	37.7
		3	Blend 1	311	100	3.65	32.7
		4	Blend 2	324	124	3.60	36.3
		5	HMGO	337	146	3.60	34.3
		8	NDF+5% Resid.	306	90	3.65	32.6
		9	NDF+10% Resid.	312	102	3.50	48.6
501-K17	Idle	2	NDF	303	85	3.42	35.5
		3	Blend 1	313	103	3.50	28.3
		4	Blend 2	322	120	3.80	42.1
		5	HMGO	334	141	3.80	35.8
		8	NDF+5% Resid.	306	91	3.60	34.7
		9	NDF+10% Resid.	313	103	3.45	34.0
TF40B	Ignition	2	NDF	300	80	3.65	41.2
		3	Blend 1	311	100	3.62	--
		4	Blend 2	324	123	3.60	39.3

TABLE A-5. EFFECT OF INCREASED FUEL TEMPERATURE ON ATOMIZATION (CONT'D)

Atomizer	Condition	Fuel No. in Tables 4 and A-1	Fuel	Fuel (K)	Temp. (°F)	Kinematic Viscosity (cSt)	SMD (μm)
		5	HMGO	336	145	3.60	28.3
		8	NDF+5% Resid.	305	89	3.62	40.2
		9	NDF+10% Resid.	310	98	3.65	46.0
TF40B	Idle	2	NDF	300	80	3.65	23.1
		3	Blend 1	312	102	3.55	14.8
		4	Blend 2	323	122	3.65	16.0
		5	HMGO	336	144	3.65	16.5
		8	NDF+5% Resid.	306	91	3.60	15.5
		9	NDF+10% Resid.	310	98	3.65	16.0
TF40B	Int. Power	2	NDF	302	84	3.45	1.7
		3	Blend 1	312	101	3.60	4.4
		4	Blend 2	325	125	3.55	5.4
		5	HMGO	335	143	3.70	4.5
		8	NDF+5% Resid.	307	92	3.60	3.9
		9	NDF+10% Resid.	311	99	3.60	3.1

CONCLUSIONS

1. For the fuels and atomizers tested, the average drop size, SMD, could be correlated with the kinematic viscosity, ν, in terms of a fuel sensitivity parameter, α,

$$SMD \sim \nu^{\alpha}$$

but the value of α varies for different atomizers, and, in some cases, varies at different flow rates for a given atomizer.

2. Of the three atomizers tested (LM2500, 501-K17, and TF40B), the 501-K17 showed the greatest fuel sensitivity. For a switch from NDF at 3.6 cSt to a 10 cSt fuel, the drop sizes for the 501-K17 would be increased by a factor 1.50. Since minimum ignition energies are proportional to SMD raised to a power of 3.0 to 4.5 (A-3), such an increase in SMD could lead to an increase in minimum spark energy required for ignition of a factor of 3.8 to 6.2. Other performance characteristics also vary with SMD raised to a power greater than unity, which underscores the importance atomization and its charcterization.

3. The atomization of NDF contaminated with very viscous residuals such as asphaltenes could be predicted from the viscosity of the overall fuel without any special accounting for the contaminants as long as particulates were not allowed to clog the atomizers.

4. The atomization performance of NDF could be duplicated by the more viscous fuels by fuel heating until their viscosities matched that of NDF. Of course, chemical differences are expected to lead to combustion problems.

5. All three atomizers exhibited significant radial variations in average drop size, with the largest drops near the outer part of the spray cone.

6. The spray density of all three atomizers was so high that tests were limited to low fuel flows. Physically blocking part of the spray would be required to make measurements at higher fuel flow rates.

RECOMMENDATIONS

1. The use of fuel heating to higher temperatures should be considered for utilization of more viscous fuels. Problems such as fuel coking would need to be considered.

2. Spray blocking techniques should be utilized to extend the measurements to higher flow rate conditions. Reference A-2 provides information on combining point measurements, which would result from spray blocking, into an overall average for the spray.

3. The Aerometrics phase/doppler drop sizer might have some advantages in the dense spray.

4. The atomization performance of the second generation dual-entry nozzle for the 501-K17 should be examined to determine if it is as fuel sensitive as the first generation single-entry nozzle. Also the effect of air swirl through the nozzle swirlers should be examined.

REFERENCES

A-1. Felton, P.G., Hamidi, A.A., and Aigal, A.K., "Multiple Scattering Effects on Particle Sizing by Laser Diffraction," Report No. 413H1C, August 1984.

A-2. Dodge, L.G., Rhodes, D.J., and Reitz, Rolf, "Comparison of Drop-Size Measurement Techniques: Malvern Laser-Diffraction and Aerometrics Phase/Doppler," to be presented at the Central States Section/The Combustion Institute, NASA/Lewis Research Center, May 1986.

A-3. Ballal, D.R., and Lefebvre, A.H., "A General Model of Spark Ignition for Gaseous and Liquid Fuel-Air Mixtures," Proceedings of the Eighteenth Symposium (International) on Combustion, The Combustion Institute, p. 1737, 1980.

APPENDIX B

COMBUSTION PERFORMANCE DATA: FLAME RADIATION AND EXHAUST SMOKE

Appendix B

Fuel No.	Composition	Flame Radiation	Exhaust Smoke							
			100% Power		75% Power		55% Power		10% Power	
			S.N.	mg/m^3	S.N.	mg/m^3	S.N.	mg/m^3	S.N.	mg/m^3
1	Jet A	116.0	17.78	2.08	13.78	1.52	11.88	1.29	4.57	0.48
2	NDF	175.4	33.51	5.52	--	--	--	--	--	--
3	NDF(70%) + HMGO(30%)	166.5	34.45	5.83	31.96	5.05	23.21	2.99	23.44	3.04
4	NDF(30%) + HMGO(70%)	187.3	36.66	6.61	33.35	5.47	23.39	3.03	23.41	3.03
5	HMGO	169.5	34.34	5.79	32.94	5.34	25.46	3.44	20.27	2.47
6	Jet A + Asphaltenes	113.0	16.94	1.95						
7	NDF + Asphaltenes (2%)	154.6	22.76	2.91	21.50	2.68	20.25	2.47	17.19	1.99
8	NDF + Asphaltenes (5%)	169.5	20.32	2.48	18.83	2.24	18.93	2.25	18.57	2.20
9	NDF & Asphaltenes (10%)	181.3	34.02	5.69	31.15	4.82	27.68	3.93	24.32	3.21
10	HMGO + Asphaltenes (2%)	181.3	34.83	5.96	33.15	5.41	28.12	4.04	19.60	2.36
11	HMGO + Asphaltenes (5%)	190.3	34.85	5.96	33.47	5.51	26.75	3.72	22.31	2.82
12	HMGO + Asphaltenes (10%)	166.5	30.08	4.53	28.46	4.12	22.53	2.87	22.54	2.87
13	NDF + (Asphaltenes - Coke) (2%)	175.4	20.40	2.49	19.60	2.36	16.49	1.89	14.00	1.55
14	NDF + (Asphaltenes - Coke) (5%)	175.4	28.81	4.20	16.94	1.95	14.63	1.64	15.39	1.74
15	NDF + (Asphaltenes - Coke) (10%)	163.5	25.79	3.51	25.33	3.41	21.17	2.62	17.50	2.00
16	HMGO + (Asphaltenes - Coke) (2%)	174.9	30.47	4.63	33.32	5.46	26.56	3.68	21.93	2.76
17	HMGO + (Asphaltenes - Coke) (5%)	188.8	30.74	4.71	28.21	4.06	24.21	3.19	20.42	2.50
18	HMGO + (Asphaltenes - Coke) (10%)	166.5	29.50	4.38	35.58	6.22	22.66	2.89	19.99	2.42
19	NDF + (Asphaltenes - Dirt) (2%)	166.5	30.88	4.74	--	--	--	--	--	--
20	NDF + (Asphaltenes - Dirt) (5%)	162.1	30.62	4.67	--	--	--	--	--	--
21	NDF + (Asphaltenes - Dirt) (10%)	159.1	30.52	4.65	--	--	--	--	--	--
22	HMGO + (Asphaltenes - Dirt) (2%)	175.4	35.15	6.07	--	--	--	--	--	--
23	HMGO + (Asphaltenes - Dirt) (5%)	191.8	32.77	5.29	--	--	--	--	--	--
24	HMGO + (Asphaltenes - Dirt) (10%)	184.0	37.99	7.14	30.25	4.57	25.84	3.52	24.65	3.27
25	NDF + 10% Slurry	157.6	37.54	6.95	36.59	6.59	34.82	5.95	31.22	4.84
26	HMGO + 10% Slurry	211.0	30.59	4.67	30.40	4.61	21.85	2.74	25.82	3.52

APPENDIX C

COMBUSTION PERFORMANCE DATA:
COMBUSTION EFFICIENCY AND GASEOUS EMISSIONS

Appendix C

Fuel No.	Description	Combustion Efficiency				Total Hydrocarbons Emissions Index				CO Emissions Index				NO_x Emission Index[1]			
		100%	75%	55%	Idle (10%)	100%	75%	55%	Idle (10%)	100%	75%	55%	Idle (10%)	100%	75%	55%	Idle (10%)
1	Jet A	99.43	98.81	98.48	95.60	4.03	12.0	12.0	40.1	11.5	25.3	42.3	122.7	6.7	5.7	4.9	2.2
2	NDF	99.57	99.12	98.68	95.40	2.20	4.63	6.67	35.6	15.1	33.3	53.9	142.7	8.8	5.1	4.7	2.0
3	70% NDF + 30% HMGO	99.59	99.06	98.90	94.94	1.33	4.40	10.7	40.8	16.5	37.1	64.7	161.2	8.3	5.9	5.2	2.9
4	30% NDF + 70% HMGO	99.54	99.03	98.10	94.36	1.67	4.30	11.6	40.2	17.7	36.7	58.4	160.0	7.6	5.7	5.1	3.2
5	HMGO	99.53	98.92	98.09	92.72	1.83	5.63	13.8	46.9	18.6	41.6	70.6	195.0	2.5	2.4	5.6	3.4
6	Jet A + Asphaltenes (2%)	99.60	99.22	98.81	95.75	2.67	4.63	9.93	40.4	12.5	30.3	50.6	123.4	7.0	5.8	4.5	2.2
7	NDF + 2% Asphaltenes	99.55	98.94	97.78	94.74	1.93	5.23	16.0	38.4	15.4	38.7	66.3	132.7	6.7	5.6	4.9	2.9
8	NDF + 5% Asphaltenes	99.50	98.87	97.62	93.84	2.30	5.93	17.8	55.0	19.8	45.2	74.1	153.6	8.4	5.4	4.6	2.8
9	NDF + 10% Asphaltenes	99.53	98.76	97.81	92.87	1.70	5.97	23.1	70.2	19.4	48.3	89.0	193.1	7.5	6.3	5.1	3.0
10	HMGO + 2% Asphaltenes	99.46	98.77	97.30	91.98	2.20	6.40	20.0	87.1	23.1	52.9	97.6	246.9	7.0	5.8	4.9	2.6
11	HMGO + 5% Asphaltenes	99.50	98.75	97.24	91.48	2.17	6.77	20.1	87.5	19.3	50.4	96.0	221.0	7.4	6.4	5.2	3.0
12	HMGO + 10% Asphaltenes	99.48	98.59	96.53	90.21	2.47	7.17	25.7	101.	23.9	57.7	119.0	285.5	7.8	6.5	2.8	2.8
13	NDF + 2% Asphaltenes + Coke	99.47	98.83	97.53	94.96	3.03	6.47	19.5	39.4	16.9	42.3	71.0	158.1	6.7	5.4	4.8	2.2
14	NDF + 5% Asphaltenes + Coke	99.41	98.75	97.46	94.45	3.40	7.03	17.2	42.5	18.3	43.5	79.1	167.7	8.8	5.5	4.4	2.8
15	NDF + 10% Asphaltenes + Coke	99.28	98.80	97.48	94.99	5.23	9.70	18.6	38.8	18.5	41.7	73.8	172.4	7.2	6.3	5.8	3.8
16	HMGO + 2% Asphaltenes + Coke	99.35	98.65	97.46	93.68	3.10	6.97	18.1	81.3	23.6	50.3	89.8	213.6	8.9	5.2	4.8	2.9
17	HMGO +5% Asphaltenes + Coke	99.38	98.69	96.92	91.83	2.97	7.87	23.1	85.1	22.8	56.8	105.5	241.4	7.8	5.9	4.8	2.9
18	HMGO + 10% Asphaltenes + Coke	99.45	98.71	95.94	91.90	2.20	5.77	44.0	87.0	21.3	51.1	88.5	201.7	7.5	6.5	5.9	3.3
19	NDF + 2% Asphaltenes + Dirt	99.63	99.09	98.87	95.19	1.33	3.83	12.7	39.1	14.9	39.1	67.8	138.6	6.8	5.9	4.5	2.8
20	NDF + 5% Asphaltenes + Dirt	99.54	99.07	97.78	94.99	1.83	4.16	14.1	38.2	18.1	38.4	74.8	148.8	6.9	5.2	4.4	2.5
21	NDF + 10% Asphaltenes + Dirt	99.41	98.81	97.33	94.54	2.87	6.27	15.8	43.8	21.1	50.8	88.9	187.3	7.1	5.3	4.5	2.1
22	HMGO + 2% Asphaltenes + Dirt	99.55	98.85	97.72	93.18	1.83	4.47	13.5	52.7	18.5	49.4	88.8	213.4	7.5	6.1	4.4	2.2
23	HMGO + 5% Asphaltenes + Dirt	99.39	98.84	97.13	91.78	3.17	5.23	20.7	76.8	21.4	47.4	102.7	256.9	7.8	6.1	4.9	2.8
24	HMGO + 10% Asphaltenes + Dirt	99.21	98.68	97.19	92.37	3.27	6.87	20.5	94.8	26.6	52.1	90.6	254.2	7.6	6.2	5.2	3.4
25	NDF + 10% Slurry with Catfines	99.34	98.81	96.65	92.17	3.53	7.16	27.0	79.3	22.4	53.1	89.9	200.8	7.1	5.6	4.7	3.2
26	HMGO + 10% Slurry with Catfines	99.47	98.84	96.20	88.93	2.73	6.23	32.2	114.	19.3	46.2	102.4	236.1	8.2	6.4	4.7	2.7

DISTRIBUTION LIST

DEPARTMENT OF DEFENSE

DEFENSE DOCUMENTATION CTR
CAMERON STATION 12
ALEXANDRIA VA 22314

DEPT. OF DEFENSE
ATTN: OASD (A&L) (MR DYCKMAN) 1
WASHINGTON DC 20301-8000

CDR
DEFENSE FUEL SUPPLY CTR
ATTN: DFSC-Q (MR MARTIN) 1
CAMERON STATION
ALEXANDRIA VA 22304-6160

DOD
ATTN: DUSDRE (RAT) (Dr. Dix) 1
ATTN: ROOM 3-D-1089, PENTAGON 1
WASHINGTON DC 20301

DEFENSE ADVANCED RES PROJ AGENCY
DEFENSE SCIENCES OFC 1
1400 WILSON BLVD
ARLINGTON VA 22209

DEPARTMENT OF THE ARMY

HG, DEPT OF ARMY
ATTN: DALO-TSE (COL BLISS) 1
DALO-TSZ-B (MR KOWALCZYK) 1
DALO-AV 1
DAMO-FDR (MAJ KNOX) 1
DAMA-ARZ (DR CHURCH) 1
DAMA-ART (LTC RINEHART) 1
WASHINGTON DC 20310

CDR
U.S. ARMY BELVOIR RESEARCH, DEVELOPMENT & ENGINEERING CTR
ATTN: STRBE-VF 10
STRBE-WC 2
FORT BELVOIR VA 22060-5606

CDR
US ARMY MATERIEL DEVEL & READINESS COMMAND
ATTN: AMCLD (DR ODOM) 1
AMCDE-SG 1
AMCDE-SS 1
AMCSM-WST (LTC DACEY) 1
5001 EISENHOWER AVE
ALEXANDRIA VA 22333-0001

CDR
US ARMY TANK-AUTOMOTIVE CMD
ATTN: AMSTA-RG (MR WHEELOCK) 1
AMSTA-TSL (MR BURG) 1
AMSTA-G 1
AMSTA-MTC (MR GAGLIO), AMSTA-MC, AMSTA-MV 1
AMSTA-UBP (MR MCCARTNEY) 1
AMSTA-MLF (MR KELLER) 1
WARREN MI 48397-5000

DIRECTOR
US ARMY MATERIEL SYSTEMS ANALYSIS ACTIVITY
ATTN: AMXSY-CM (MR NIEMEYER) 1
AMXSY-CR 1
ABERDEEN PROVING GROUND MD 21005-5006

DIRECTOR
APPLIED TECHNOLOGY LAB
U.S. ARMY R&T LAB (AVSCOM)
ATTN: SAVDL-ATL-ATP (MR MORROW) 1
SAVDL-ATL-ASV 1
FORT EUSTIS VA 23604-5577

CDR
US ARMY GENERAL MATERIAL & PETROLEUM ACTIVITY
ATTN: STRGP-F (MR ASHBROOK) 1
STRGP-FE, BLDG 85-3 1
STRGP-FT 1
NEW CUMBERLAND PA 17070-5008

HQ, DEPT. OF ARMY
ATTN: DAEN-DRM 1
WASHINGTON DC 20310

CDR
US ARMY RES & STDZN GROUP
(EUROPE)
ATTN: AMXSN-UK-RA (DR OERTEL) 1
AMXSN-UK-SE (LTC NICHOLS) 1
BOX 65
FPO NEW YORK 09510

CDR, US ARMY AVIATION R&D CMD
ATTN: AMSAV-EP (MR EDWARDS) 1
AMSAV-NS 1
4300 GOODFELLOW BLVD
ST LOUIS MO 63120-1798

CDR
US ARMY YUMA PROVING GROUND
ATTN: STEYP-MT-TL-M
(MR DOEBBLER) 1
YUMA AZ 85364-9130

PROJ MGR, BRADLEY FIGHTING
VEHICLE SYS
ATTN: AMCPM-FVS-M 1
WARREN MI 48397

PROG MGR, M113 FAMILY OF VEHICLES
ATTN: AMCPM-M113-T 1
WARREN MI 48397

PROJ MGR, MOBILE ELECTRIC POWER
ATTN: AMCPM-MEP-TM 1
7500 BACKLICK ROAD
SPRINGFIELD VA 22150

PROJ OFF, AMPHIBIOUS AND WATER
CRAFT
ATTN: AMCPM-AWC-R 1
4300 GOODFELLOW BLVD
ST LOUIS MO 63120

CDR
US ARMY EUROPE & SEVENTH ARMY
ATTN: AEAGG-FMD 1
AEAGD-TE 1
APO NY 09403

CDR
THEATER ARMY MATERIAL MGMT
CENTER (200TH)-DPGM
DIRECTORATE FOR PETROL MGMT
ATTN: AEAGD-MMC-PT-Q 1
APO NY 09052

CDR
US ARMY RESEARCH OFC
ATTN: SLCRO-ZC 1
SLCRO-EG (DR MANN) 1
SLCRO-CB (DR GHIRARDELLI) 1
P O BOX 12211
RSCH TRIANGLE PARK NC 27709-2211

PROG MGR, TACTICAL VEHICLE
ATTN: AMCPM-TV 1
WARREN MI 48397

DIR
US ARMY AVIATION R&T LAB
(AVSCOM)
ATTN: SAVDL-AS (MR WILSTEAD) 1
AMES RSCH CTR
MAIL STOP 207-5
MOFFET FIELD CA 94035

CDR
TRADOC COMBINED ARMS TEST
ACTIVITY
ATTN: ATCT-CA 1
FORT HOOD TX 76544

CDR
TOBYHANNA ARMY DEPOT
ATTN: SDSTO-TP-S 1
TOBYHANNA PA 18466

CDR
US ARMY LEA
ATTN: DALO-LEP 1
NEW CUMBERLAND ARMY DEPOT
NEW CUMBERLAND PA 17070

CDR
US ARMY GENERAL MATERIAL &
PETROLEUM ACTIVITY
ATTN: STRGP-FW (MR PRICE) 1
BLDG 247, DEFENSE DEPOT TRACY
TRACY CA 95376

PROJ MGR, LIGHT ARMORED VEHICLES
ATTN: AMCPM-LA-E 1
WARREN MI 48397

CDR
US ARMY ORDNANCE CENTER &
SCHOOL
ATTN: ATSL-CD-CS 1
ABERDEEN PROVING GROUND MD
21005

CDR
US ARMY FOREIGN SCIENCE & TECH CENTER
ATTN: AMXST-MT-1 1
AMXST-BA 1
FEDERAL BLDG
CHARLOTTESVILLE VA 22901

CDR
AMC MATERIEL READINESS SUPPORT ACTIVITY (MRSA)
ATTN: AMXMD-MO (MR BROWN) 1
LEXINGTON KY 40511-5101

PROJECT MANAGER, LIGHT COMBAT VEHICLES
ATTN: AMCPM-LCV-TC 1
WARREN, MI 48397

HQ, US ARMY T&E COMMAND
ATTN: AMSTE-TO-O 1
AMSTE-CM-R-O 1
AMSTE-TE-T (MR RITONDO) 1
ABERDEEN PROVING GROUND MD 21005-5006

CDR, US ARMY ARMAMENT MUNITIONS & CHEMICAL COMMAND ARMAMENT RESEARCH & DEVELOPMENT CTR
ATTN: AMSMC-LC 1
AMSMC-SC 1
DOVER NJ 07801-5001

CDR, US ARMY TROOP SUPPORT COMMAND
ATTN: AMSTR-ME 1
AMSTR-S 1
AMSTRE-E 1
4300 GOODFELLOW BLVD
ST LOUIS MO 63120-1798

CDR
CONSTRUCTION ENG RSCH LAB
ATTN: CERL-EM 1
CERL-ZT 1
CERL-EH 1
P O BOX 4005
CHAMPAIGN IL 61820

TRADOC LIAISON OFFICE
ATTN: ATFE-LO-AV 1
4300 GOODFELLOW BLVD
ST LOUIS MO 63120-1798

DIRECTOR
US ARMY RSCH & TECH LAB (AVSCOM)
PROPULSION LABORATORY
ATTN: SAVDL-PL-D (MR ACURIO) 1
21000 BROOKPARK ROAD
CLEVELAND OH 44135-3127

CDR
US ARMY NATICK RES & DEV LAB
ATTN: STRNA-YE (DR KAPLAN) 1
STRNA-U 1
NATICK MA 01760-5000

CDR
US ARMY TRANSPORTATION SCHOOL
ATTN: ATSP-CD-MS (MR HARNET) 1
FORT EUSTIS VA 23604-5000

PROJ MGR, PATRIOT PROJ OFFICE
ATTN: AMCPM-MD-T-C 1
U.S. ARMY MISSILE COMMAND
REDSTONE ARSENAL AL 35898

CDR
US ARMY QUARTERMASTER SCHOOL
ATTN: ATSM-CD 1
ATSM-TD 1
ATSM-PFS 1
FORT LEE VA 23801

HQ, US ARMY ARMOR CENTER AND FORT KNOX
ATTN: ATSB-CD 1
FORT KNOX KY 40121

CDR
COMBINED ARMS COMBAT DEVELOPMENT ACTIVITY
ATTN: ATZL-CAT-E 1
ATZL-CAT-A 1
FORT LEAVENWORTH KA 66027-5300

CDR
US ARMY LOGISTICS CTR
ATTN: ATCL-MS (MR A MARSHALL) 1
ATCL-C 1
FORT LEE VA 23801-6000

PROJECT MANAGER
PETROLEUM & WATER LOGISTICS
ATTN: AMCPM-PWS 1
4300 GOODFELLOW BLVD
ST LOUIS MO 63120-1798

CDR
US ARMY FIELD ARTILLERY SCHOOL
ATTN: ATSF-CD 1
FORT SILL OK 73503-5600

CDR
US ARMY ENGINEER SCHOOL
ATTN: ATZA-TSM-G 1
ATZA-CDM 1
ATZA-CDD 1
FORT BELVOIR VA 22060-5606

CDR
US ARMY INFANTRY SCHOOL
ATTN: ATSH-CD-MS-M 1
FORT BENNING GA 31905-5400

CDR
US ARMY AVIATION CTR & FT RUCKER
ATTN: ATZQ-DI 1
FORT RUCKER AL 36362

PROG MGR, TANK SYSTEMS
ATTN: AMCPM-M1E1-SM 1
AMCPM-M60 1
WARREN MI 48397

CDR
US ARMY ARMOR & ENGINEER BOARD
ATTN: ATZK-AE-AR 1
ATZK-AE-LT 1
FORT KNOX KY 40121

CDR
6TH MATERIEL MANAGEMENT CENTER
19TH SUPPORT BRIGADE 1
APO SAN FRANCISCO 96212-0172

CHIEF, U.S. ARMY LOGISTICS
ASSISTANCE OFFICE, FORSCOM
ATTN: AMXLA-FO (MR PITTMAN) 1
FT MCPHERSON GA 30330

DEPARTMENT OF THE NAVY

CDR
NAVAL AIR PROPULSION CENTER
ATTN: PE-33 (MR D'ORAZIO) 1
P O BOX 7176
TRENTON NJ 06828

CDR
NAVAL SEA SYSTEMS CMD
ATTN: CODE 05M4 (MR R LAYNE) 1
WASHINGTON DC 20362-5101

CDR
DAVID TAYLOR NAVAL SHIP R&D CTR
ATTN: CODE 2830 (MR BOSMAJIAN) 1
CODE 2759 (MR STRUCKO) 1
CODE 2831 1
ANNAPOLIS MD 21402

CDR
NAVAL SHIP ENGINEERING CENTER
ATTN: CODE 6764 1
PHILADELPHIA PA 19112

DEPARTMENT OF THE NAVY
HQ, US MARINE CORPS
ATTN: LPP 1
LMM/2 1
WASHINGTON DC 20380

CDR
NAVAL AIR SYSTEMS CMD
ATTN: CODE 53645 (MR MEARNS) 1
WASHINGTON DC 20361

CDR
NAVAL RESEARCH LABORATORY
ATTN: CODE 6170 1
CODE 6180 1
CODE 6110 (DR HARVEY) 1
WASHINGTON DC 20375

CDR
NAVAL FACILITIES ENGR CTR
ATTN: CODE 1202B (MR R BURRIS) 1
200 STOVAL ST
ALEXANDRIA VA 22322

CDR
NAVAL AIR ENGR CENTER
ATTN: CODE 92727 1
LAKEHURST NJ 08733

COMMANDING GENERAL
US MARINE CORPS DEVELOPMENT
& EDUCATION COMMAND
ATTN: DO74 (LTC WOODHEAD) 1
QUANTICO VA 22134

OFFICE OF THE CHIEF OF NAVAL RESEARCH
ATTN: OCNR-126 (MR ZIEM) 1
ARLINGTON, VA 22217-5000

CHIEF OF NAVAL OPERATIONS
ATTN: OP 413 1
WASHINGTON DC 20350

CDR
NAVY PETROLEUM OFC
ATTN: CODE 43 (MR LONG) 1
CAMERON STATION
ALEXANDRIA VA 22304-6180

DEPARTMENT OF THE AIR FORCE

HQ, USAF
ATTN: LEYSF 1
WASHINGTON DC 20330

HQ AIR FORCE SYSTEMS CMD
ATTN: AFSC/DLF (MAJ VONEDA) 1
ANDREWS AFB MD 20334

CDR
US AIR FORCE WRIGHT AERONAUTICAL LAB
ATTN: AFWAL/POSF (MR CHURCHILL) 1
WRIGHT-PATTERSON AFB OH 45433

CDR
SAN ANTONIO AIR LOGISTICS CTR
ATTN: SAALC/SFT (MR MAKRIS) 1
SAALC/MMPRR 1
KELLY AIR FORCE BASE TX 78241

CDR
WARNER ROBINS AIR LOGISTIC CTR
ATTN: WRALC/MMTV (MR GRAHAM) 1
ROBINS AFB GA 31098

CDR
USAF 3902 TRANSPORTATION SQUADRON
ATTN: LGTVP (MR VAUGHN) 1
OFFUTT AIR FORCE BASE NE 68113

CDR
HQ 3RD USAF
ATTN: LGSF 1
APO NEW YORK 09127

CDR
DET 29
ATTN: SA-ALC/SFM 1
CAMERON STATION
ALEXANDRIA VA 22314

OTHER GOVERNMENT AGENCIES

NATIONAL AERONAUTICS AND SPACE ADMINISTRATION
VEHICLE SYSTEMS AND ALTERNATE FUELS PROJECT OFFICE
ATTN: MR CLARK 1
LEWIS RESEARCH CENTER
CLEVELAND OH 44135

DEPARTMENT OF TRANSPORTATION
FEDERAL AVIATION ADMINISTRATION
ATTN: AWS-110 1
800 INDEPENDENCE AVE, SW
WASHINGTON DC 20590

US DEPARTMENT OF ENERGY
CE-151
ATTN: MR ECKLUND 1
FORRESTAL BLDG.
1000 INDEPENDENCE AVE, SW
WASHINGTON DC 20585

ENVIRONMENTAL PROTECTION AGENCY
AIR POLLUTION CONTROL 1
2565 PLYMOUTH ROAD
ANN ARBOR MI 48105

END

1-87

DTIC